

U.S. DEPARTMENT OF  
**ENERGY**

Office of  
Science

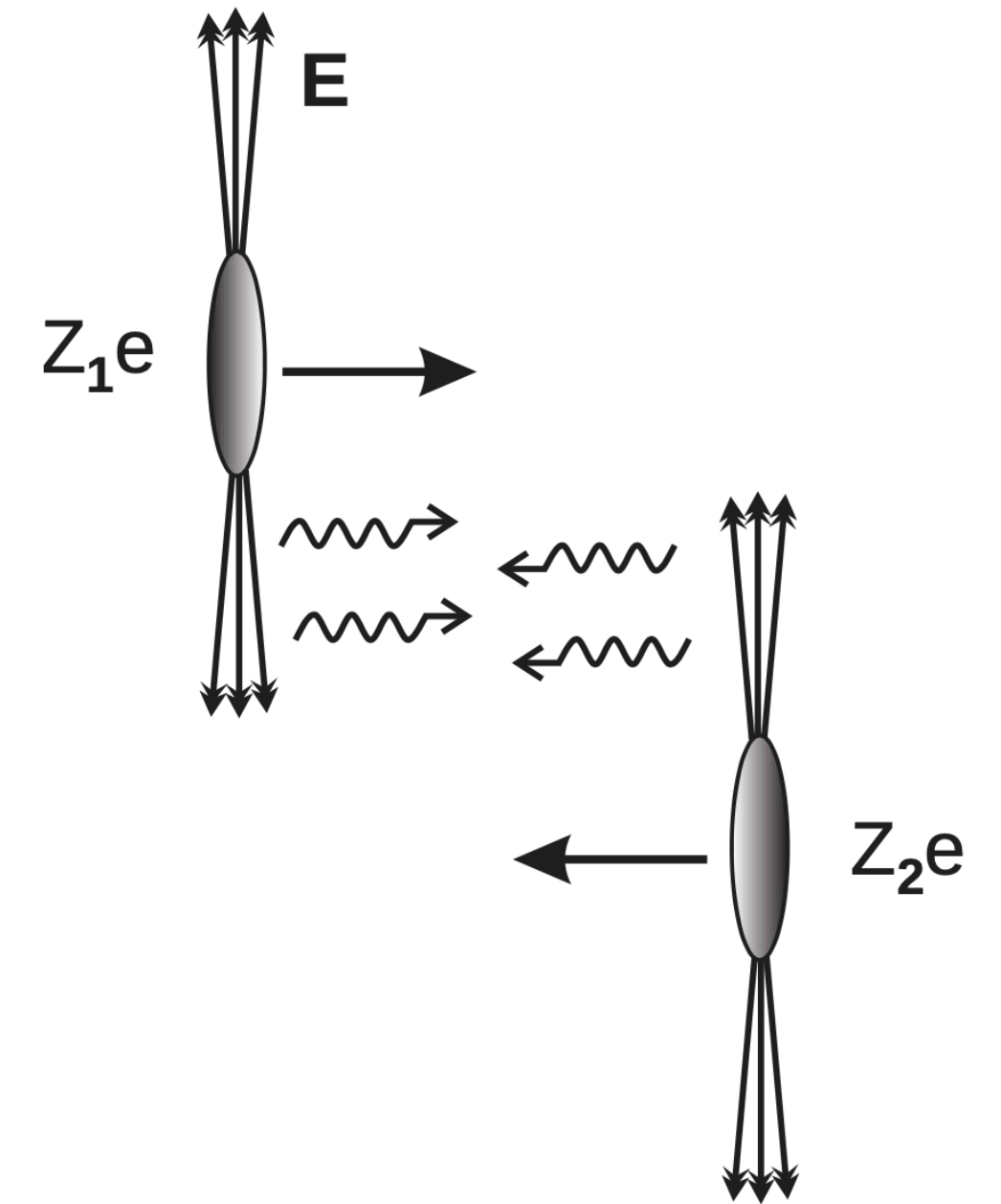
# THEORY OF VECTOR MESON PHOTO PRODUCTION

BJÖRN SCHENKE, BROOKHAVEN NATIONAL LABORATORY

The first international workshop on the physics of Ultra Peripheral Collisions  
Playa del Carmen  
12/11/2023

# Ultrapерipheral collisions (UPC)

- At an impact parameter  $|b_T| > 2R_A$  nuclei are photon sources
- Photons are quasi-real  $Q^2 \lesssim 1/R_A^2$
- High energy  $\gamma + \gamma, \gamma + p, \gamma + A$  at RHIC and LHC
- Ignoring interference, the cross section for vector meson production is a convolution of photon flux  $n^{A_1}$  from nucleus  $A_1$  and the  $\gamma A_2$  cross section (and vice versa):



$$\frac{d\sigma^{AA \rightarrow VAA'}}{dt} = n^{A_2}(\omega_2) \sigma_{\gamma A_1 \rightarrow VA'_1}(y) + n^{A_1}(\omega_1) \sigma_{\gamma A_2 \rightarrow VA'_2}(-y)$$

$y$  is the rapidity of the VM and photon energies are  $\omega_1 = (M_V/2)e^y, \omega_2 = (M_V/2)e^{-y}$

# Interference effects

C. A. Bertulani, S. R. Klein and J. Nystrand, *Ann. Rev. Nucl. Part. Sci.* 55 (2005) 271

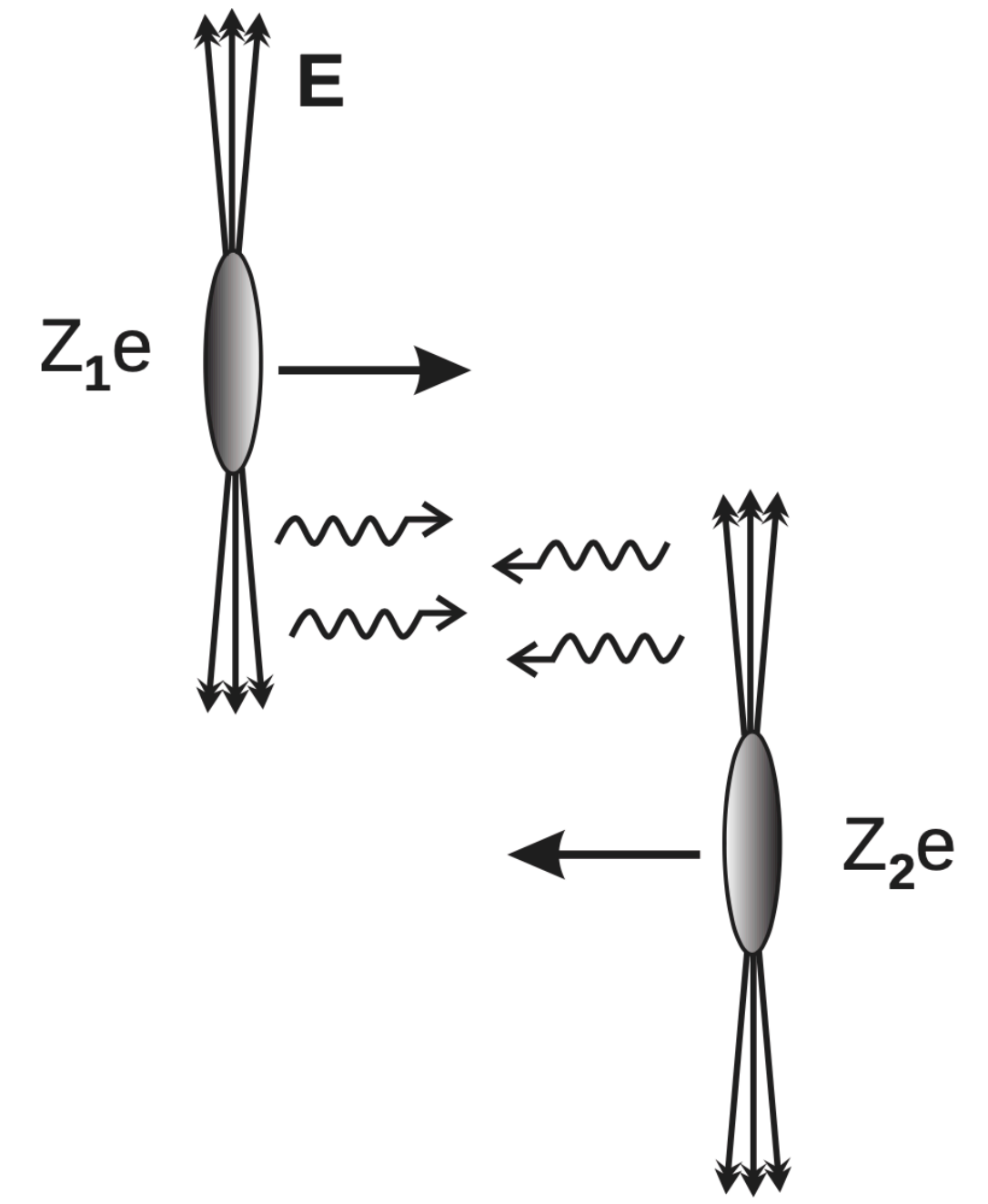
Interference is important for the differential cross-section in A+A, especially at midrapidity. There

$$\frac{d\sigma}{d|t|} = \frac{1}{16\pi} \int d^2\mathbf{B} |A_1 - A_2|^2 \theta(|\mathbf{B}| - 2R_A)$$

Interference is destructive in A+A because of negative parity of the VM

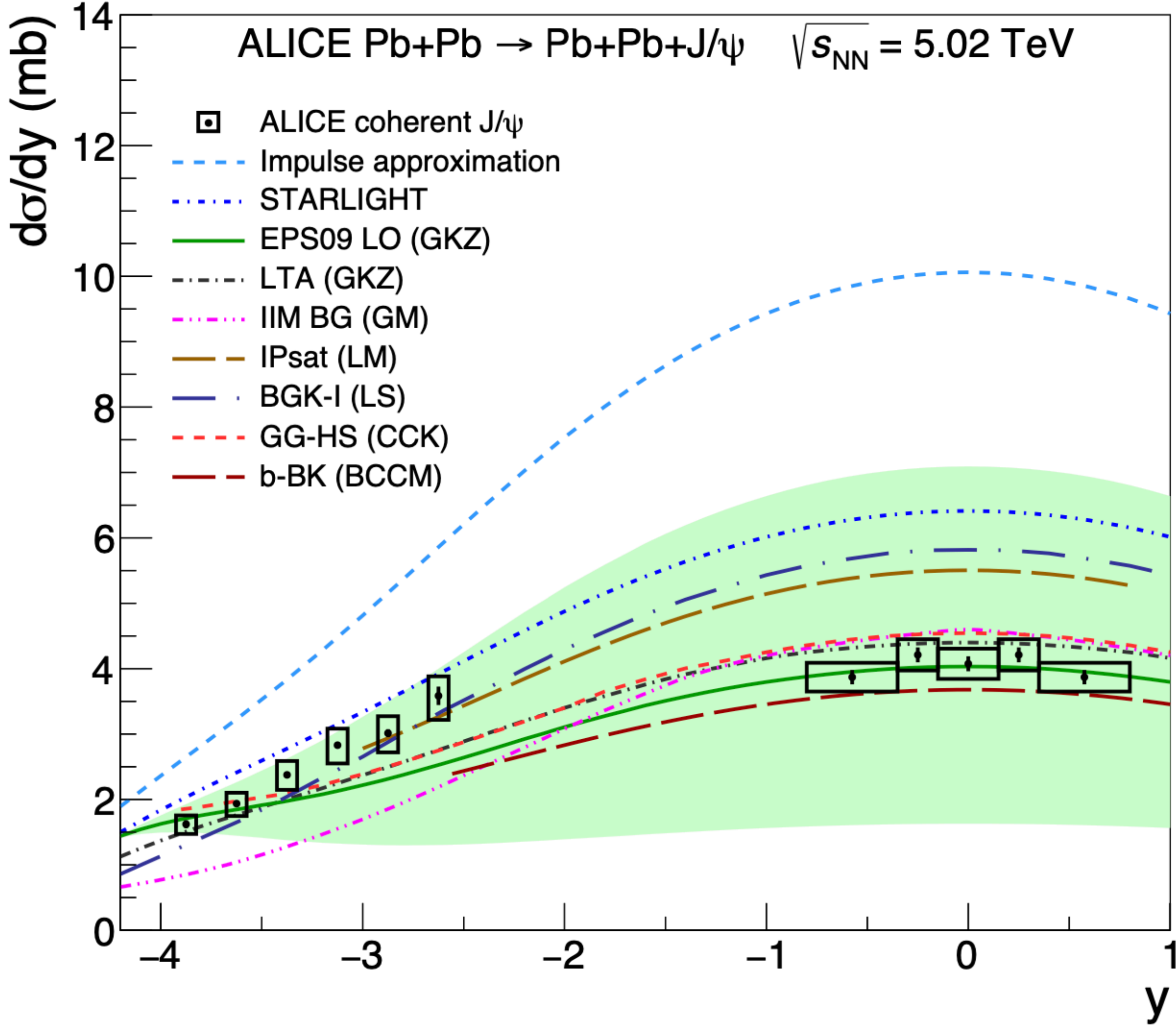
$$\left. \frac{d\sigma^{A_1+A_2 \rightarrow V+A_1+A_2}}{d|t|dy} \right|_{y=0} = 2 \int d^2\mathbf{B} n(\omega, |\mathbf{B}|) \frac{d\sigma^{\gamma+A \rightarrow V+A}}{d|t|} [1 - \cos(\Delta \cdot \mathbf{B})] \theta(|\mathbf{B}| - 2R_A)$$

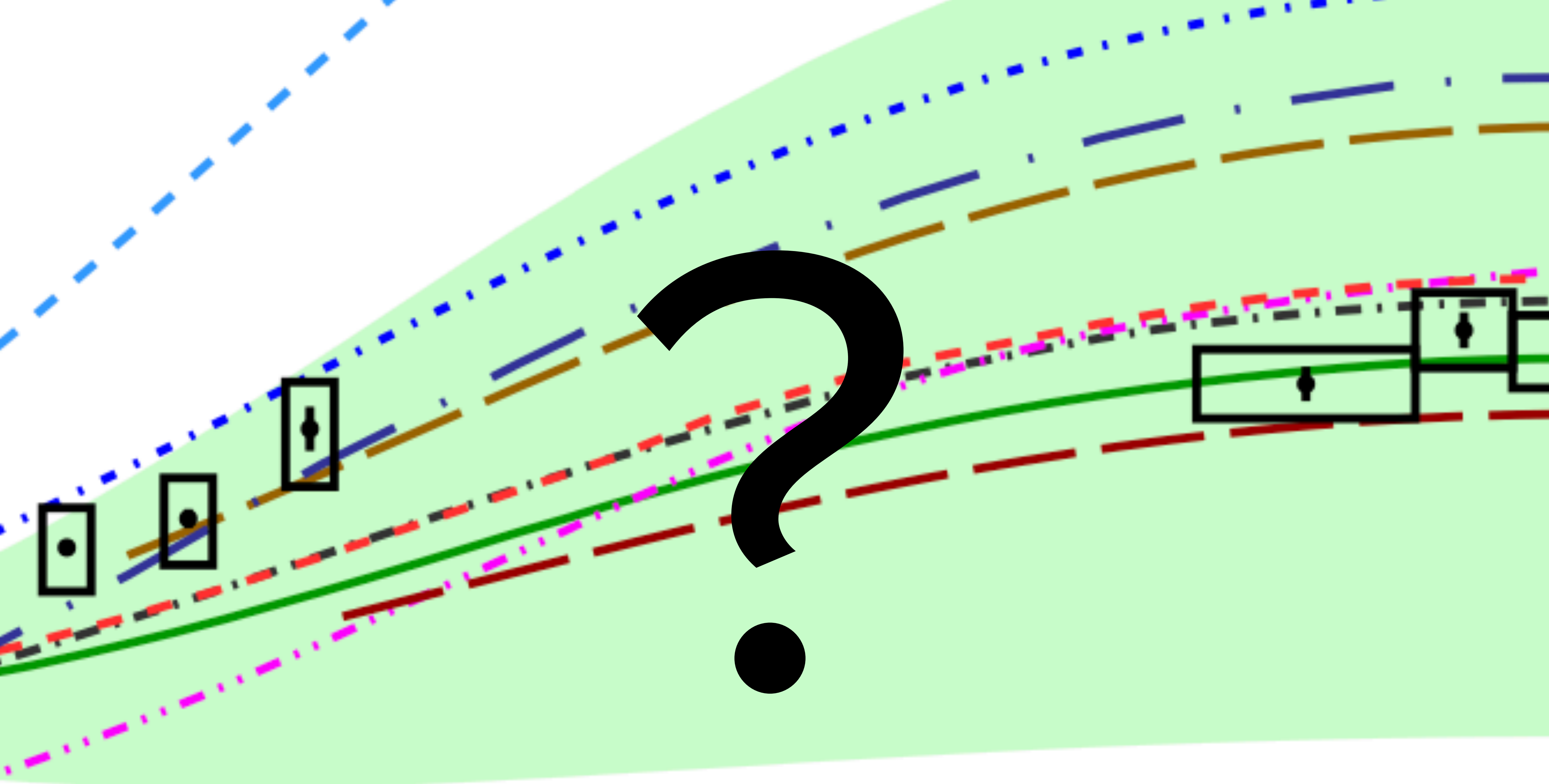
with  $t = -\Delta^2$



# Coherent $J/\psi$ production

ALICE Collaboration, Eur. Phys. J. C 81 (2021) 712





# Coherent $J/\psi$ production

M.G. Ryskin, Z.Phys.C 57 (1993) 89-92 (for proton)

LO pQCD: V. Guzey, M. Zhalov, JHEP 1310, 207 (2013)

$$\sigma_{\gamma A \rightarrow V A}(W_{\gamma p}) = C_A(\mu^2) [\alpha_s(\mu^2) x g_A(x, \mu^2)]^2 \Phi_A(t_{\min})$$

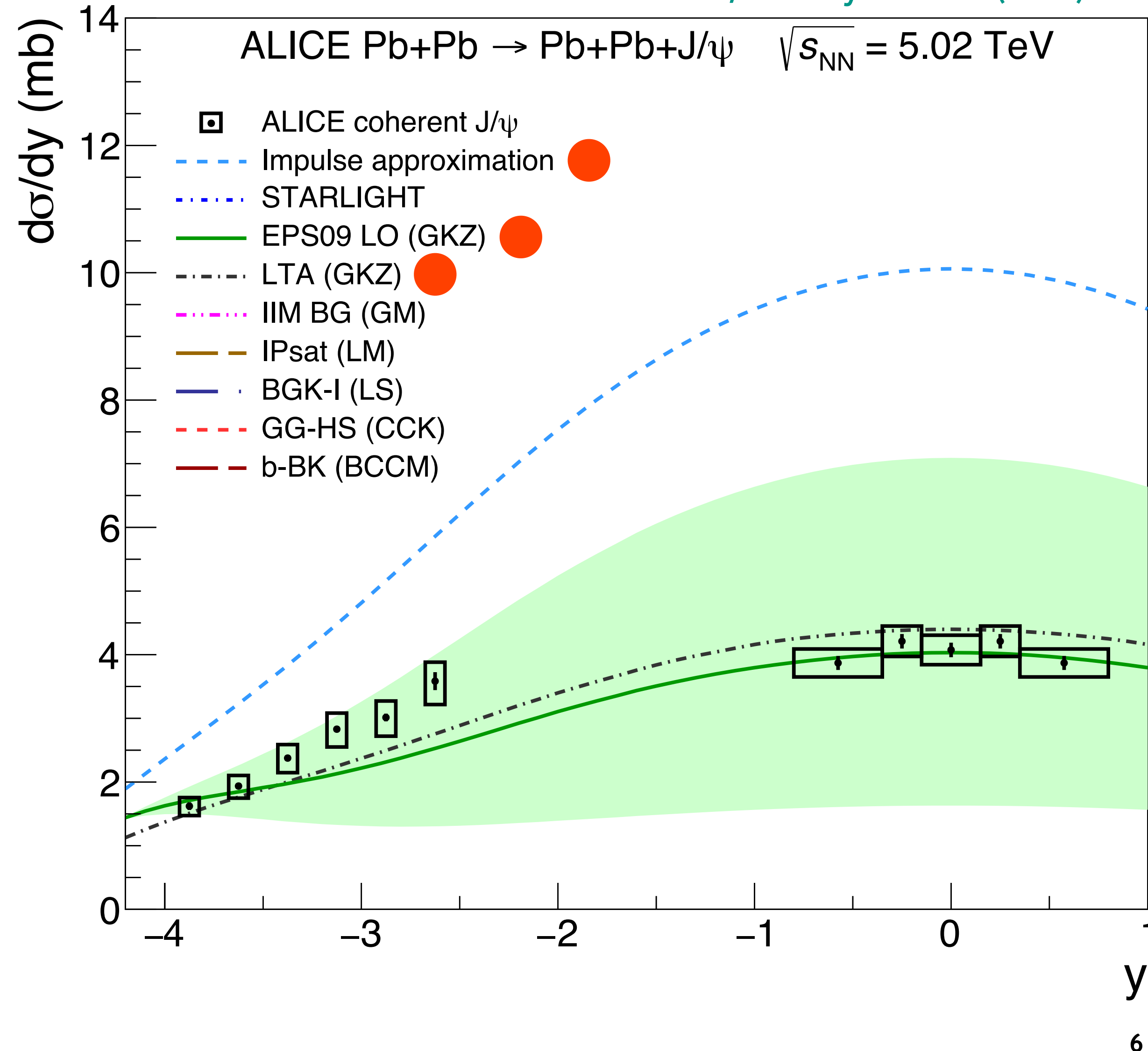
$$= \frac{C_A(\mu^2)}{C_p(\mu^2)} \frac{d\sigma_{\gamma p \rightarrow V p}(W_{\gamma p}, t=0)}{dt} \left[ \frac{x g_A(x, \mu^2)}{A x g_p(x, \mu^2)} \right]^2 \Phi_A(t_{\min})$$

$$\downarrow$$

$$C_p(\mu^2) [\alpha_s(\mu^2) x g_p(x, \mu^2)]^2 \quad R_g(x, \mu^2)$$

$$\Phi_A(t_{\min}) = \int_{-\infty}^{t_{\min}} dt |F_A(t)|^2$$

ALICE Collaboration, Eur. Phys. J. C 81 (2021) 712



— Impulse approximation:  $R_g = 1$

## LTA (GKZ):

V. Guzey, E. Kryshen, M. Zhalov, Phys. Rev. C 93, 055206 (2016)

$R_g$  from Leading Twist Nuclear Shadowing

L. Frankfurt, V. Guzey and M. Strikman, Phys. Rept. 512, 255 (2012)

## EPS09 (GKZ):

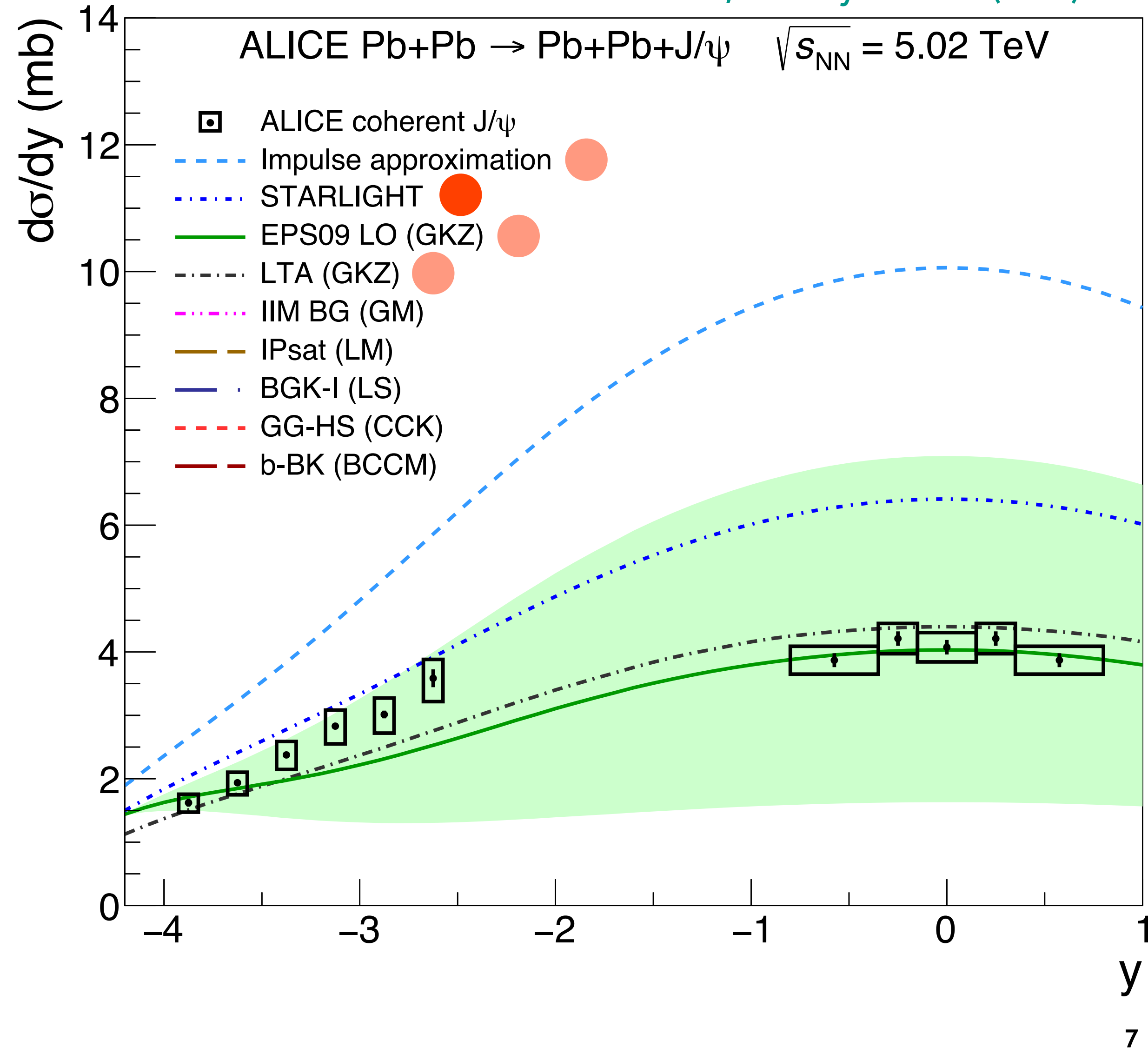
$R_g$  from EPS09 nuclear parton distribution functions

K. J. Eskola, H. Paukkunen and C. A. Salgado, JHEP 0904, 065 (2009)

$$x = M_V^2 / W_{\gamma p}^2 \quad \mu^2 = 3 \text{ GeV}^2$$

# Coherent $J/\psi$ production

ALICE Collaboration, Eur. Phys. J. C 81 (2021) 712



## STARLIGHT:

Spencer R. Klein, Joakim Nystrand, Janet Seger, Yuri Gorbunov, Joey Butterworth, Comput.Phys.Commun. 212 (2017) 258-268

STARLIGHT includes **Glauber-like rescattering**

$$\begin{aligned} \sigma(AA \rightarrow AAV) &= 2 \int dk \frac{dN_\gamma(k)}{dk} \sigma(\gamma A \rightarrow VA) \\ &= 2 \int_0^\infty dk \frac{dN_\gamma(k)}{dk} \int_{t_{min}}^\infty dt \left. \frac{d\sigma(\gamma A \rightarrow VA)}{dt} \right|_{t=0} |F(t)|^2, \end{aligned}$$

Using vector meson dominance and optical theorem:

$$\frac{d\sigma(\gamma A \rightarrow VA)}{dt} = \frac{\alpha \sigma_{tot}^2(\gamma A \rightarrow VA)}{4f_v^2}$$

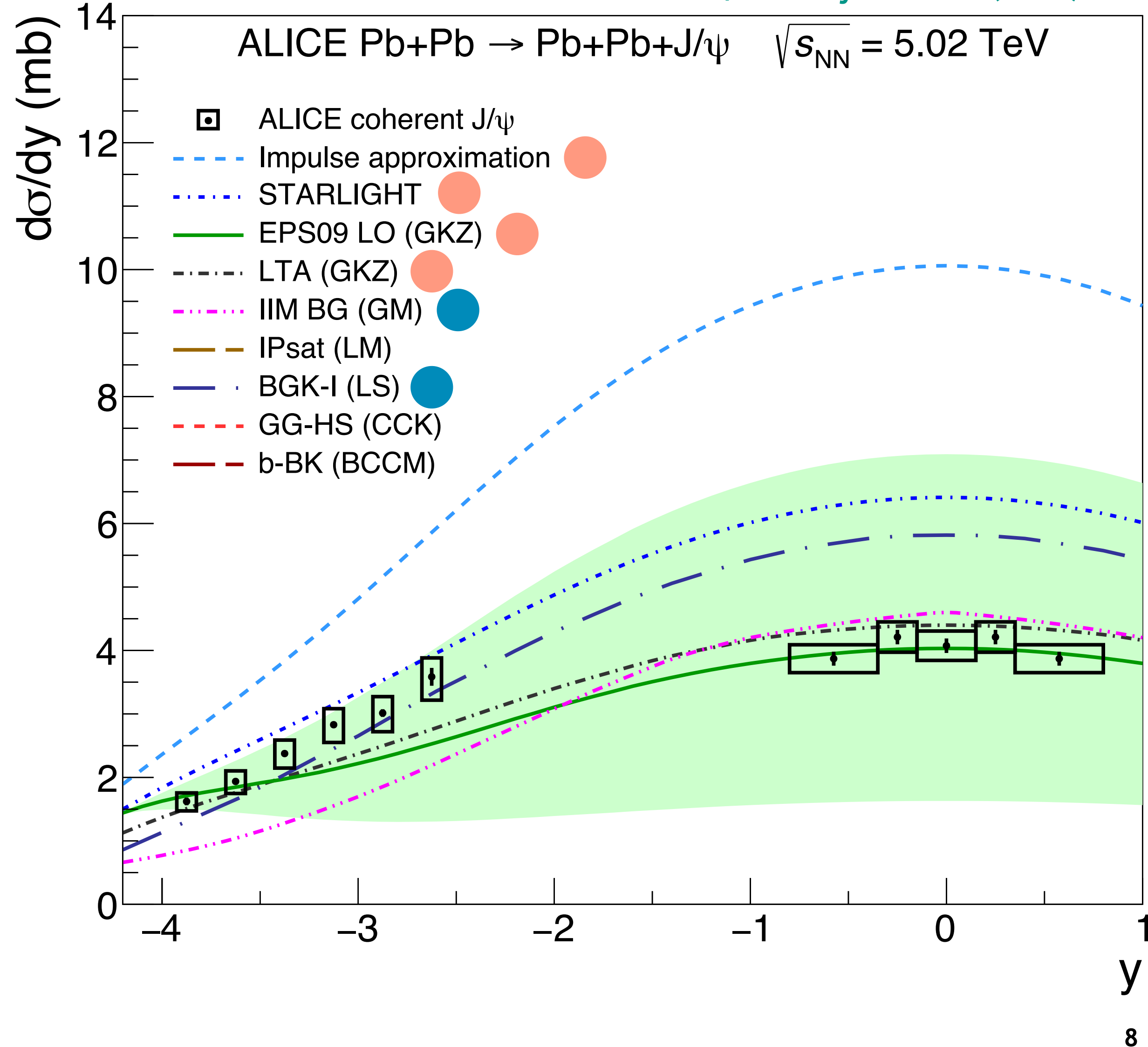
$$\text{with } \sigma_{tot}(\gamma A \rightarrow VA) = \int d^2\vec{b} \left( 1 - e^{-\sigma_{tot}(\gamma p \rightarrow Vp) T_{AA}(\vec{b})} \right)$$

$f_v$  is the vector meson-photon coupling

Spencer R. Klein, Joakim Nystrand, Phys.Rev.C 60 (1999) 014903

# Coherent $J/\psi$ production

ALICE Collaboration, Eur. Phys. J. C 81 (2021) 712



## IIM BG (GM):

G. Sampaio dos Santos, M.V.T. Machado, J. Phys. G. 42 105001 (2015)

$$\sigma(\gamma A \rightarrow VA) = \int d^2b \left| \langle \Psi^V | 1 - \exp \left[ -\frac{1}{2} \sigma_{dip} T_A \right] | \Psi^\gamma \rangle \right|^2$$

with a parametrization of the dipole cross section that is fit to HERA data

$$\sigma_{dip}(x, r) = \sigma_0 \begin{cases} 0.7 \left( \frac{\bar{r}^2}{4} \right)^{\gamma_{eff}(x, r)}, & \text{for } \bar{r} \leq 2, \\ 1 - \exp \left[ -a \ln^2(b \bar{r}) \right], & \text{for } \bar{r} > 2, \end{cases}$$

E. Iancu, K. Itakura and S. Munier, Phys. Lett. B 590, 199 (2004)

$$\bar{r} = r Q_s(x)$$

## BGK-I (LS):

A. Łuszczak and W. Schäfer, Phys. Rev. C 99 no. 4, (2019) 044905

Expresses  $\sigma_{dip}$  in terms of the gluon distribution and includes DGLAP. Also includes the real part of the dipole-nucleon amplitude.

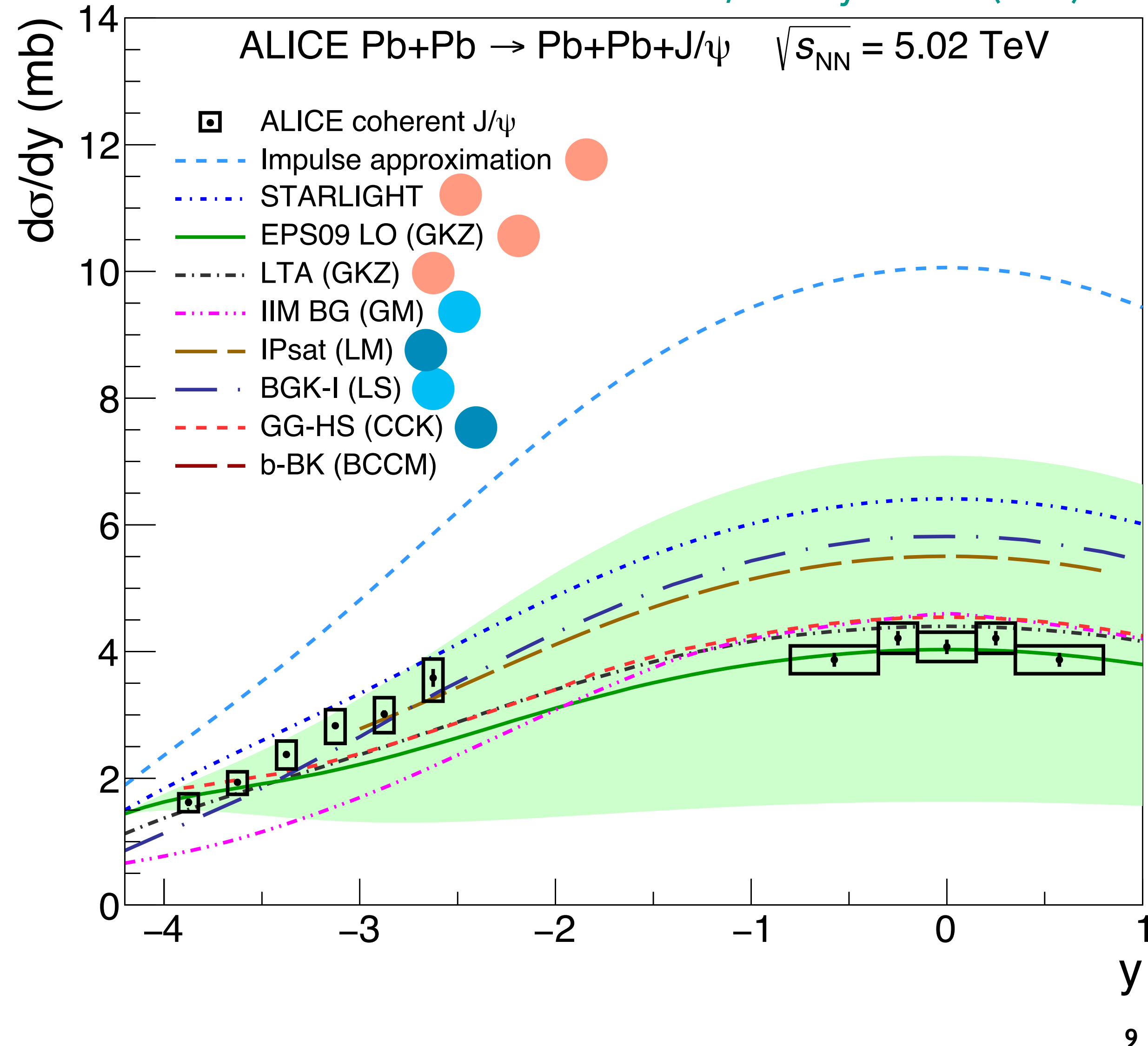
$$\sigma_{dip} = \sigma_0 \left( 1 - \exp \left[ -\frac{\pi^2 r^2 \alpha_s(\mu^2) x g(x, \mu^2)}{3 \sigma_0} \right] \right)$$

$$xg(x, \mu_0^2) = A_g x^{-\lambda_g} (1-x)^{C_g} \quad \text{and then DGLAP}$$



# Coherent $J/\psi$ production

ALICE Collaboration, Eur. Phys. J. C 81 (2021) 712



## IPsat (LM)

T. Lappi, H. Mäntysaari, Phys.Rev. C87 (2013) 032201

Like BGK but also including explicit impact parameter dependence

$$\sigma_{\text{dip-A}}(x, \vec{r}) = \int d^2\vec{b} \frac{d\sigma_{q\bar{q}}}{d^2\vec{b}}$$

$$\frac{d\sigma_{q\bar{q}}}{d^2\vec{b}} = 2 \left[ 1 - \exp \left( -\frac{\pi^2}{2N_c} r^2 \alpha_S(\mu^2) x g(x, \mu^2) T(b) \right) \right]$$

$$T_G(b) = \frac{1}{2\pi B_G} \exp \left( -\frac{b^2}{2B_G} \right), \quad \int d^2\vec{b} T_G(b) = 1$$

## GG-HS (CCK)

J. Cepila, J. G. Contreras, M. Krelina, Phys.Rev.C 97 (2018) 2, 024901

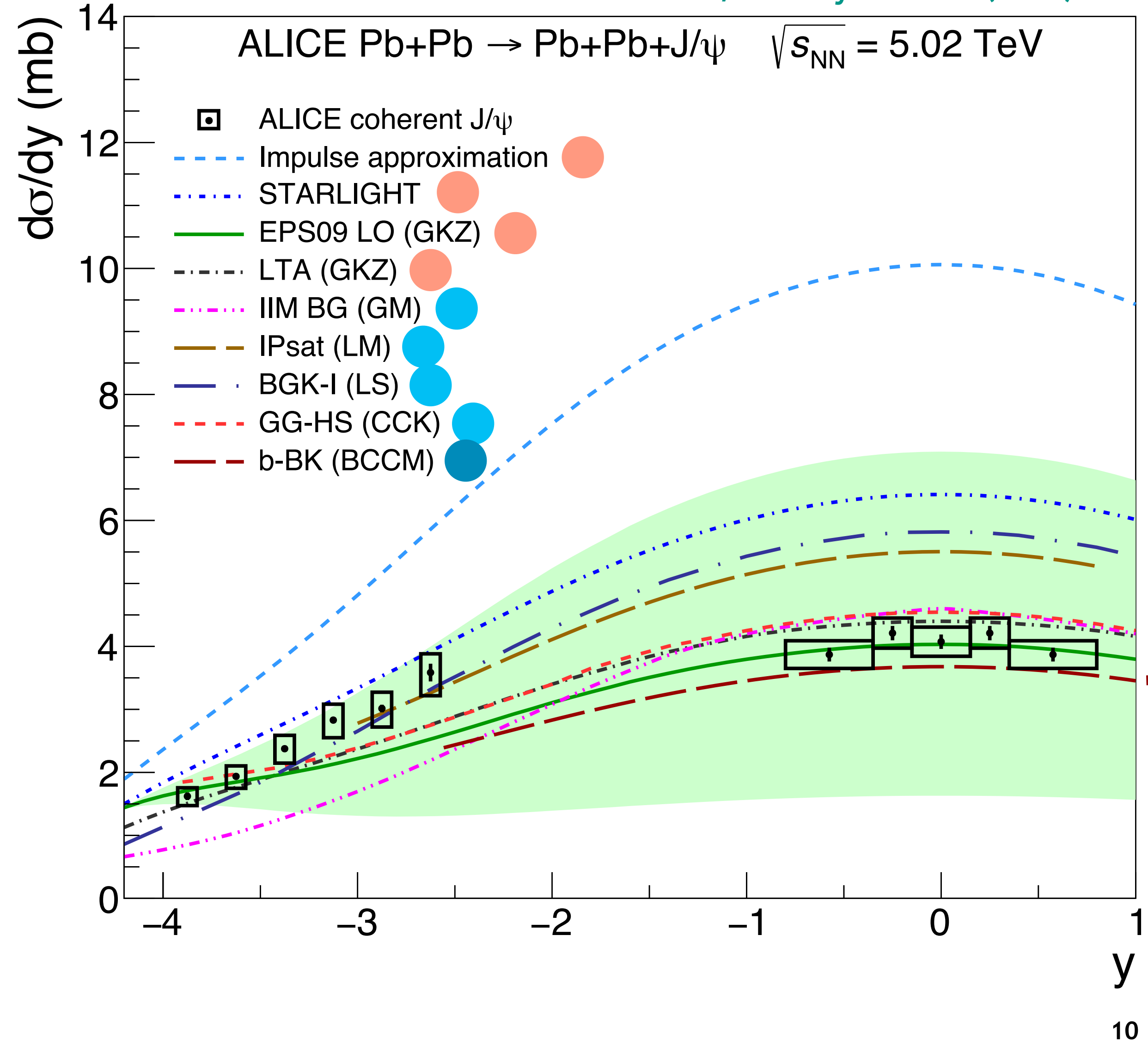
Includes the impact parameter dependence (and hot spots) but drops the DGLAP

$$\sigma_{\text{dip-A}} = 2 \left[ 1 - \exp \left( -\frac{1}{2} \sigma_{\text{dip}}(x, r) T_A(b) \right) \right]$$

$$\sigma_{\text{dip}}(x, r) = \sigma_0 \left[ 1 - \exp(-r^2 Q_s^2(x)/4) \right]$$

# Coherent $J/\psi$ production

ALICE Collaboration, Eur. Phys. J. C 81 (2021) 712



## b-BK (BCCM)

Dipole model including impact parameter dependent BK evolution  
 D.Bendova, J. Cepila, J. G. Contreras, M. Matas  
 Phys.Lett.B 817 (2021) 136306

$$\mathcal{A}_{T,L}(x, Q^2, \vec{\Delta}) = i \int d\vec{r} \int_0^1 \frac{dz}{4\pi} \int d\vec{b} |\Psi_V^* \Psi_{\gamma^*}|_{T,L} \exp \left[ -i \left( \vec{b} - (1-z)\vec{r} \right) \cdot \vec{\Delta} \right] \frac{d\sigma^{q\bar{q}}}{d\vec{b}}$$

$$\frac{d\sigma^{q\bar{q}}}{d\vec{b}} = 2N(\vec{r}, \vec{b}; x)$$

dipole scattering amplitude (solution to the BK equation)

# Leading twist shadowing

L. Frankfurt, V. Guzey, M. Strikman, M. Zhalov  
 JHEP 0308:043,2003

Make use of QCD factorization theorem for the hard diffractive scattering

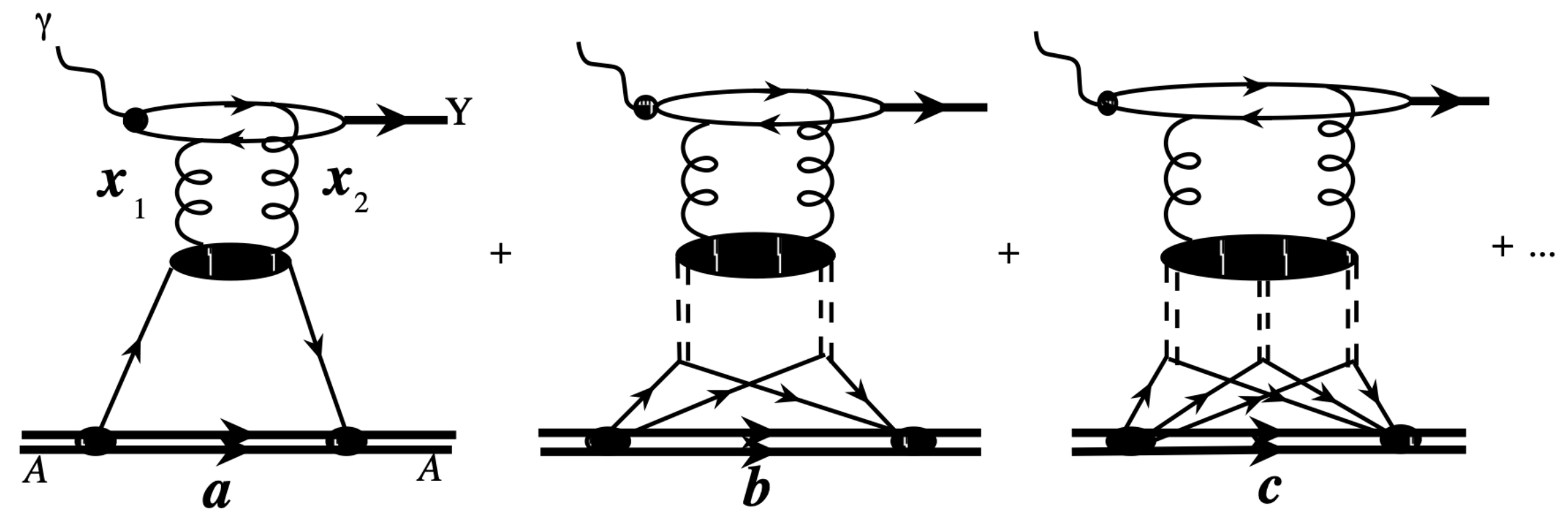


Figure 1: High energy quarkonium photoproduction in the leading twist approximation.

Amplitude is the convolution of the wave function of the meson at the zero transverse separation between the quark and antiquark, the hard interaction block, and the generalized parton distribution (GPD) of the target,  $g_T(x_1, x_2, Q^2, t_{\min})$  approximated by  $g_A(x = (x_1 + x_2)/2)$

$$\begin{aligned} \sigma_{\gamma A \rightarrow V A}(W_{\gamma p}) &= C_A(\mu^2) [\alpha_s(\mu^2) x g_A(x, \mu^2)]^2 \Phi_A(t_{\min}) \\ &= \frac{C_A(\mu^2)}{C_p(\mu^2)} \frac{d\sigma_{\gamma p \rightarrow V p}(W_{\gamma p}, t=0)}{dt} \left[ \frac{x g_A(x, \mu^2)}{A x g_p(x, \mu^2)} \right]^2 \Phi_A(t_{\min}) \end{aligned}$$

with the nuclear gluon density distribution

$$g_A(x, \mu^2) = A g_p(x, \mu^2) - 8\pi \Re \left[ \frac{(1-i\eta)^2}{1+\eta^2} \int d^2b \int_{-\infty}^{\infty} dz_1 \int_{-\infty}^{\infty} dz_2 \int_x^{x_{\mathbb{P}}^0} dx_{\mathbb{P}} g_N^D(x/x_{\mathbb{P}}, x_{\mathbb{P}}, \mu^2, t_{\min}) \rho_A(\vec{b}, z_1) \rho_A(\vec{b}, z_2) e^{ix_{\mathbb{P}} m_N (z_1 - z_2)} e^{-\frac{1}{2} \sigma_{\text{eff}}(x, \mu^2) (1-i\eta) \int_{z_1}^{z_2} dz \rho_A(\vec{b}, z)} \right]$$

and  $\Phi_A(t_{\min}) = \int_{-\infty}^{t_{\min}} dt |F_A(t)|^2$

inelastic shadowing via phase shifts

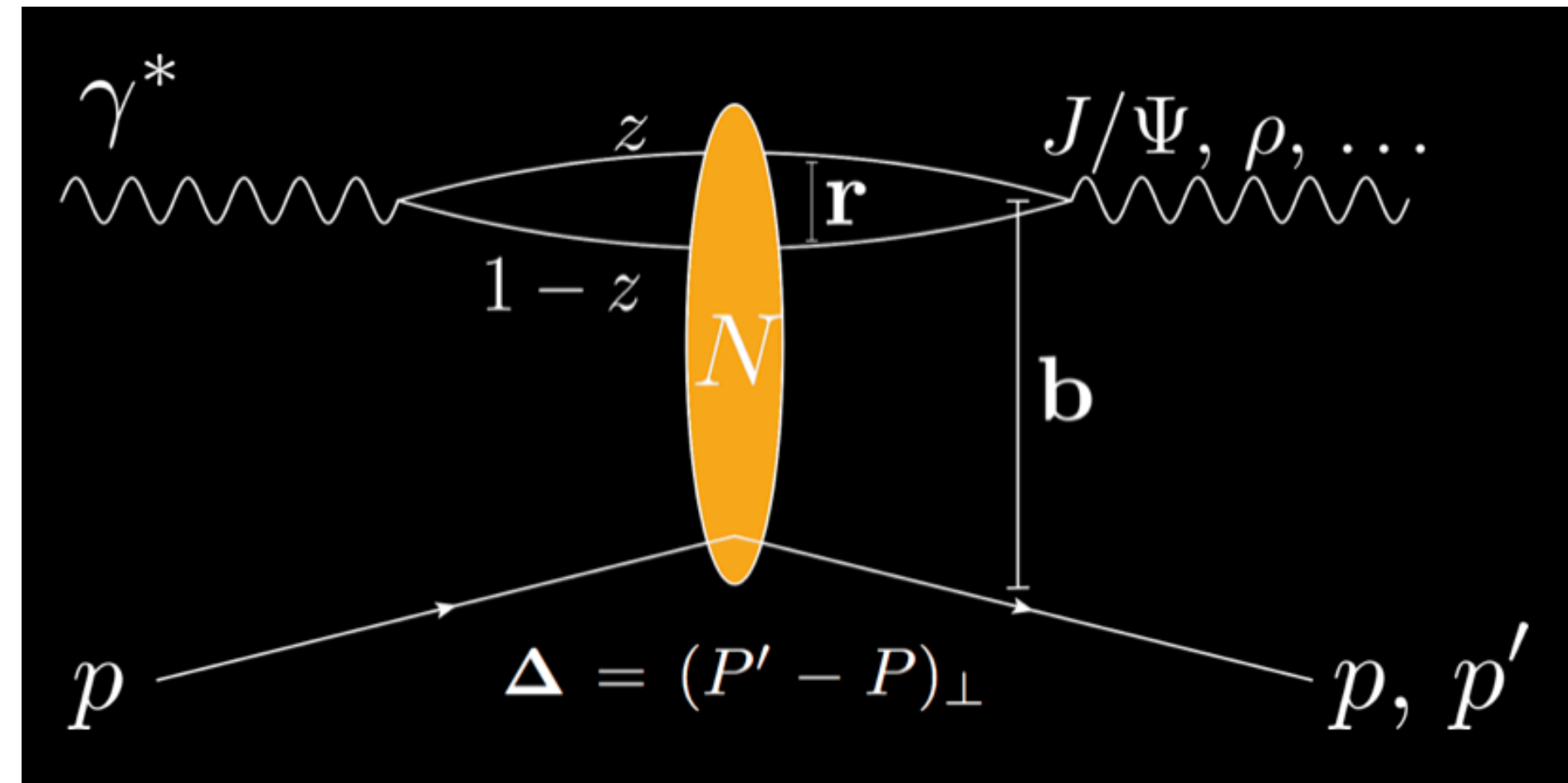
interaction with 3 or more nucleons  
 "attenuation factor"

# Dipole picture

H. Mäntysaari, B. Schenke, Phys. Rev. Lett. 117 (2016) 052301; Phys.Rev. D94 (2016) 034042

High energy factorization:

- $\gamma^* \rightarrow q\bar{q} : \psi^\gamma(r, Q^2, z)$
- $q\bar{q}$  dipole scatters with amplitude  $N$
- $q\bar{q} \rightarrow V : \psi^V(r, Q^2, z)$



$$\mathcal{A}_{T,L}^{\gamma^* N \rightarrow V N}(x_{\mathbb{P}}, Q^2, \mathbf{\Delta}) = i \int d^2\mathbf{r} \int d^2\mathbf{b} \int \frac{dz}{4\pi} \\ \times (\Psi^* \Psi_V)_{T,L}(Q^2, \mathbf{r}, z) \\ \times e^{-i[\mathbf{b} - (\frac{1}{2} - z)\mathbf{r}] \cdot \mathbf{\Delta}} 2N(\mathbf{b}, \mathbf{r}, x_{\mathbb{P}}).$$

$$\frac{d\sigma^{q\bar{q}}}{d\vec{b}} = 2N(\vec{r}, \vec{b}; x)$$

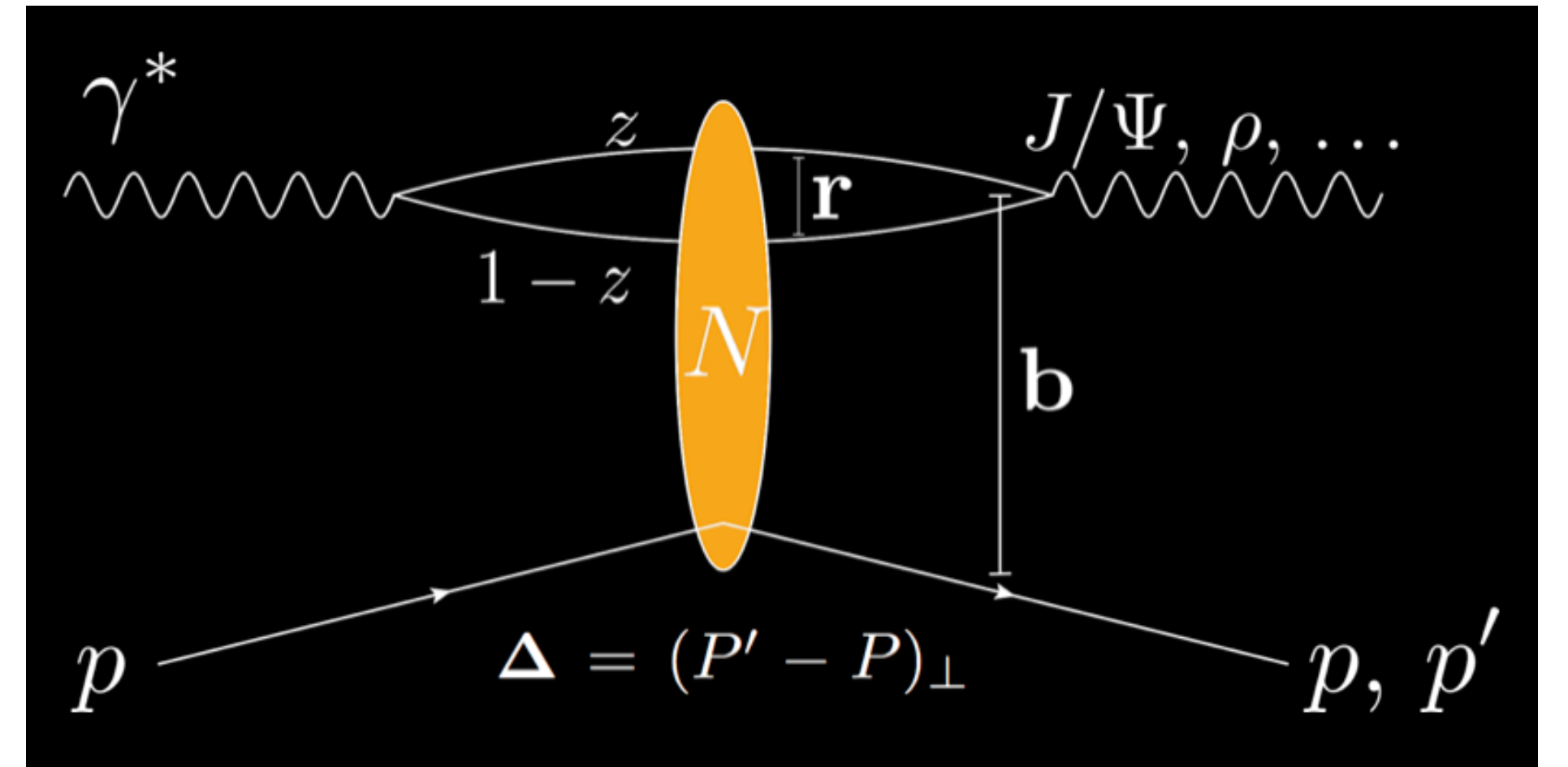
- Impact parameter  $\mathbf{b}$  is the Fourier conjugate of transverse momentum transfer  $\mathbf{\Delta} \rightarrow$   
**Access to spatial structure** ( $t = -\Delta^2$ )

# Color glass condensate formalism

H. Mäntysaari, B. Schenke, Phys. Rev. Lett. 117 (2016) 052301; Phys.Rev. D94 (2016) 034042

Compute the Wilson lines using color charges whose correlator depends on  $\vec{b}_\perp$  (for example using MV model):

$$\langle \rho^a(\mathbf{b}_\perp) \rho^b(\mathbf{x}_\perp) \rangle = g^2 \mu^2(x, \mathbf{b}_\perp) \delta^{ab} \delta^{(2)}(\mathbf{b}_\perp - \mathbf{x}_\perp)$$



$$N(\vec{r}, x, \vec{b}) = N(\vec{x} - \vec{y}, x, (\vec{x} + \vec{y})/2) = 1 - \text{Tr}(\mathbf{V}(\vec{x}) \mathbf{V}^\dagger(\vec{y})) / N_c$$

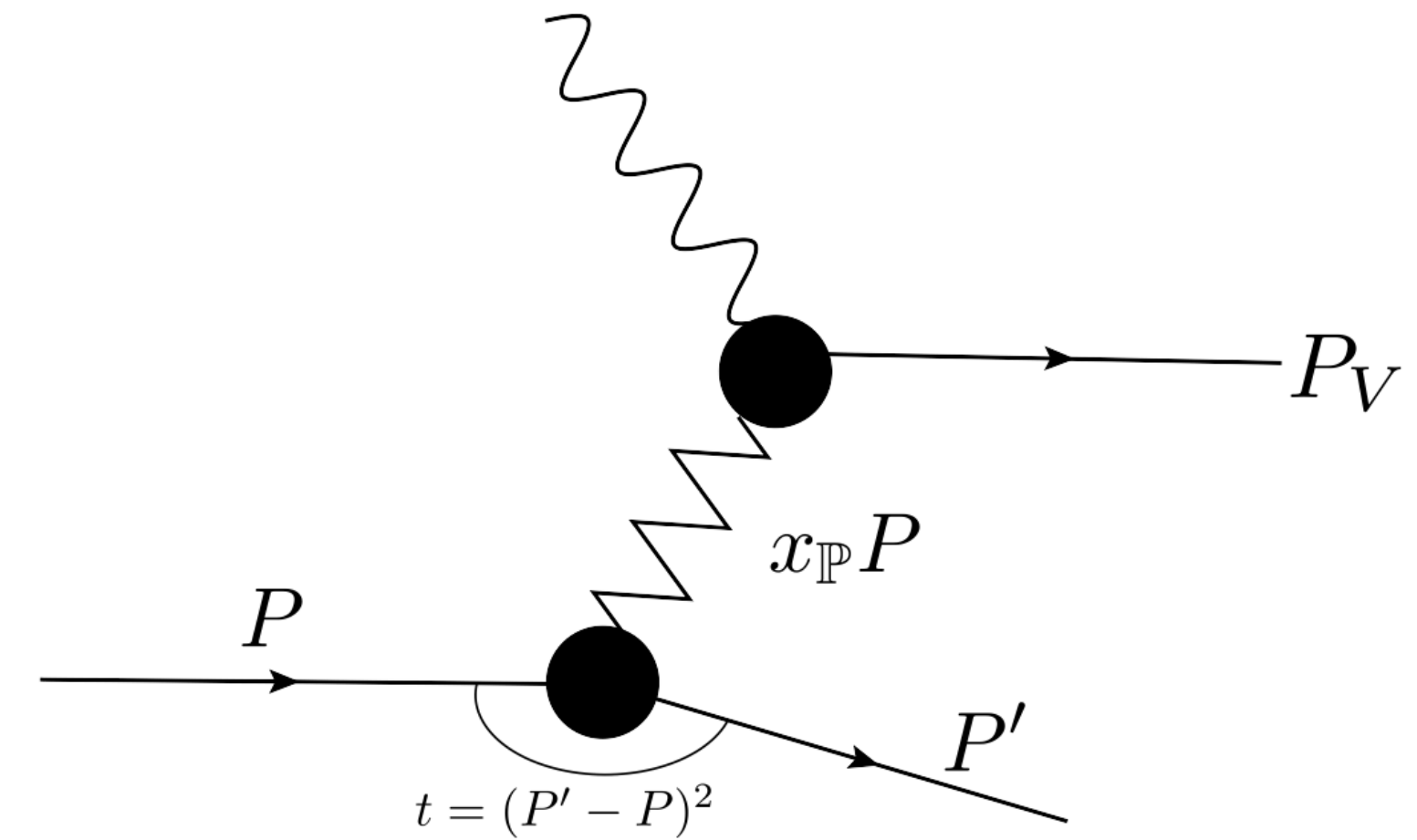
The trace appears at the level of the amplitude, because we project on a **color singlet**

$$A \sim \int d^2b dz d^2r \psi^* \psi^V(\vec{r}, z, Q^2) e^{-i(\vec{b} - (\frac{1}{2} - z)\vec{r}) \cdot \vec{\Delta}} N(\vec{r}, x, \vec{b})$$

# Diffractive vector meson production

— Coherent diffraction: 
$$\frac{d\sigma^{\gamma^*p \rightarrow Vp}}{dt} = \frac{1}{16\pi} \left| \left\langle A^{\gamma^*p \rightarrow Vp} \left( x_P, Q^2, \vec{\Delta} \right) \right\rangle \right|^2$$

sensitive to the average size of the target



— Incoherent diffraction: 
$$\frac{d\sigma^{\gamma^*p \rightarrow Vp^*}}{dt} = \frac{1}{16\pi} \left( \left\langle \left| A^{\gamma^*p \rightarrow Vp} \left( x_P, Q^2, \vec{\Delta} \right) \right|^2 \right\rangle - \left| \left\langle A^{\gamma^*p \rightarrow Vp} \left( x_P, Q^2, \vec{\Delta} \right) \right\rangle \right|^2 \right)$$

sensitive to fluctuations (including geometric ones)

H. Kowalski, L. Motyka, G. Watt, Phys.Rev. D 74 (2006) 074016

A. Caldwell, H. Kowalski, EDS 09, 190-192, e-Print: 0909.1254 [hep-ph]

M. L. Good and W. D. Walker, Phys. Rev. 120 (1960) 1857

H. I. Miettinen and J. Pumplin, Phys. Rev. D18 (1978) 1696

Y. V. Kovchegov and L. D. McLerran, Phys. Rev. D60 (1999) 054025

A. Kovner and U. A. Wiedemann, Phys. Rev. D64 (2001) 114002

# CGC calculation: Model impact parameter dependence (in nucleons)

H. Mäntysaari, B. Schenke, Phys. Rev. Lett. 117 (2016) 052301; Phys.Rev. D94 (2016) 034042

1) Assume Gaussian proton shape:

$$T(\vec{b}) = T_p(\vec{b}) = \frac{1}{2\pi B_p} e^{-b^2/(2B_p)}$$

2) Assume a substructure of the nucleon. For example Gaussian distributed and Gaussian shaped hot spots:

$$P(b_i) = \frac{1}{2\pi B_{qc}} e^{-b_i^2/(2B_{qc})} \quad (\text{angles uniformly distributed})$$

$$T_p(\vec{b}) = \frac{1}{N_q} \sum_{i=1}^{N_q} T_q(\vec{b} - \vec{b}_i) \quad \text{with } N_q \text{ hot spots;} \quad T_q(\vec{b}) = \frac{1}{2\pi B_q} e^{-b^2/(2B_q)}$$

# Diffractive $J/\psi$ production in e+p at HERA

Nucleon parameters  $B_{q'}$ ,  $B_{qc'}$  can be constrained by e+p scattering data from HERA

Exclusive diffractive  $J/\psi$  production in e+p:

Incoherent x-sec sensitive to fluctuations

H. Mäntysaari, B. Schenke, Phys. Rev. Lett. 117 (2016) 052301

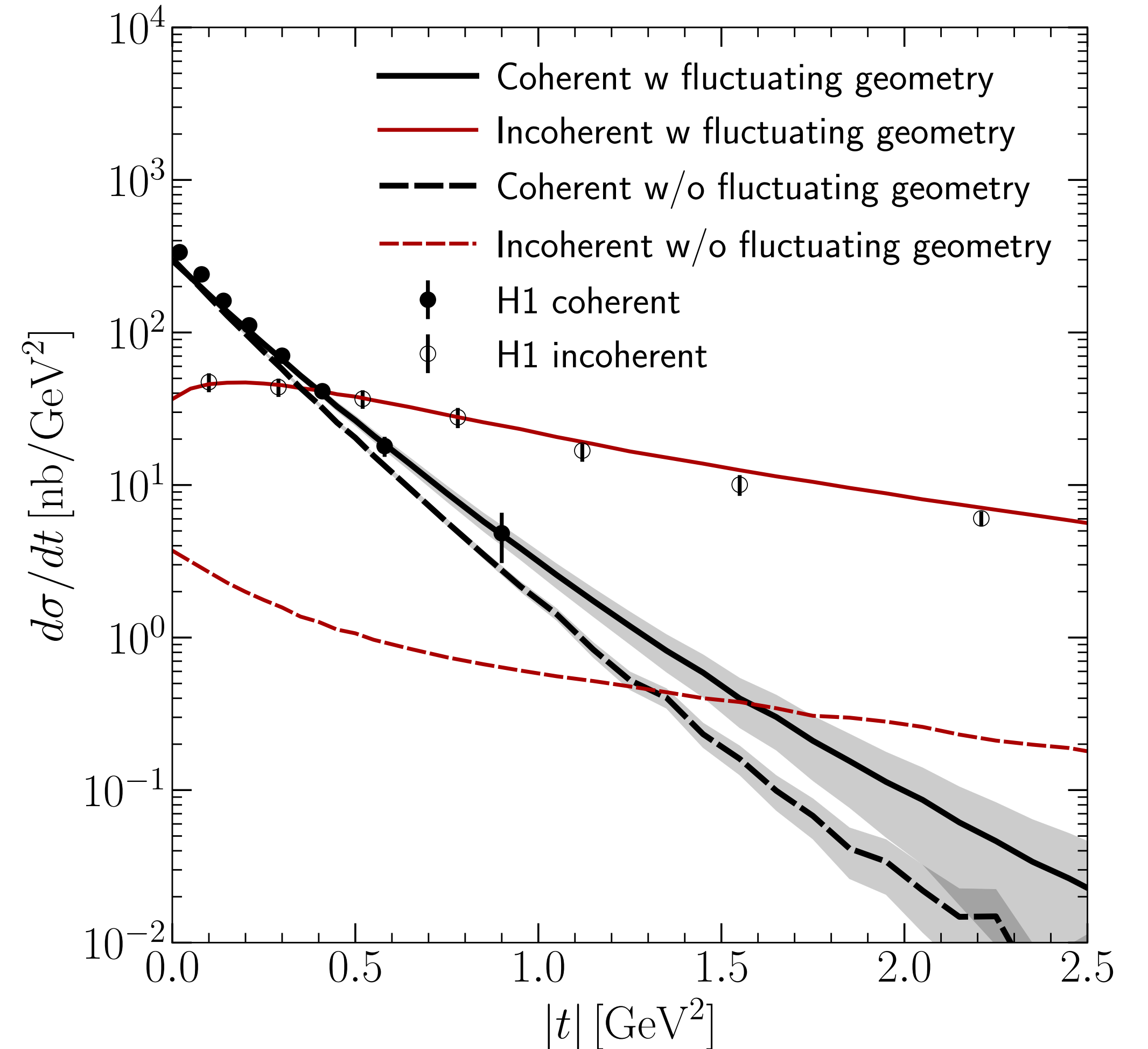
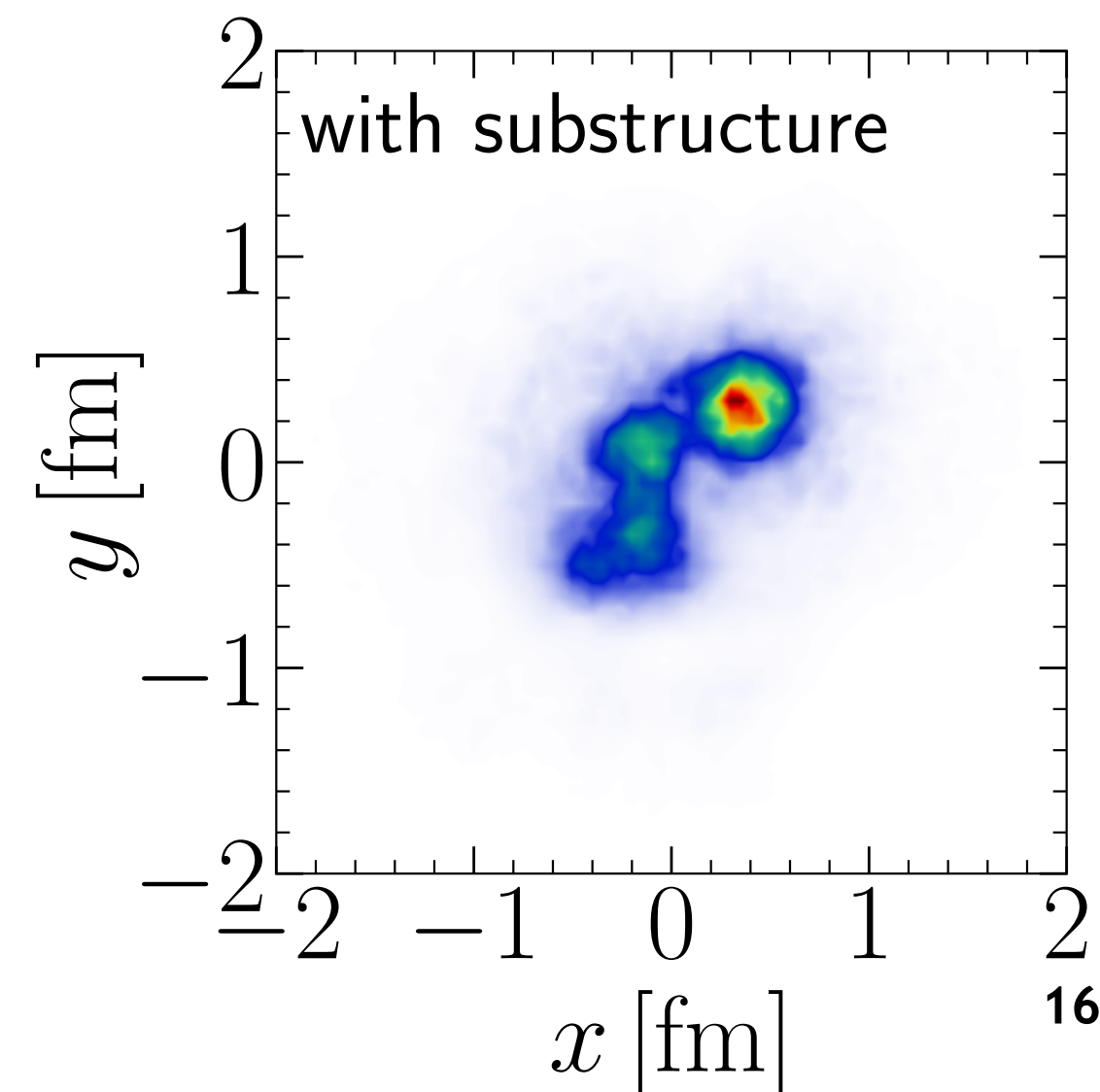
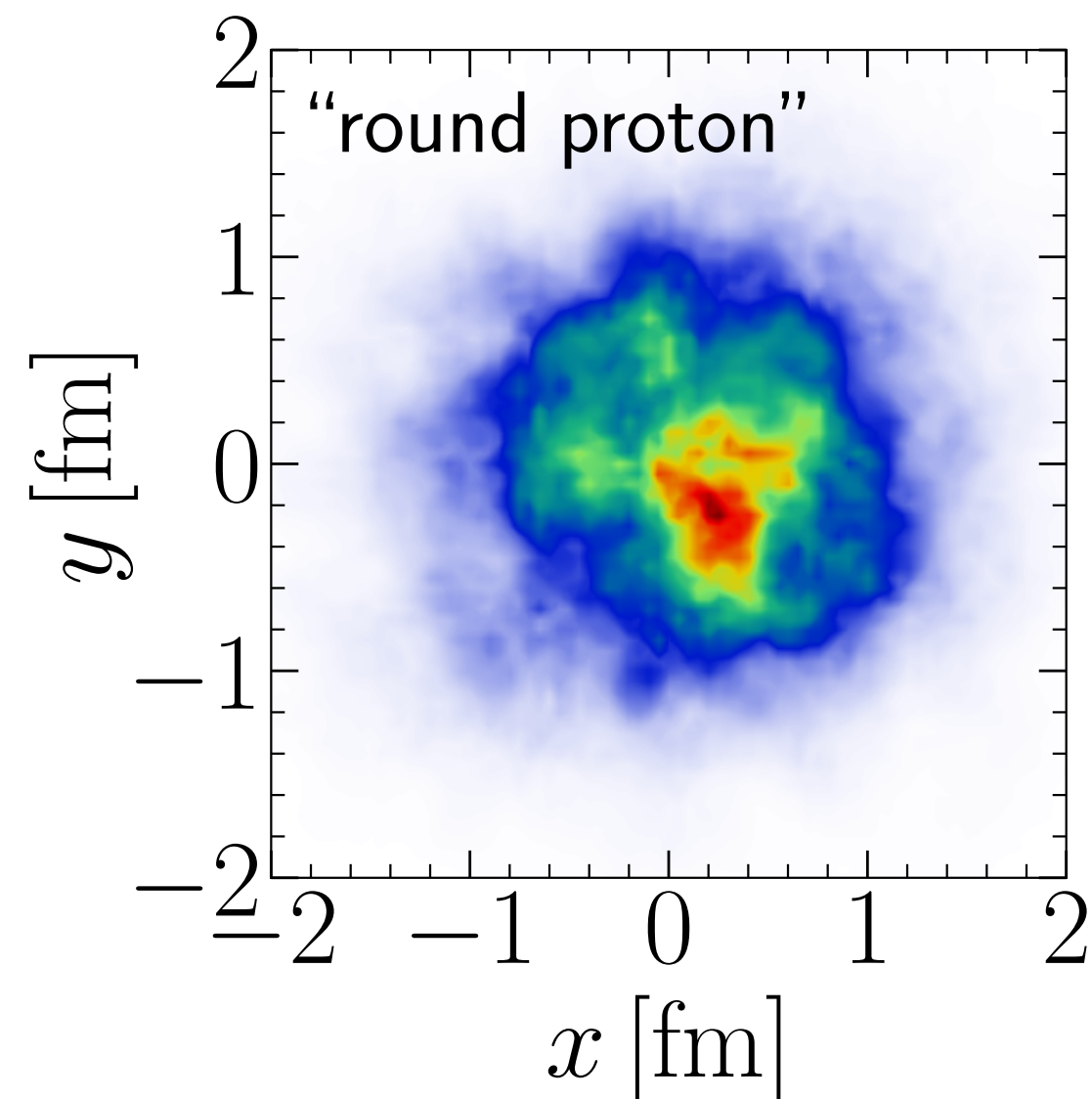
Phys.Rev. D94 (2016) 034042

also see:

S. Schlichting, B. Schenke, Phys.Lett. B739 (2014) 313-319

H. Mäntysaari, Rep. Prog. Phys. 83 082201 (2020)

B. Schenke, Rep. Prog. Phys. 84 082301 (2021)



H1 Collaboration, Eur. Phys. J. C73 (2013) no. 6 2466



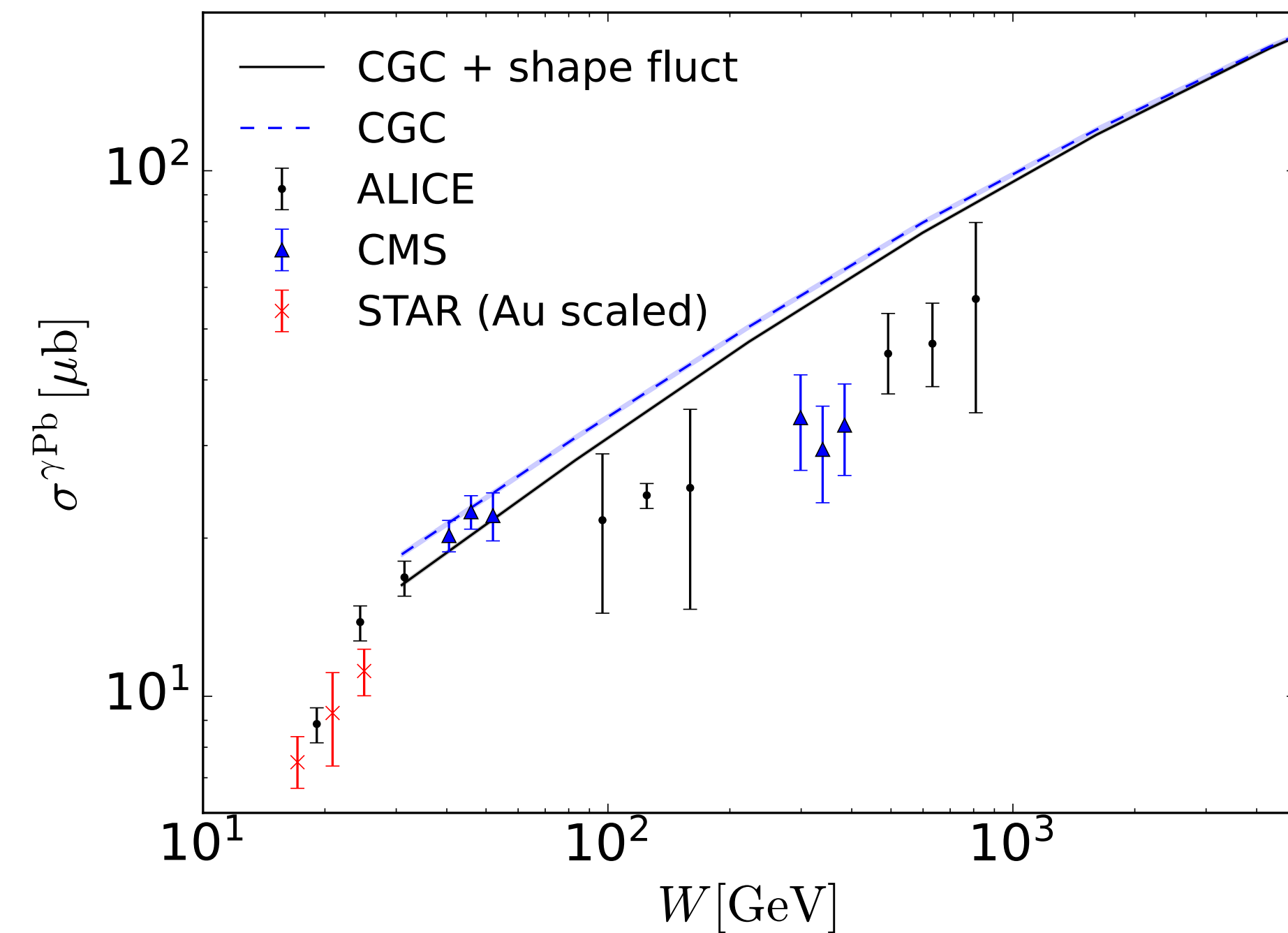
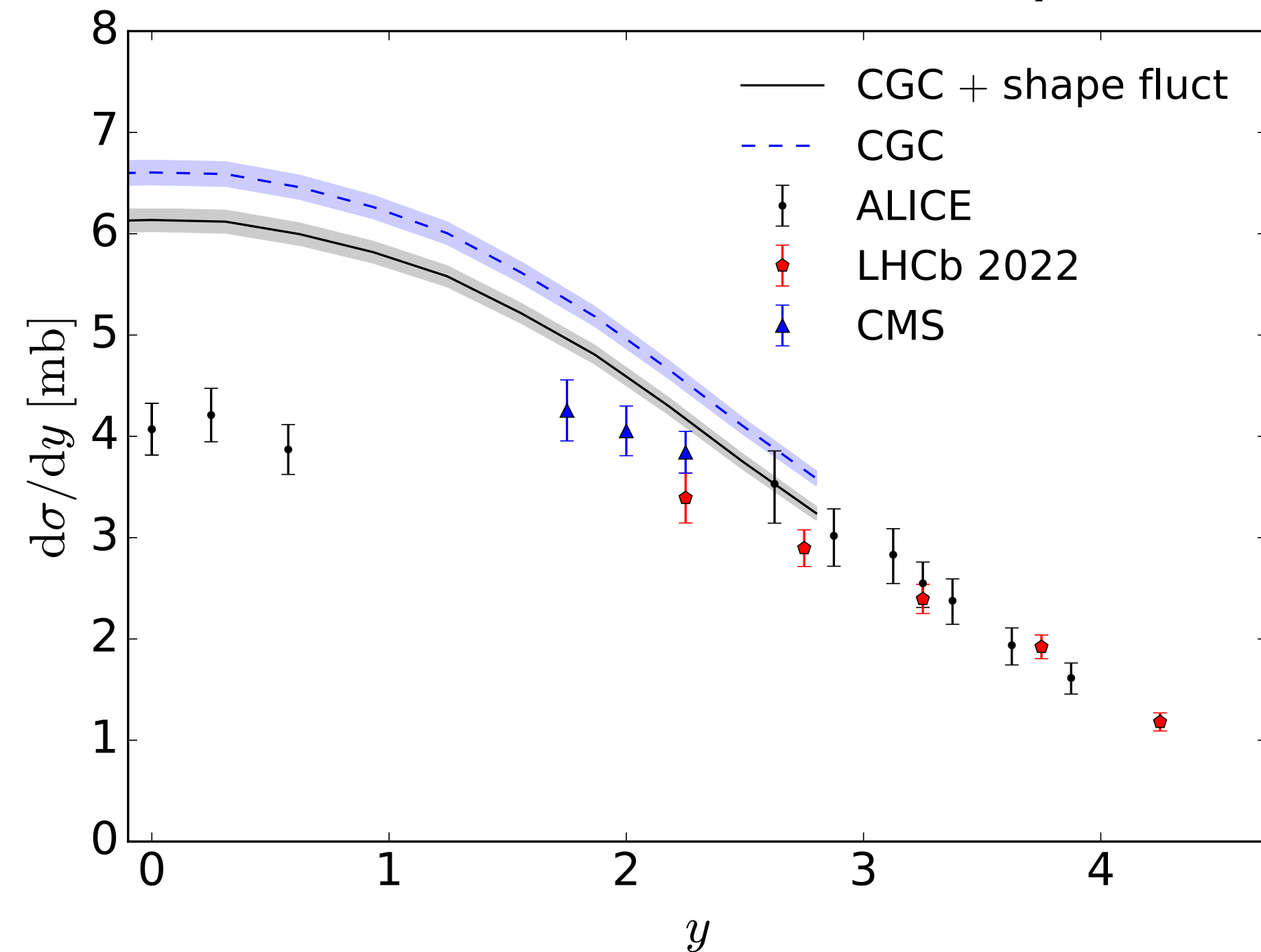
# Back to UPCs: Coherent cross section

H. Mäntysaari, F. Salazar, B. Schenke, *Phys.Rev.D* 106 (2022) 7, 074019 and [arXiv:2312.04194](https://arxiv.org/abs/2312.04194)

Calculation is constrained by HERA  $J/\psi$  production data

$$\text{Pb+Pb} \rightarrow \text{Pb+Pb+}J/\psi$$

$$\gamma+\text{Pb} \rightarrow J/\psi + \text{Pb}$$



Larger suppression when including shape fluctuations: Hotter hot spots; larger local  $Q_s$

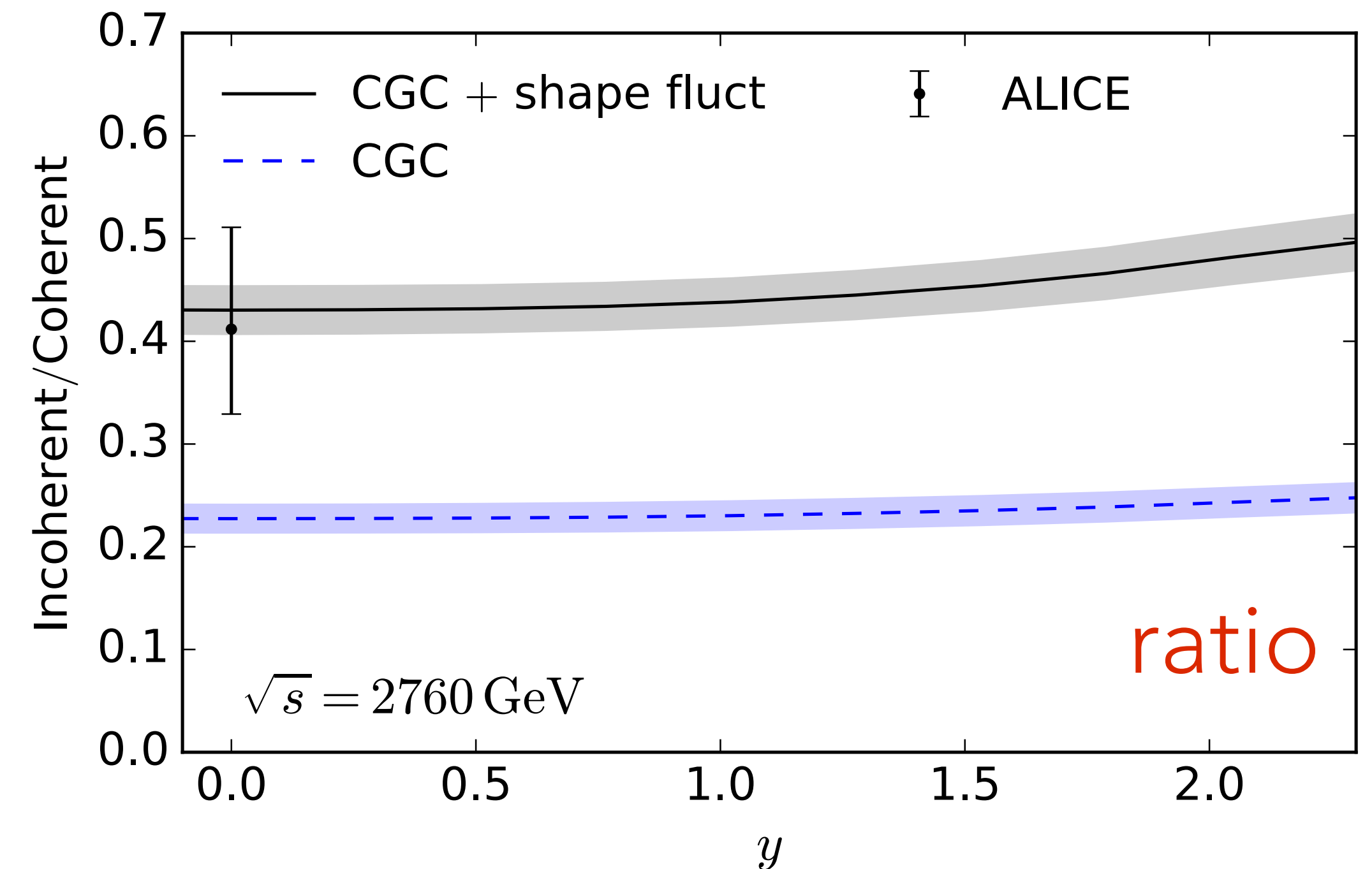
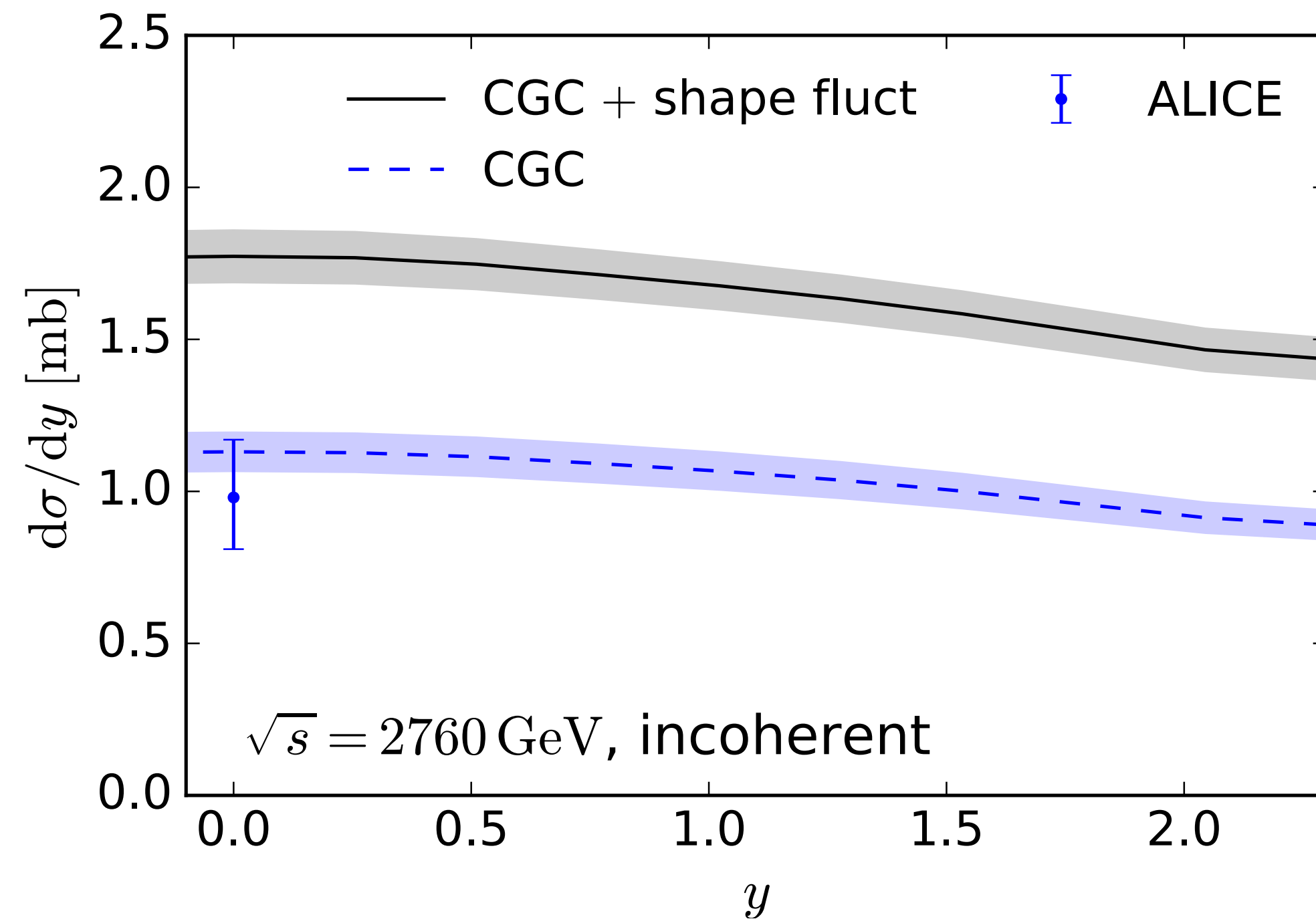
ALICE Collaboration, S. Acharya et. al., *Eur. Phys. J. C*81 (2021) no. 8 712 [[arXiv:2101.04577](https://arxiv.org/abs/2101.04577)]

CMS Collaboration, A. Tumasyan et. al., [arXiv:2303.16984](https://arxiv.org/abs/2303.16984)

LHCb Collaboration, R. Aaij et. al., *JHEP* 06 146 (2023) [[arXiv:2206.08221](https://arxiv.org/abs/2206.08221)]

# Incoherent cross section

H. Mäntysaari, F. Salazar, B. Schenke, Phys.Rev.D 106 (2022) 7, 074019



More fluctuations when including shape fluctuations  $\rightarrow$  larger incoherent cross section  
Ratio of coherent to incoherent well described (both coh. and incoh. overestimated)

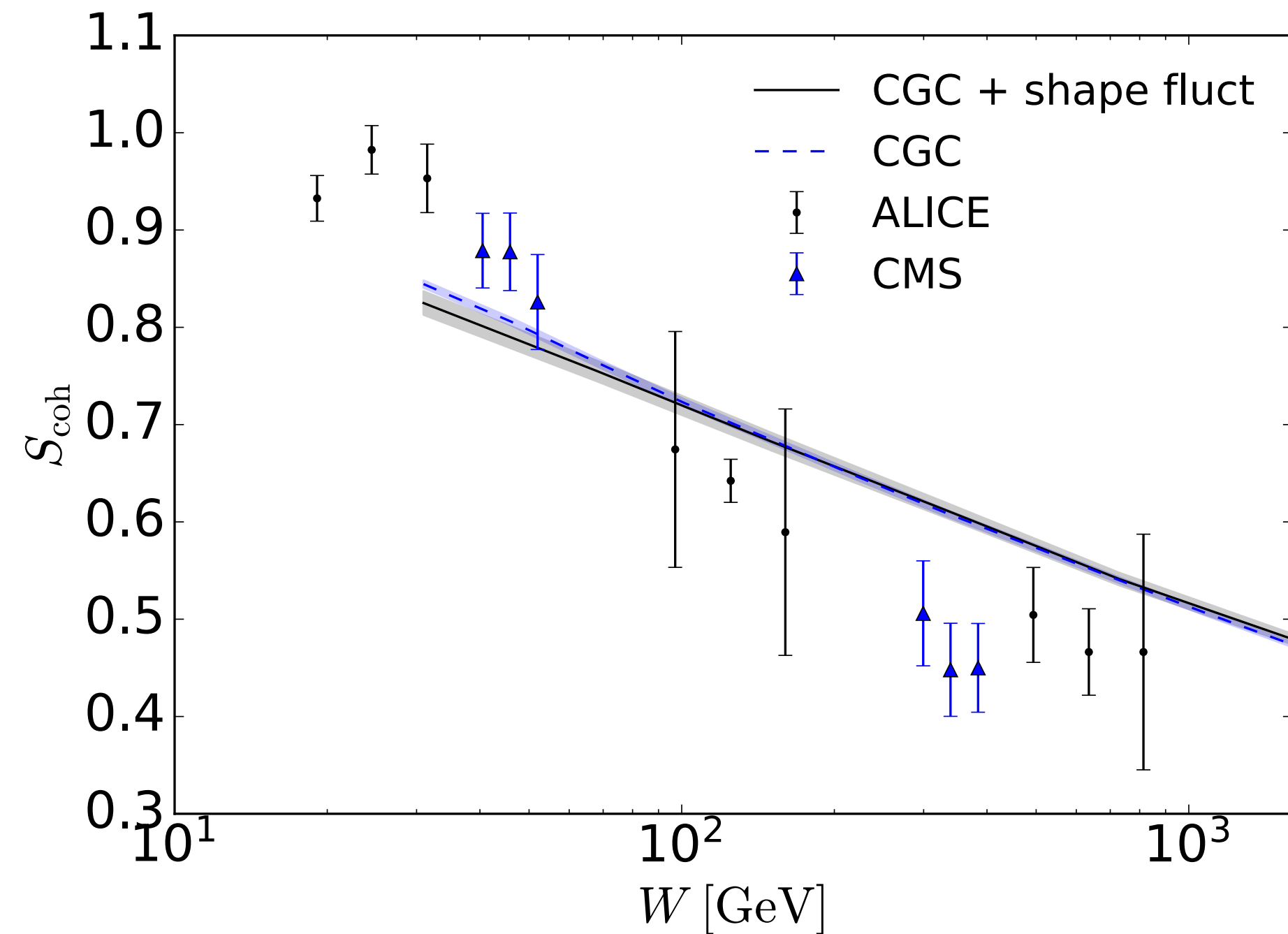
ALICE Eur. Phys. J. C73 (2013) no. 11 2617

# Nuclear suppression

H. Mäntysaari, F. Salazar, B. Schenke, [arXiv:2312.04194](https://arxiv.org/abs/2312.04194)

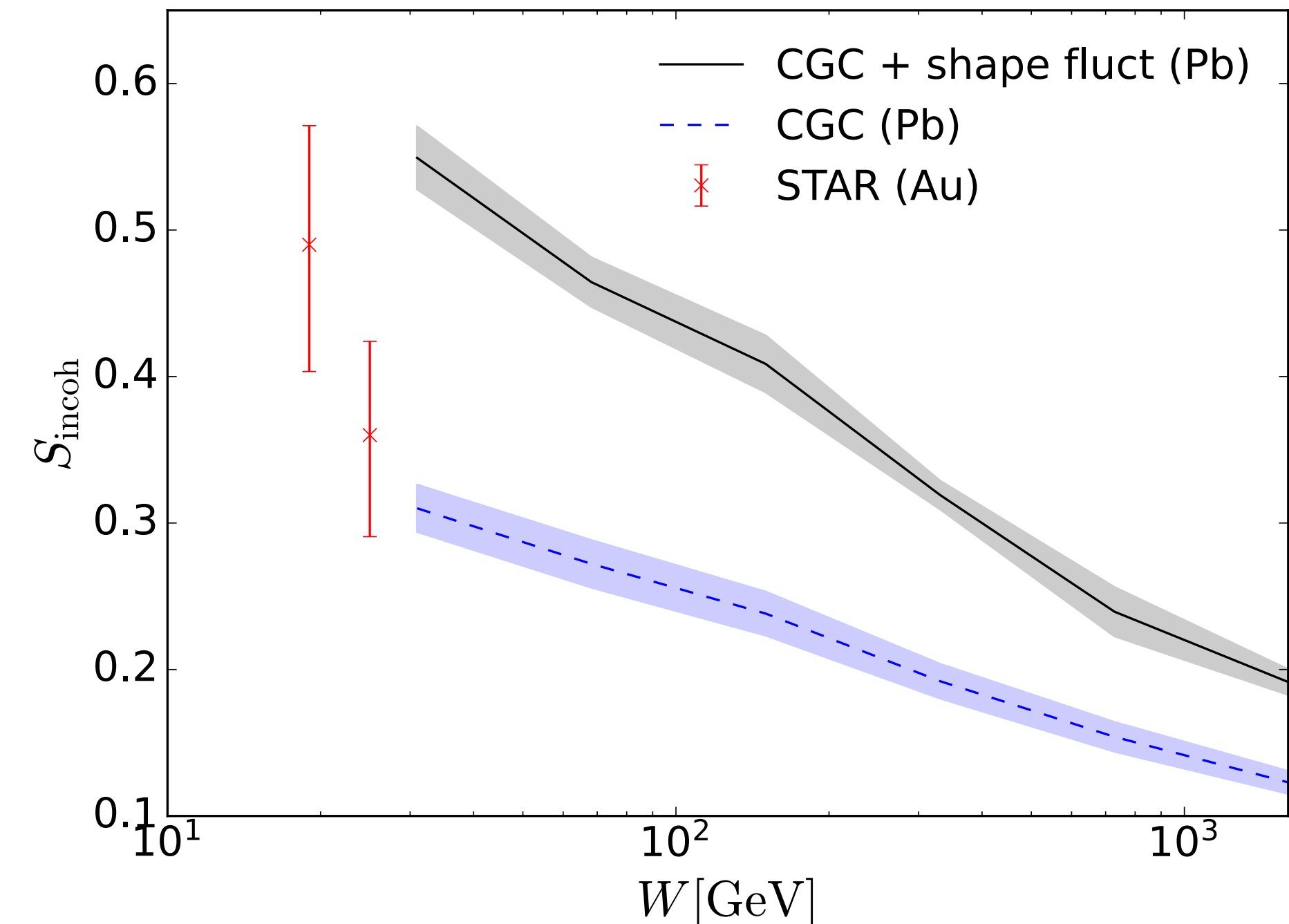
$$S_{\text{coh}} = \sqrt{\frac{\sigma^{\gamma A}}{\sigma^{\text{IA}}}} \quad \sigma^{\text{IA}} = \frac{d\sigma^{\gamma p}}{dt}(t=0) \int_{-t_{\text{min}}} dt |F(t)|^2$$

Coherent



$$S_{\text{incoh}} = \frac{\sigma^{\gamma+A \rightarrow J/\psi+A^*}}{A(\sigma^{\gamma+p \rightarrow J/\psi+p^*} + \sigma^{\gamma+p \rightarrow J/\psi+p})}$$

Incoherent



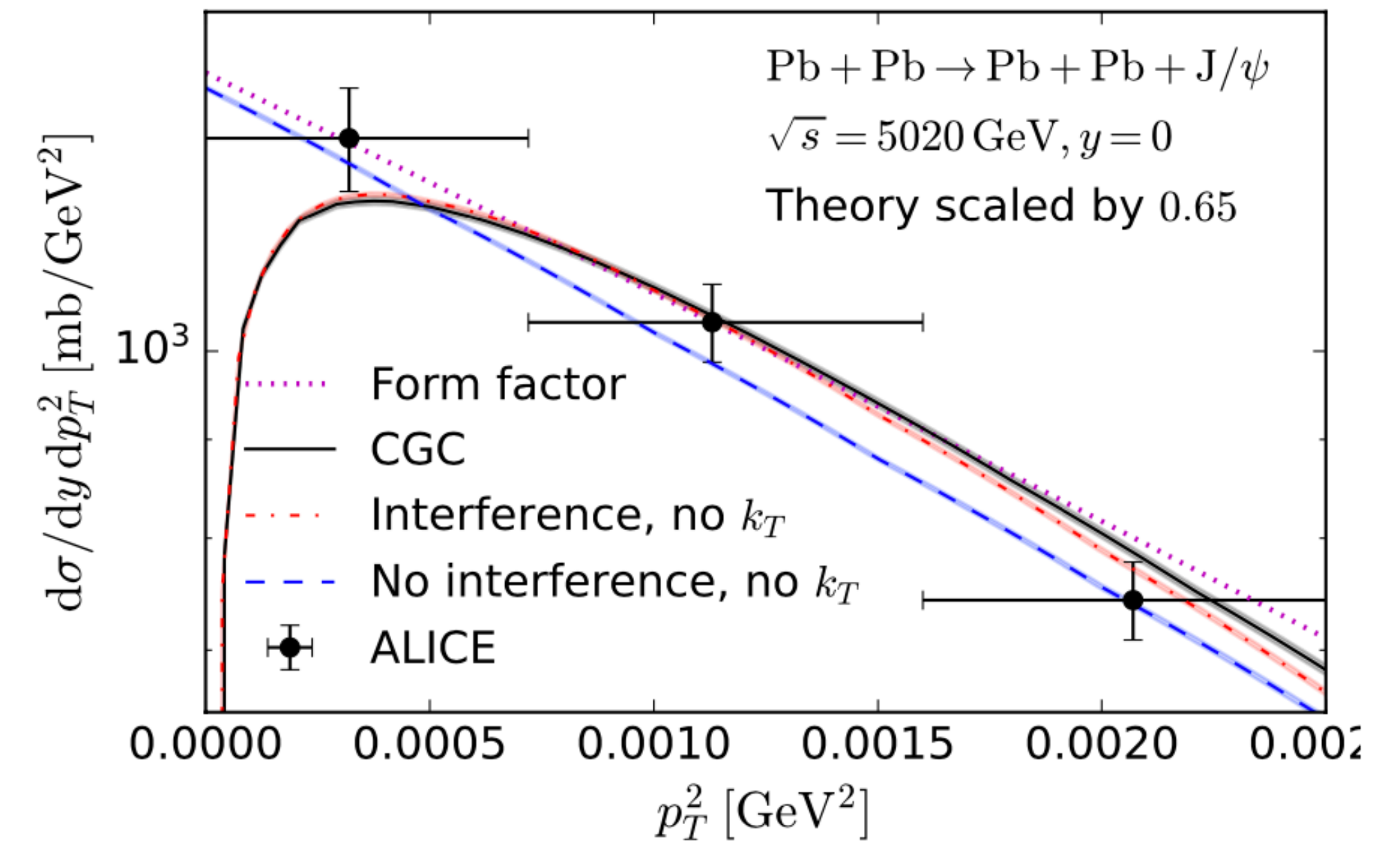
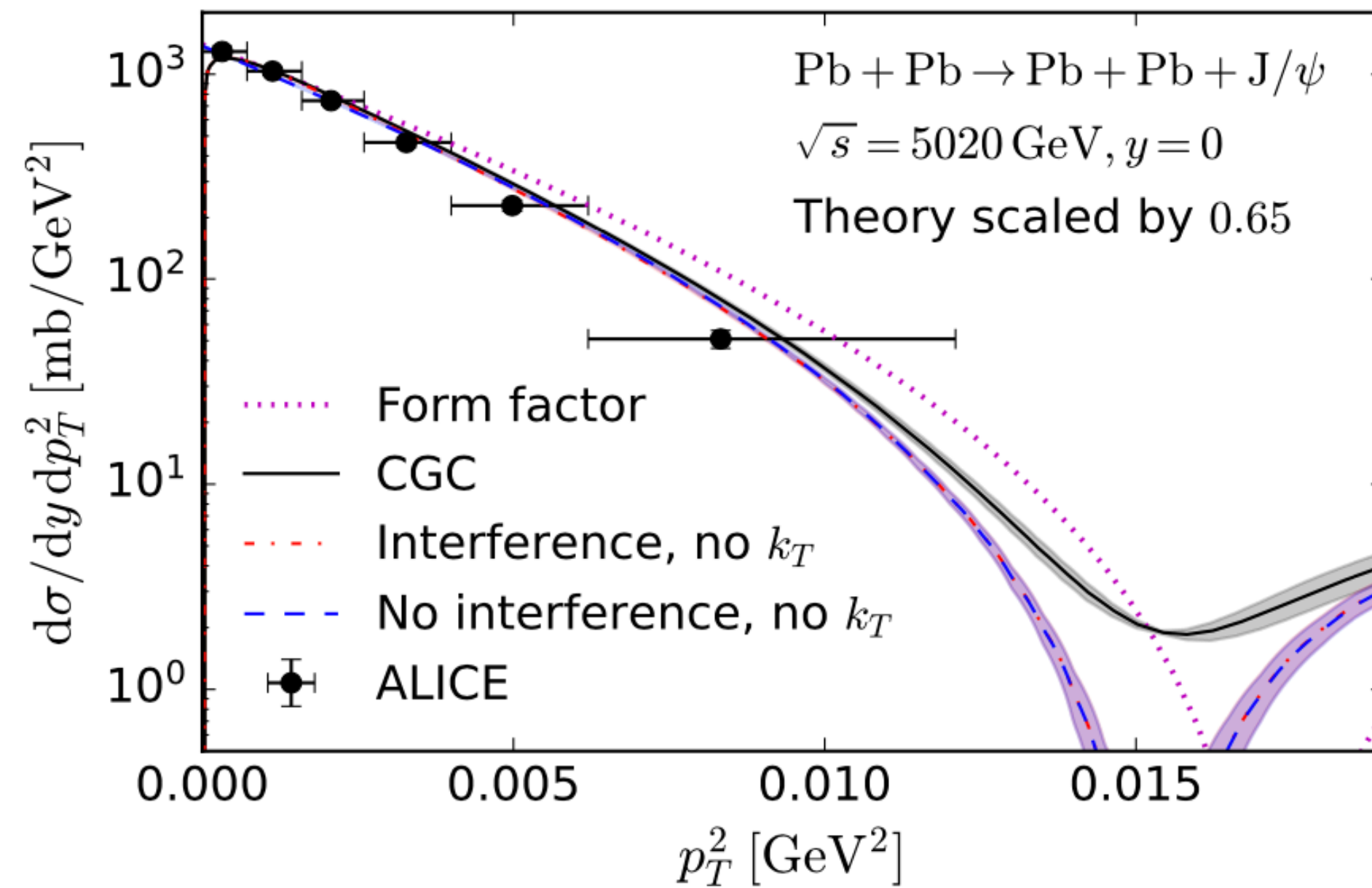
CMS Collaboration, A. Tumasyan et. al., [arXiv:2303.16984](https://arxiv.org/abs/2303.16984) [nucl-ex]

ALICE Collaboration, S. Acharya et al, *JHEP* 10 119 (2023) [[arXiv:2305:19060](https://arxiv.org/abs/2305.19060)]

STAR Collaboration, [arXiv:2311.13637](https://arxiv.org/abs/2311.13637) [nucl-ex]

# Pb+Pb UPCs at midrapidity

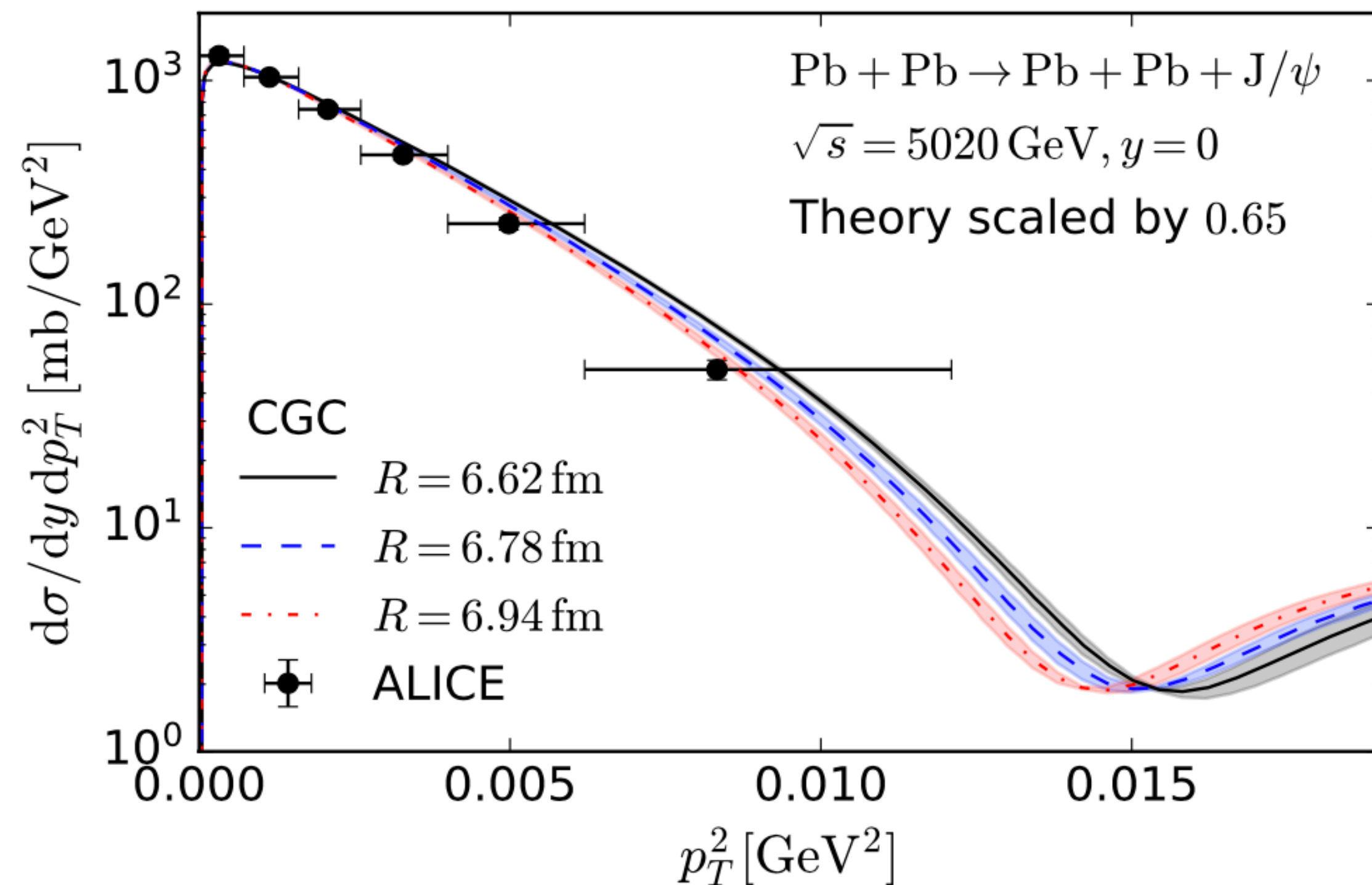
H. Mäntysaari, F. Salazar, B. Schenke, Phys.Rev.D 106 (2022) 7, 074019 ALICE Collaboration, Phys.Lett.B 817 (2021) 136280



- UPC: Photon  $k_T \leq 1/R_A \neq 0$ : important around dips, small effect on  $p_T$  integrated  $\sigma$
- Interference (both nuclei can emit  $\gamma$ ):  $d\sigma/dp_T^2 \rightarrow 0$  when  $p_T \rightarrow 0$   
Stronger effect predicted than seen in the ALICE data
- Calculated spectra not steep enough, although the ALICE  $\gamma + \text{Pb}$  data is well described  
 $\Rightarrow$  photon  $k_T$  effect included differently?
- Need a larger Pb than what we get with standard Woods-Saxon parameters

# Effect of the nuclear size

H. Mäntysaari, F. Salazar, B. Schenke, Phys.Rev.D 106 (2022) 7, 074019



- Steep enough spectrum obtained with a larger nucleus
- Neutron skin effect?

STAR measurements of diffractive photo production of  $\rho$  mesons and study of interference patterns in the angular distribution of  $\rho^0 \rightarrow \pi^+ \pi^-$  decays also indicate that strong-interaction nuclear radii of Au and U are larger than the charge radii  
[STAR Collaboration, 2204.01625](#)

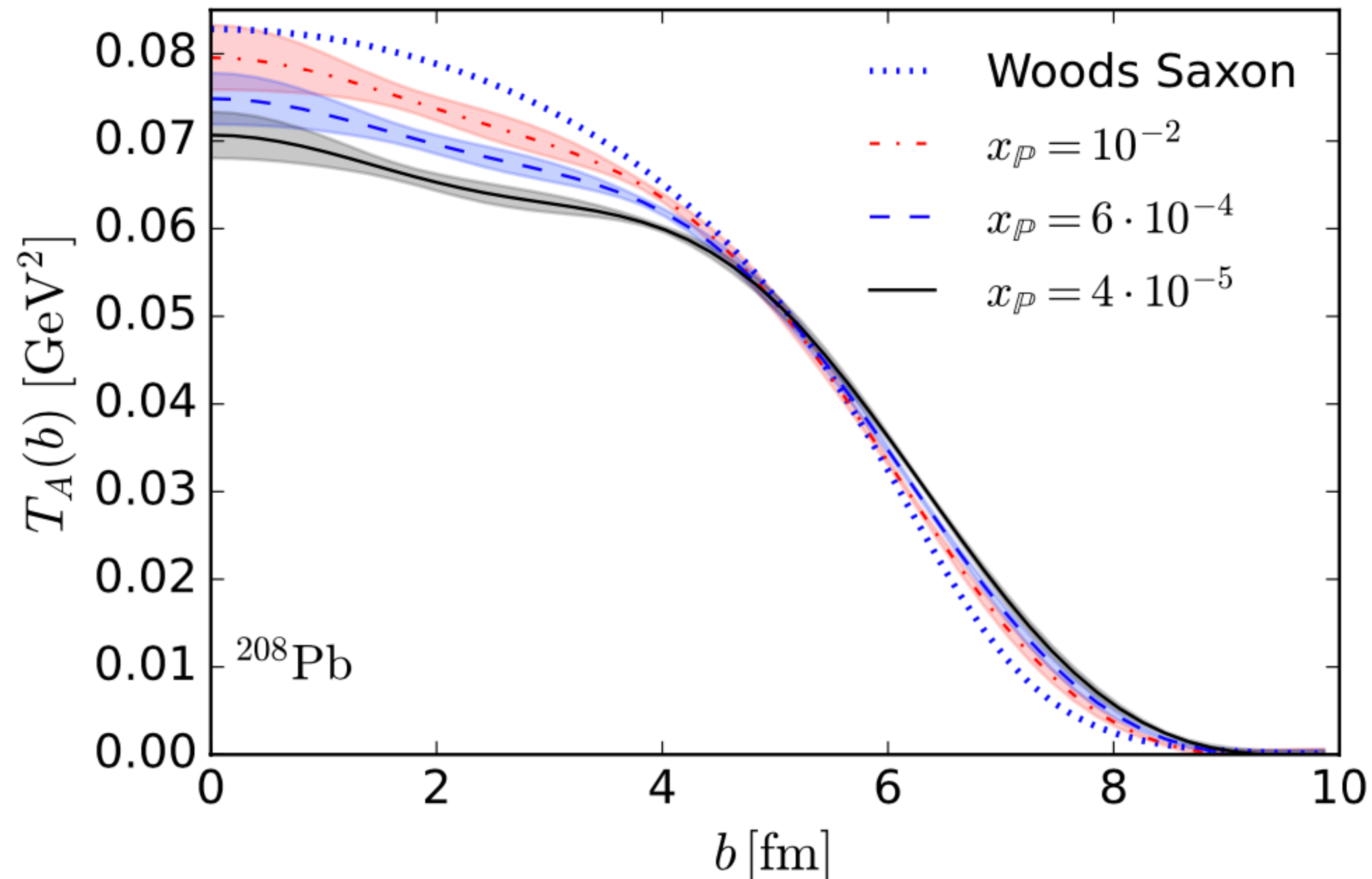
[ALICE Collaboration, Phys.Lett.B 817 \(2021\) 136280](#)

# Saturation effects on nuclear geometry

H. Mäntysaari, F. Salazar, B. Schenke, Phys.Rev.D 106 (2022) 7, 074019

Fourier transform to coordinate space

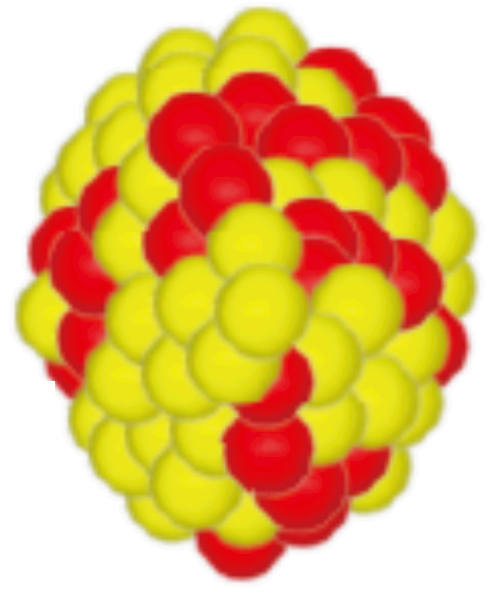
$$T_A(b) \propto \int \Delta d\Delta J_0(b\Delta) (-1)^n \sqrt{\frac{d\sigma^{\gamma^* + \text{Pb} \rightarrow \text{J}/\psi + \text{Pb}}}{d|t|}},$$



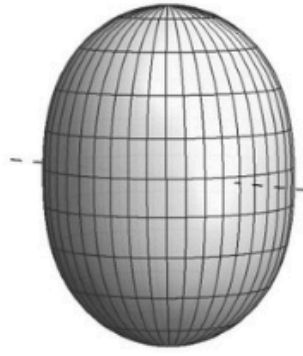
JIMWLK evolution leads to growth of the nucleus towards small  $x$  and depletion near the center (normalized so  $\int d^2b T_A(b) = 208$ )

# Effects of deformation on diffractive cross sections: Uranium

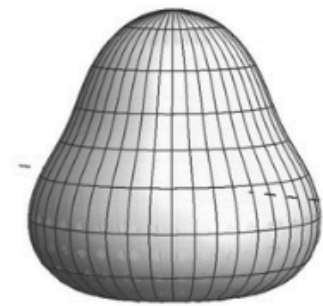
H. Mäntysaari, B. Schenke, C. Shen, W. Zhao, *Phys. Rev. Lett.* **131**, 062301 (2023)



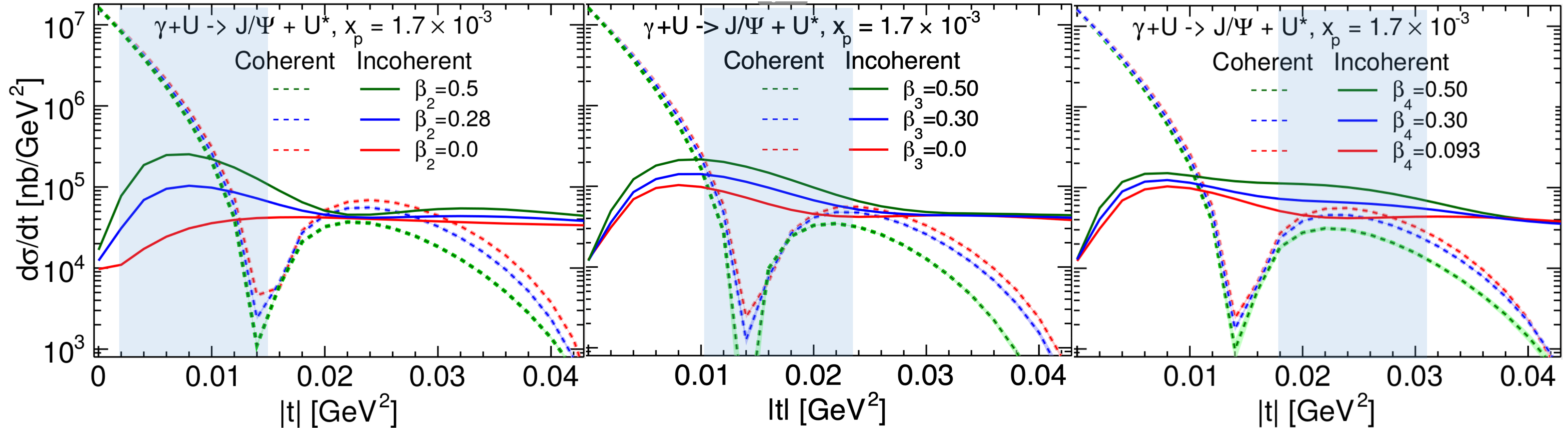
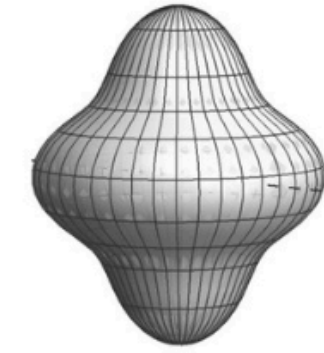
$\beta_2$



$\beta_3$



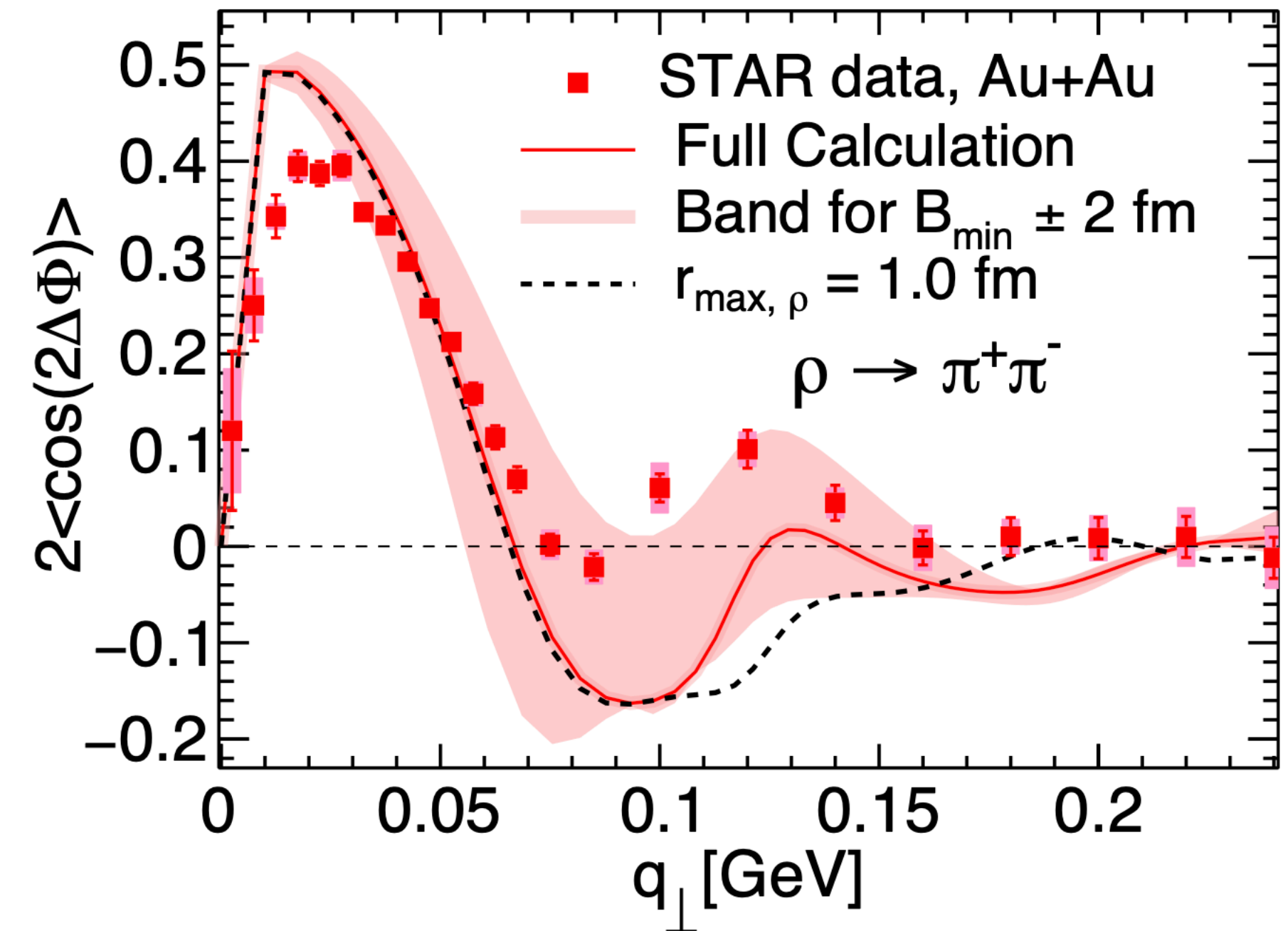
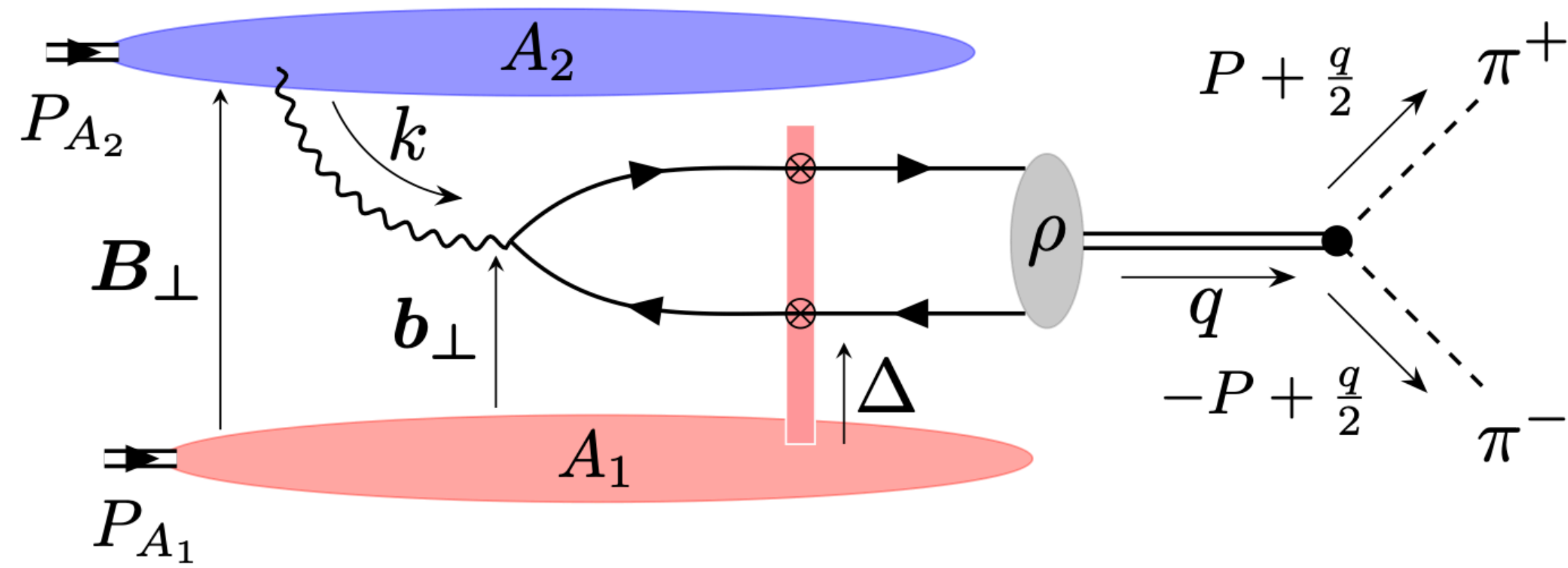
$\beta_4$



- $\beta_2$  ,  $\beta_3$  and  $\beta_4$  modify fluctuations at different length scales:  
Change incoherent cross section in different  $|t|$  regions

# Angular anisotropies: Interference effects - $\rho$ production

Heikki Mäntysaari, Farid Salazar, Björn Schenke, Chun Shen, Wenbin Zhao, arXiv:2310.15300



$$\frac{d\sigma^{\rho \rightarrow \pi^+ \pi^-} (\phi \rightarrow K^+ K^-)}{d^2\mathbf{P}_\perp d^2\mathbf{q}_\perp dy_1 dy_2} = \frac{1}{4(2\pi)^3} \frac{P_\perp^2 f^2}{(Q^2 - M_V^2)^2 + M_V^2 \Gamma^2} \left\{ C_0(x_1, x_2, |\mathbf{q}_\perp|) + C_2(x_1, x_2, |\mathbf{q}_\perp|) \cos(2(\phi_{\mathbf{P}_\perp} - \phi_{\mathbf{q}_\perp})) \right\}$$

where

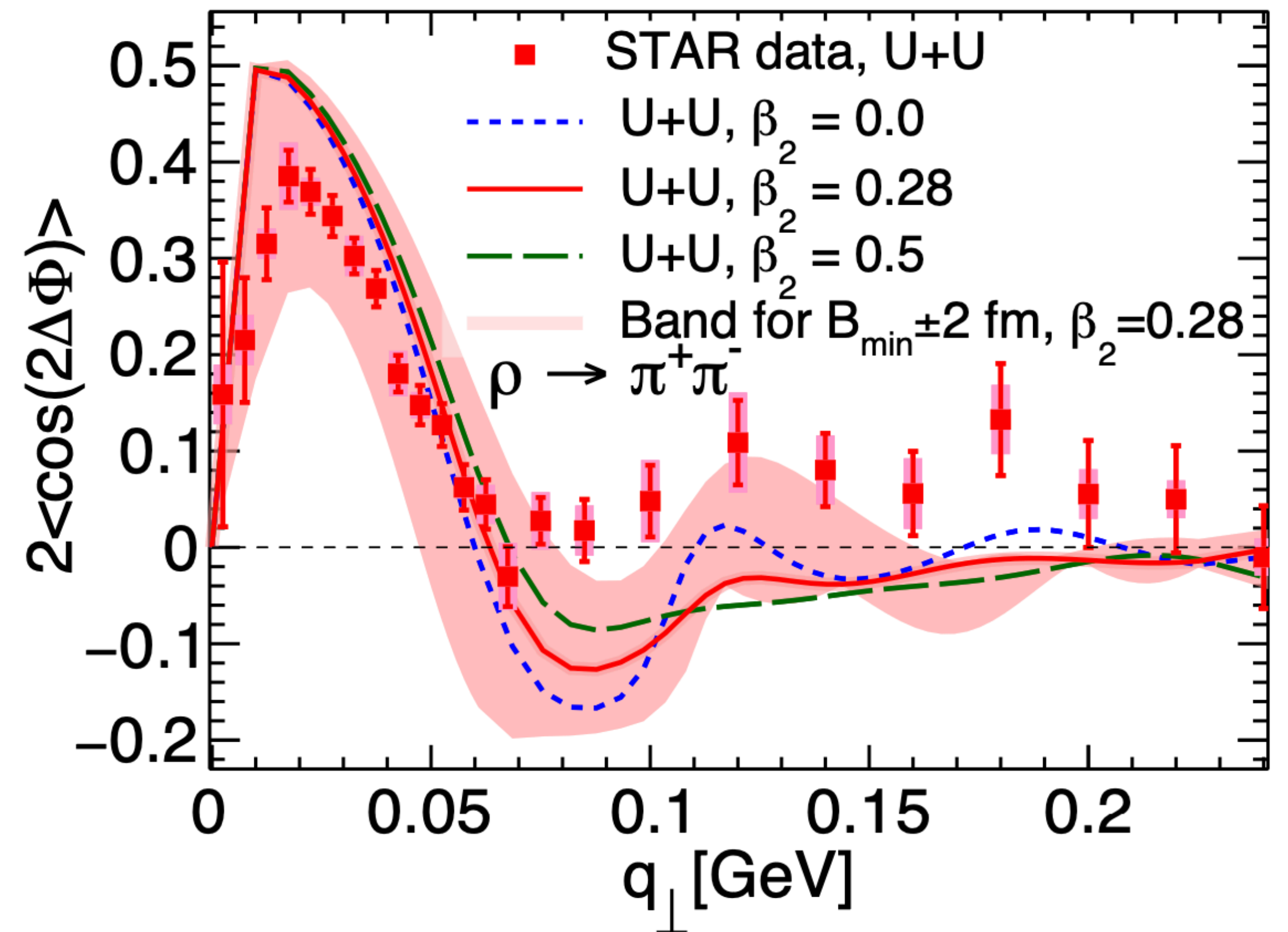
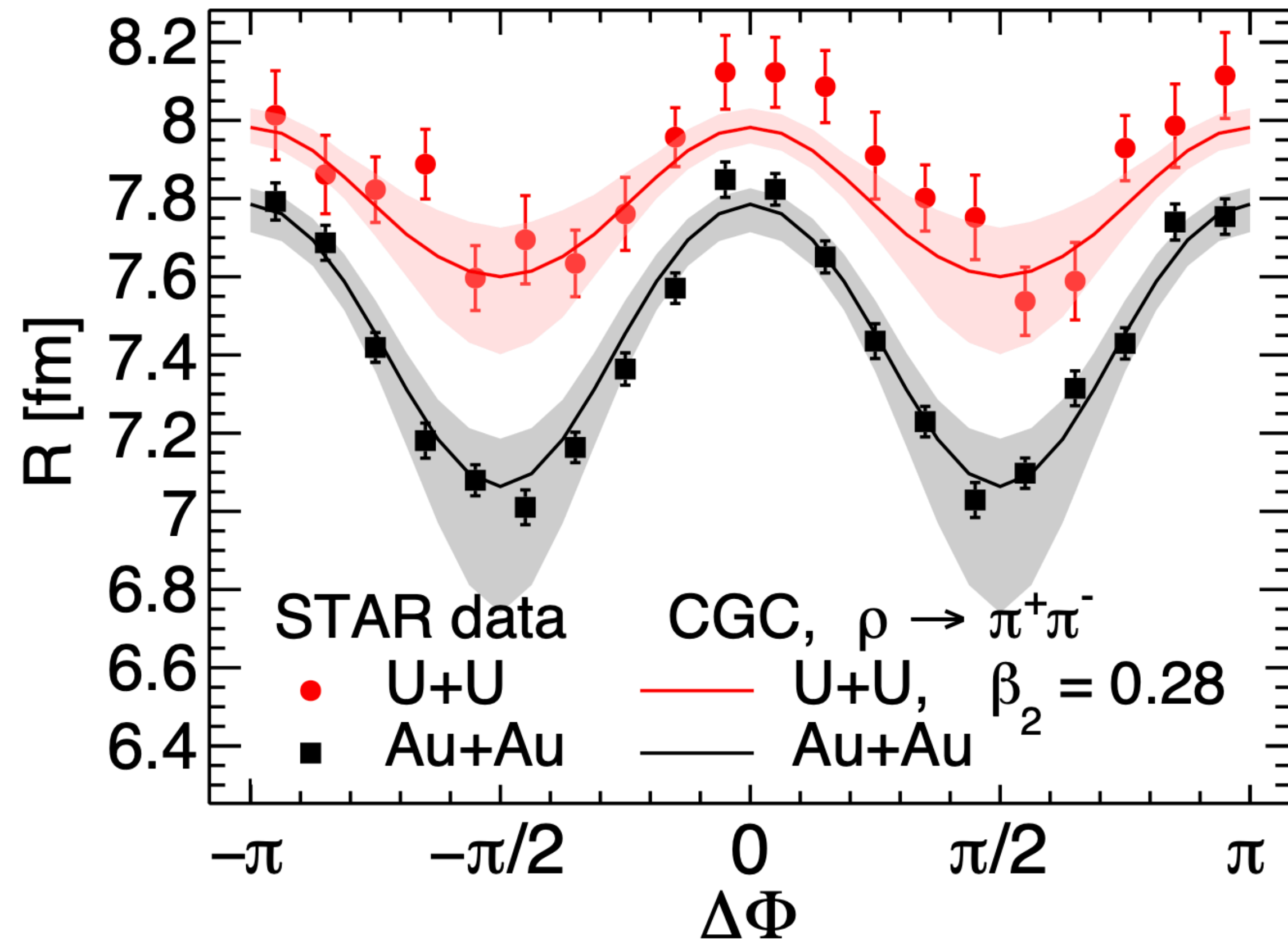
$$C_0(x_1, x_2, |\mathbf{q}_\perp|) = \left\langle \int d^2\mathbf{B}_\perp \mathcal{M}^i(x_1, x_2, \mathbf{q}_\perp, \mathbf{B}_\perp) \mathcal{M}^{\dagger,i}(x_1, x_2, \mathbf{q}_\perp, \mathbf{B}_\perp) \Theta(|\mathbf{B}_\perp| - B_{\min}) \right\rangle_\Omega, \text{ and}$$

$$C_2(x_1, x_2, |\mathbf{q}_\perp|) = \left( \frac{2\mathbf{q}_\perp^i \mathbf{q}_\perp^j}{q_\perp^2} - \delta^{ij} \right) \left\langle \int d^2\mathbf{B}_\perp \mathcal{M}^i(x_1, x_2, \mathbf{q}_\perp, \mathbf{B}_\perp) \mathcal{M}^{\dagger,j}(x_1, x_2, \mathbf{q}_\perp, \mathbf{B}_\perp) \Theta(|\mathbf{B}_\perp| - B_{\min}) \right\rangle_\Omega$$



# Effects of nuclear radius and deformation

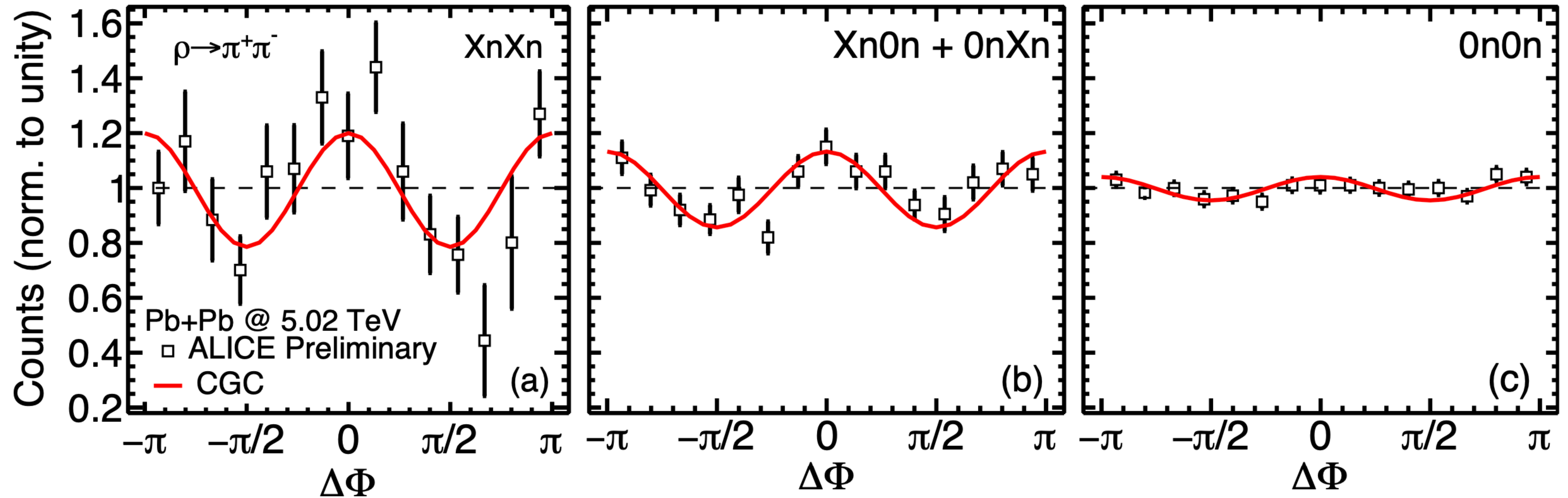
Heikki Mäntysaari, Farid Salazar, Björn Schenke, Chun Shen, Wenbin Zhao, arXiv:2310.15300



Large effect from the differences in minimal impact parameter  $B_{\min}$

# Varying impact parameter distribution at LHC

Heikki Mäntysaari, Farid Salazar, Björn Schenke, Chun Shen, Wenbin Zhao, arXiv:2310.15300



More neutrons in the forward direction prefers smaller impact parameters  
Modulation decreases for larger impact parameter

# NLO pQCD exclusive J/ψ photoproduction

[K. J. Eskola, C. A. Flett, V. Guzey, T. Löytäinen, H. Paukkunen, Phys.Rev.C 106 \(2022\) 3, 035202, \[arXiv:2203.11613\]](#)

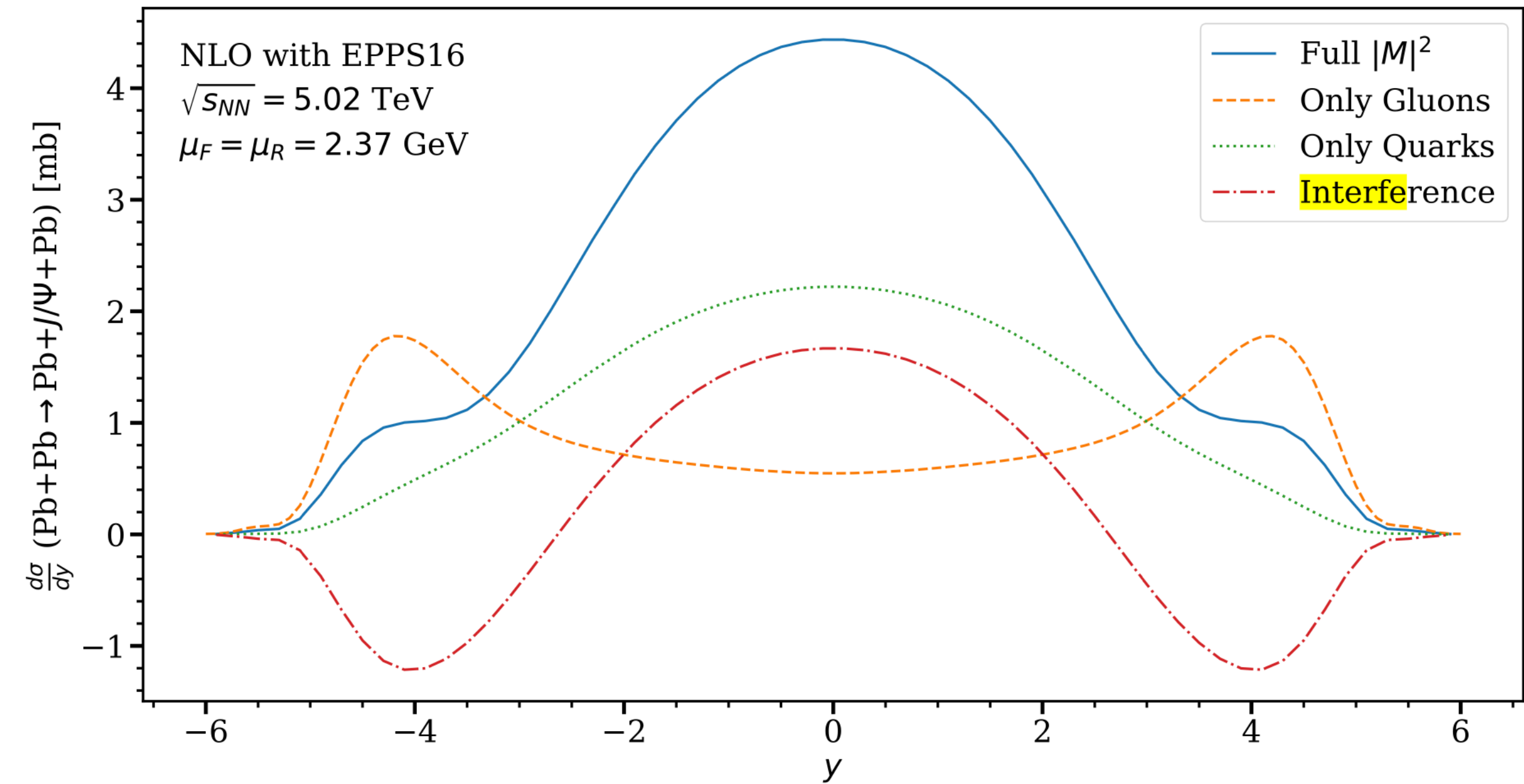
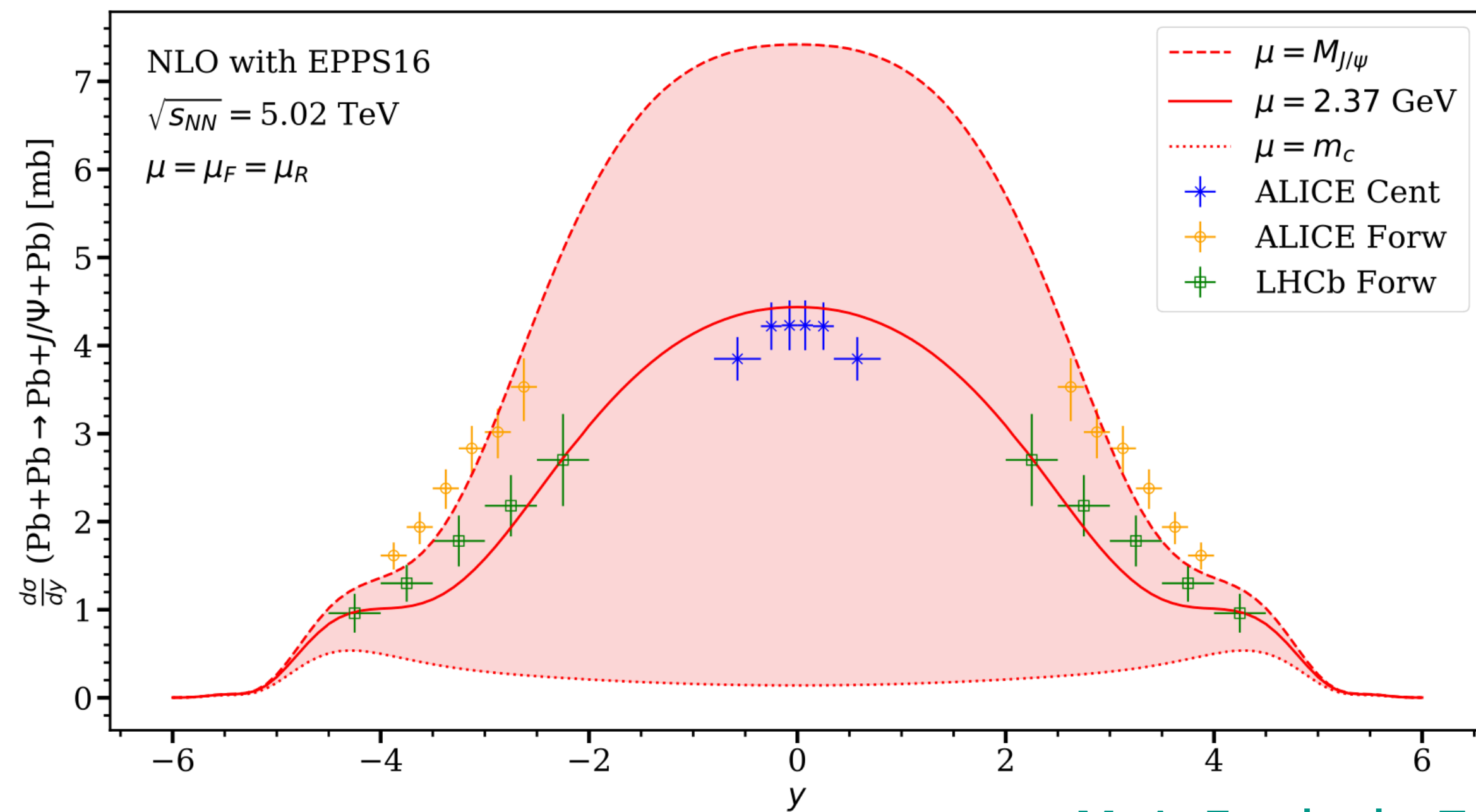
based on NLO pQCD calculation using collinear factorization at the amplitude level

(factorization of the amplitude into calculable NLO pQCD pieces and the GPDs, which in the forward limit become the usual PDFs)

[D. Y. Ivanov, A. Schafer, L. Szymanowski, G. Krasnikov, Eur. Phys. J. C 34 \(2004\) no. 3 297 \[arXiv:hep-ph/0401131\]](#)

The LO and NLO gluon amplitudes dominate over the NLO quark contribution.

But LO and NLO gluon amplitudes cancel to a large degree, due to their opposite signs



[M. A. Escobedo, T. Lappi, Phys. Rev. D 101, 034030 \(2020\)](#)

For NLO in the dipole picture see:

[H. Mäntysaari, J. Penttala, Letters B 823 \(2021\) 136723](#)

[H. Mäntysaari, J. Penttala, JHEP 08 \(2022\) 247](#)

# Discussion: Ryskin vs. dipole model

Shashank Anand, Tobias Toll, Phys. Rev. C 100, 024901 (2019); <https://arxiv.org/pdf/1807.10888.pdf>  
 also Kopeliovich arXiv:1602.00298

Scattering amplitudes for a proton target:

Ryskin 
$$\mathcal{A}_T^{\gamma^* p \rightarrow J/\Psi p} = i4\pi^2 \sqrt{\frac{\Gamma_{ee}^{J/\Psi} M_{J/\Psi}^3}{3\alpha_{\text{EM}}}} \alpha_s(\mu^2) xg(x, \mu^2) \underbrace{F_N^{2G}(t)}_{\text{proton form factor}} \frac{2\mu^2 + t}{(2\mu^2)^3} \quad (\text{form that LTA calculation uses})$$

IPsat 
$$\mathcal{A}_{T,L}^{\gamma^* p \rightarrow J/\Psi p} = i \int_0^\infty 2\pi r dr \int_0^1 \frac{dz}{4\pi} \int_0^\infty 2\pi b db (\Psi_{J/\Psi}^* \Psi)_{T,L} J_0(b\Delta) J_0([1-z]r\Delta) \frac{d\sigma_{q\bar{q}}}{d^2\vec{b}}$$

$$\frac{d\sigma_{q\bar{q}}}{d^2\vec{b}} = 2 \left( 1 - \exp \left( -\frac{\pi^2}{2N_c} r^2 \alpha_s(\mu_{\text{dip}}^2) xg(x, \mu_{\text{dip}}^2) T(b) \right) \right)$$

Take the hard scattering (small  $r$  limit) and non-relativistic limits (where  $z = 1/2$ ) of the Dipole Model (IPSat) and assume  $\mu_{\text{dip}}^2 = \mu^2$ : The results are equivalent

The second difference is how nuclear effects are computed.

# Discussion: LTA calculations vs dipole picture and CGC

- Dipole approximation includes Gribov inelastic shadowing corrections to all orders of multiple interactions [Kopeliovich arXiv:1602.00298](#)
- In the limit of very small  $x = Q^2/2m_N\nu$  the coherence time is longer than nuclear size and “frozen” dipole picture is appropriate ( $\nu$  is photon energy)
- If the coherence time is smaller than nuclear size scale one should correct for dipole size fluctuations during the propagation in the nucleus, which corresponds to inclusion of the phase shifts between DIS amplitudes on different nucleons.
- “ $e^{i(z_1-z_2)m_Nx_{\mathbb{P}}}$  factor can be safely set to unity for  $x \leq 10^{-2}$ ” [Frankfurt, Guzey, Strikman Physics Reports 512 \(2012\) 255-393](#)
- In that case, what is the difference between LTA (with attenuation factor) and CGC?
- Does BK take care of the higher Fock states in the dipole? (also when applied to target fields?) (see [Kopeliovich arXiv:1602.00298](#)) or is it ignoring shorter coherence times for  $q\bar{q}g$  that should be taken into account?

# Summary

- Many different models, mainly based on LO pQCD or the dipole model. Predictions for coherent cross sections in UPC can vary strongly even between similar models
- Nuclear suppression in the CGC seems to be too weak. Why?
- Interference effects and dependence on nuclear target are well described for VM production in UPCs
- Differential exclusive VM production is sensitive to nuclear structure
- Going to NLO is important to make quantitative predictions
- Ryskin formula and dipole model are equivalent in certain limit
- LTA differs from eikonal dipole picture by taking into account phase shifts (which may not matter at small  $x$ ) and treating different Fock states in the projectile explicitly. In the CGC the LLx small- $x$  evolution should take care of some of the corrections, full NLO CGC calculations further include  $q\bar{q}g$  contributions that are not log enhanced

# BACKUP

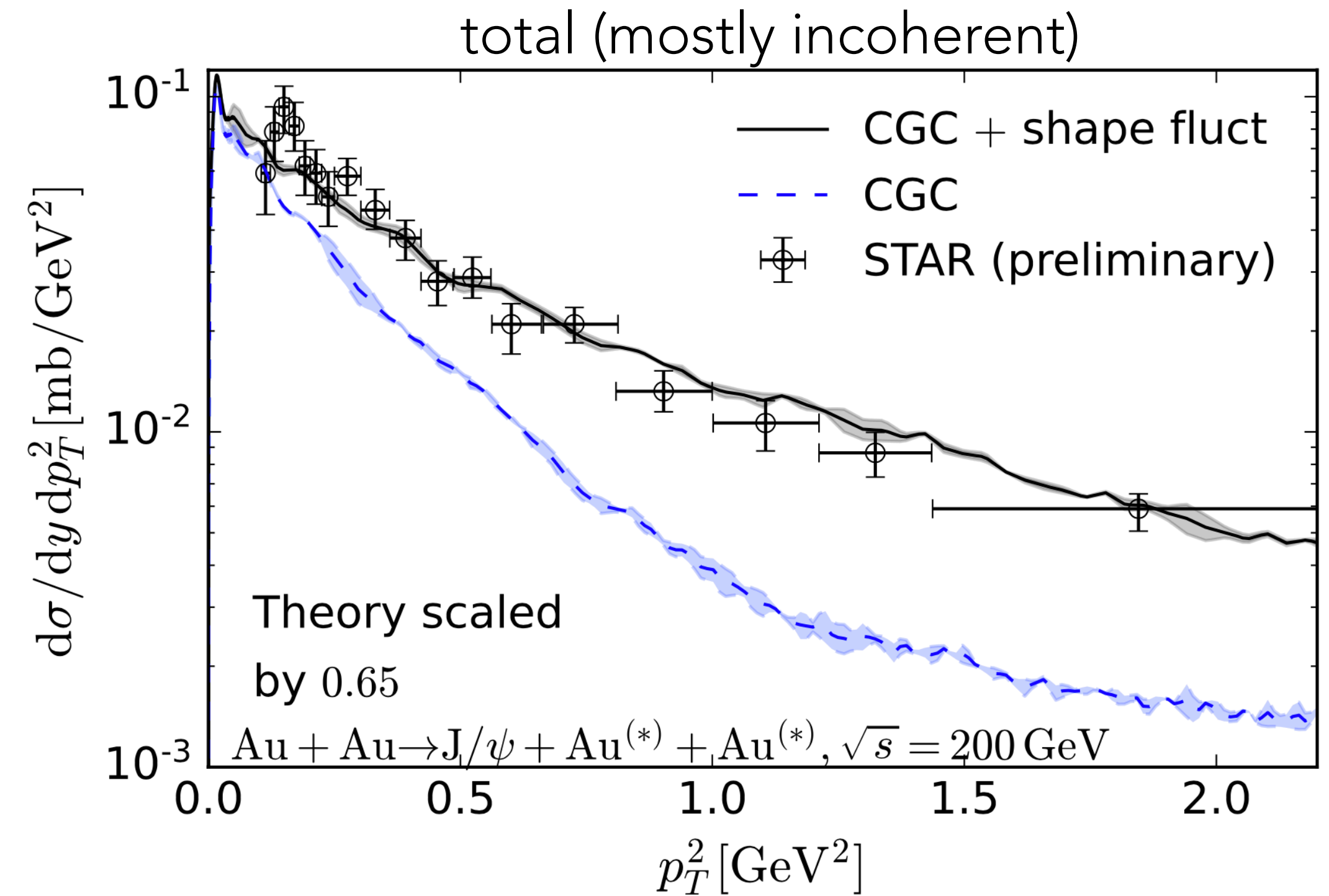
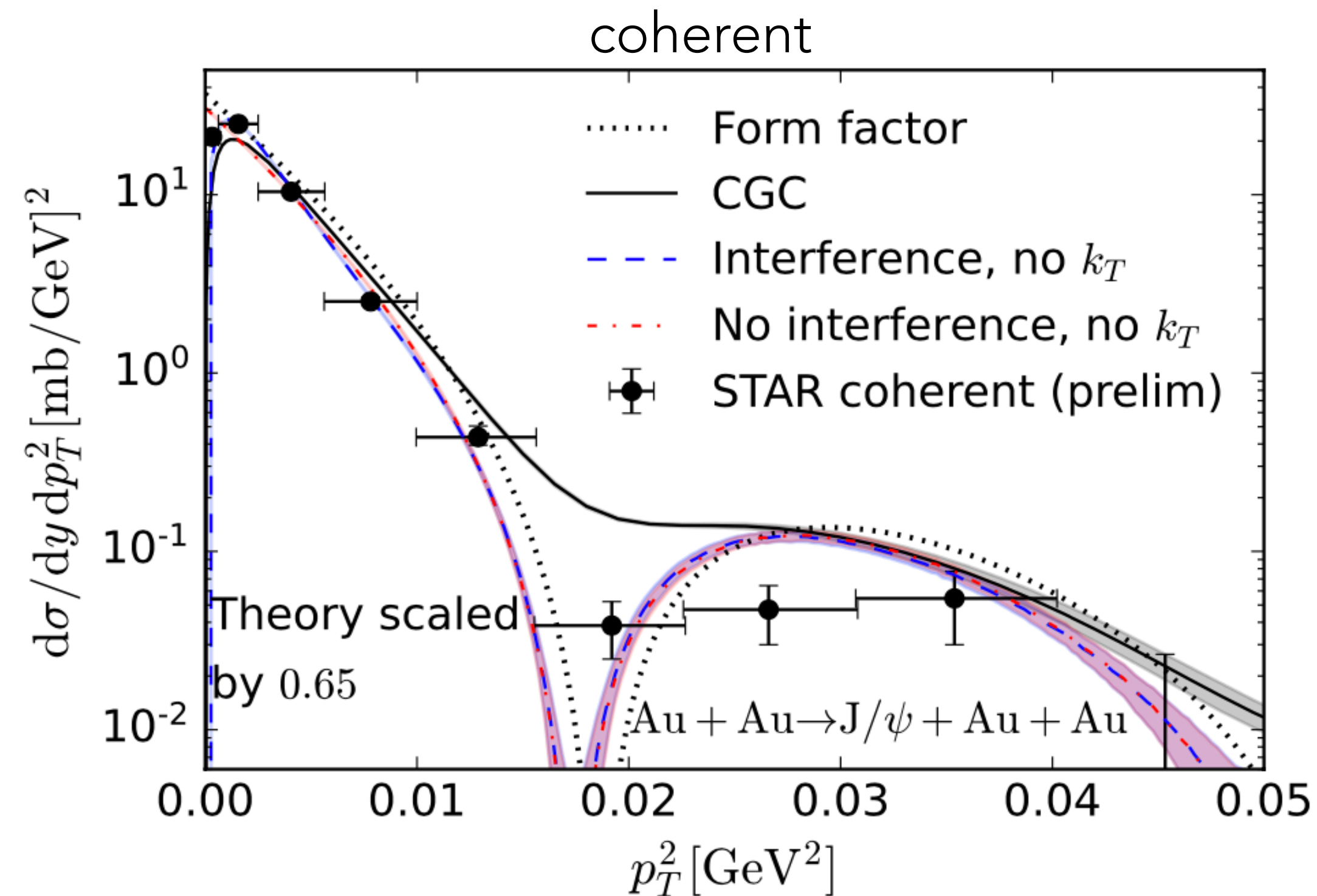
# Discussion: LTA calculations vs dipole picture and CGC

- Dipole approximation includes Gribov inelastic shadowing corrections to all orders of multiple interactions [Kopeliovich arXiv:1602.00298](#)
- In the limit of very small  $x = Q^2/2m_N\nu$  the coherence time is longer than nuclear size and “frozen” dipole picture is appropriate
- If the coherence time is smaller than nuclear size scale one should correct for dipole size fluctuations during the propagation in the nucleus, which corresponds to inclusion of the phase shifts between DIS amplitudes on different nucleons.
- “ $e^{i(z_1-z_2)m_Nx_{\mathbb{P}}}$  factor can be safely set to unity for  $x \leq 10^{-2}$ ” [Frankfurt, Guzey, Strikman Physics Reports 512 \(2012\) 255-393](#)
- In that case, what is the difference between LTA (with attenuation factor) and CGC?
- Does BK take care of the higher Fock states in the dipole? (also when applied to target fields?) (see [Kopeliovich arXiv:1602.00298](#)) or is it ignoring shorter coherence times for  $q\bar{q}g$  that should be taken into account?



# Comparing to RHIC results

H. Mäntysaari, F. Salazar, B. Schenke, Phys.Rev.D 106 (2022) 7, 074019 STAR data: W. Schmidke, Presentation at the CFNS Workshop on Photon-Induced Interactions, April 2021

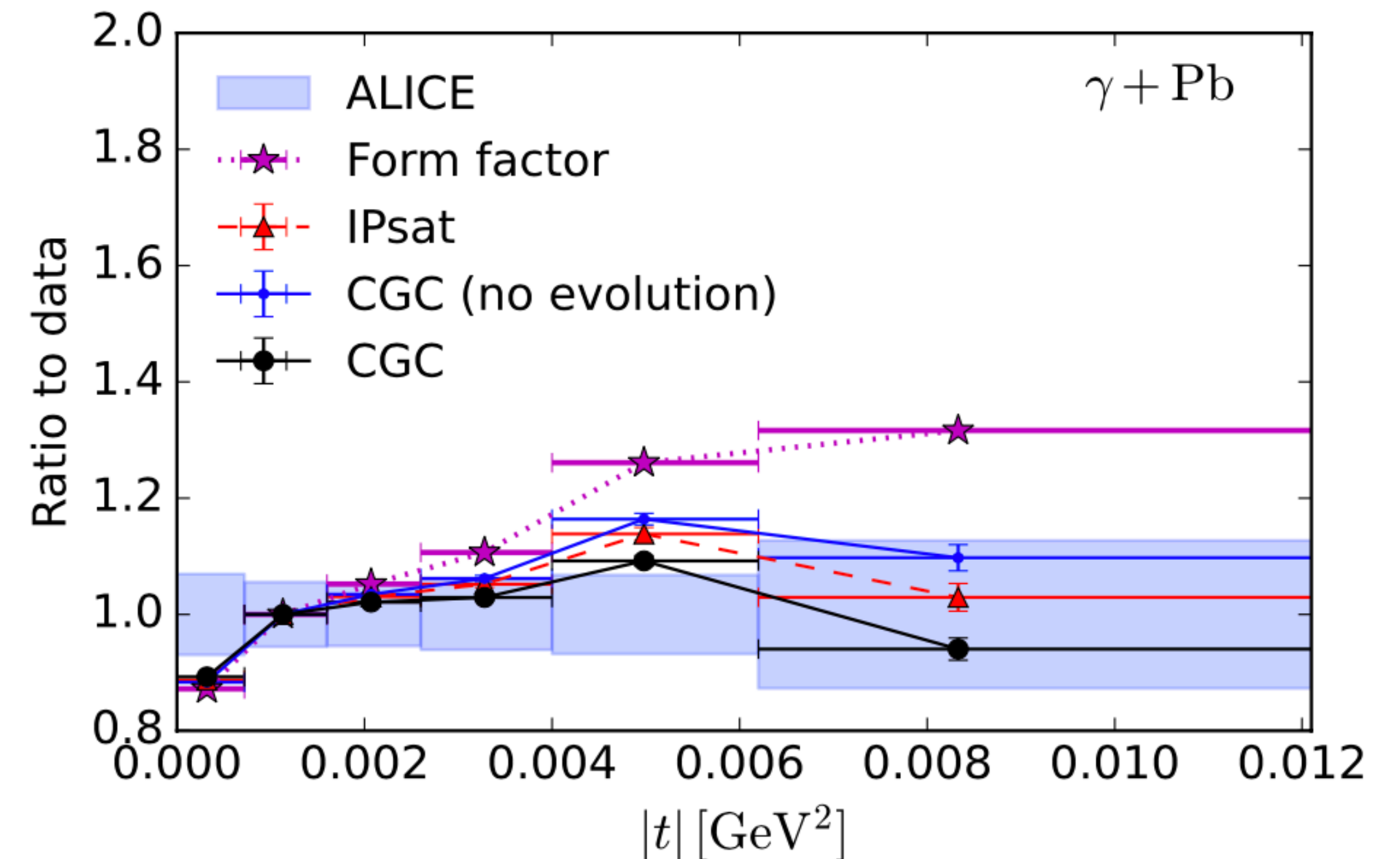
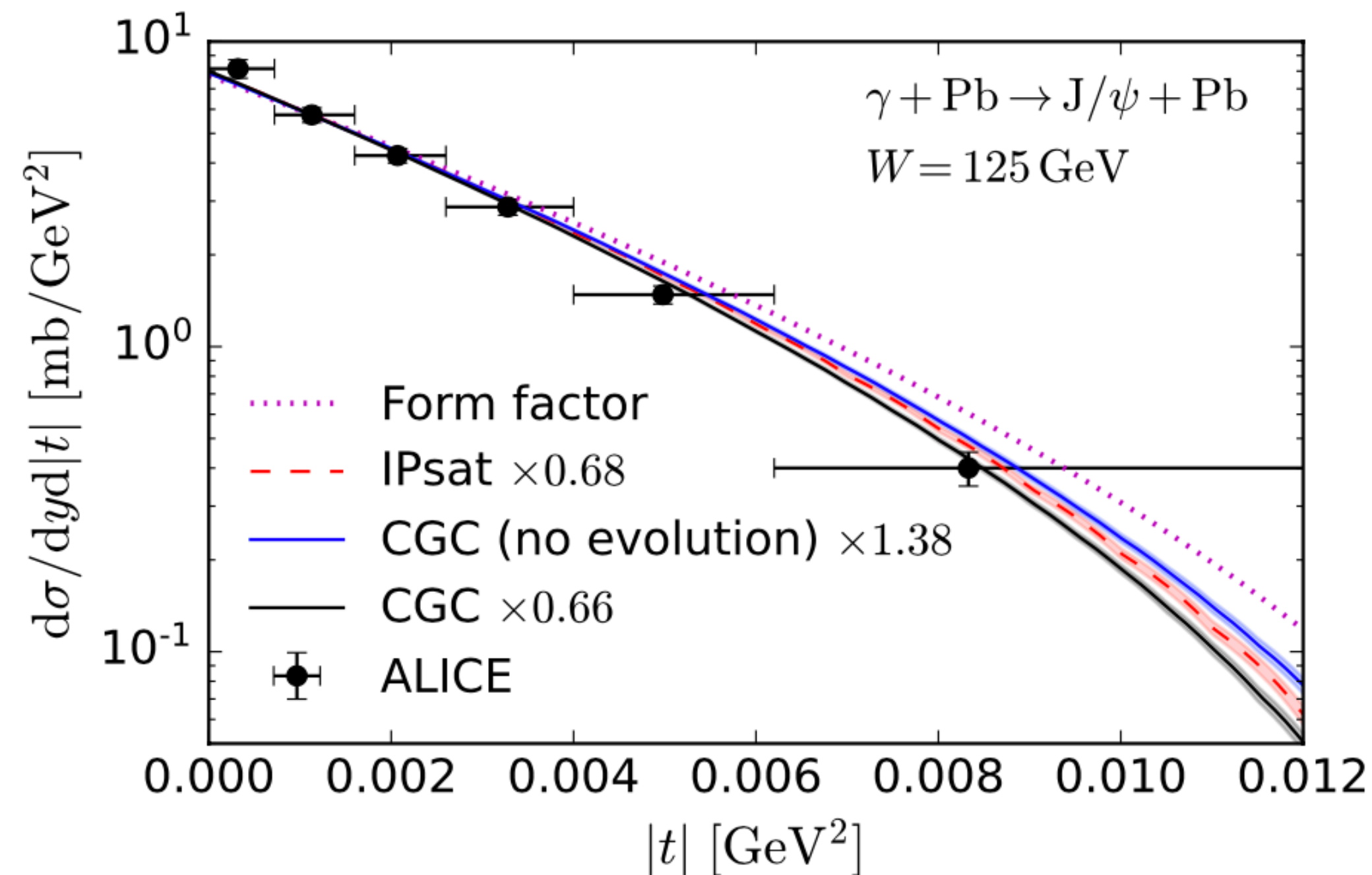


- Normalization scaled down (from HERA) same way as for comparison to ALICE data
- Inclusion of interference effect improves agreement with STAR data
- Photon  $k_T$  effect seems too strong
- Incoherent well described with subnucleon fluctuations included

# UPCs: $\gamma$ +Pb measurement - Role of saturation effects

H. Mäntysaari, F. Salazar, B. Schenke, Phys.Rev.D 106 (2022) 7, 074019

Here, ALICE removed interference and photon  $k_T$  effects to get the  $\gamma$ +Pb cross section

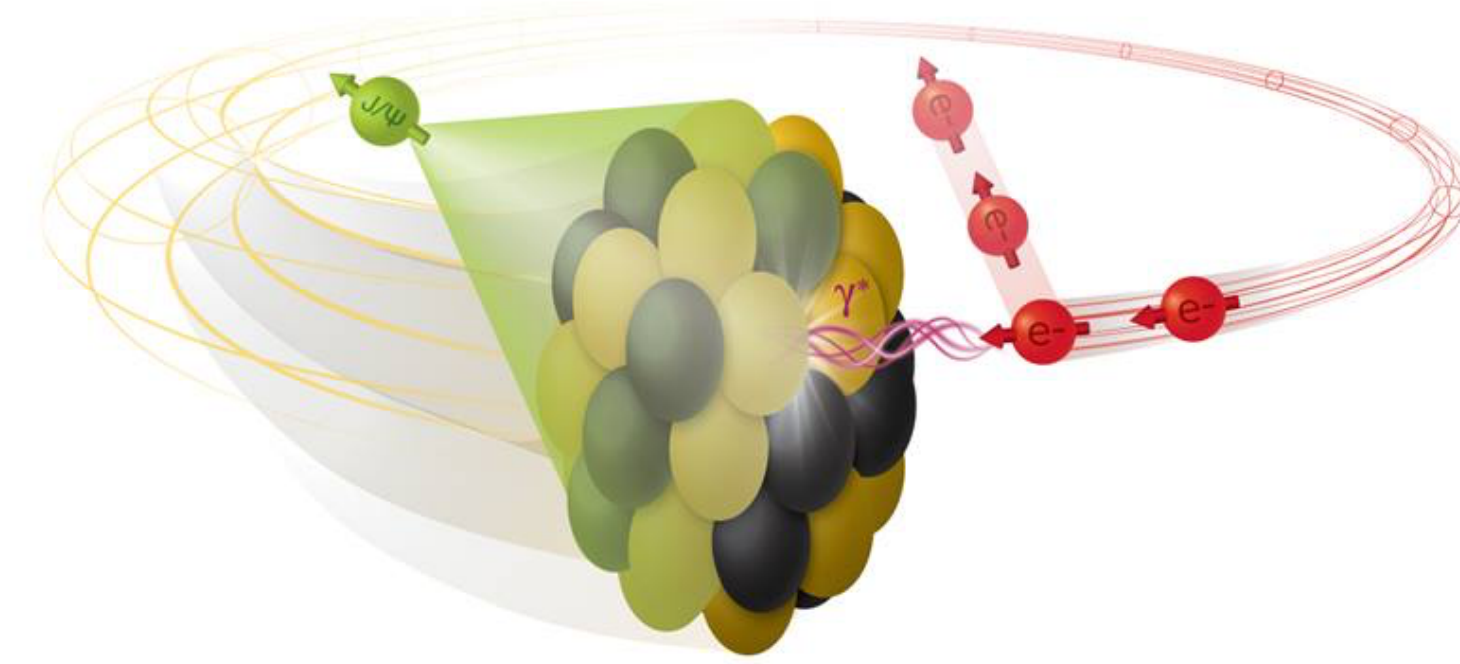


ALICE Collaboration, Phys.Lett.B 817 (2021) 136280

Saturation effects improve agreement with experimental data significantly  
Multiplicative factor included to better compare to the shape. Suppression not enough.

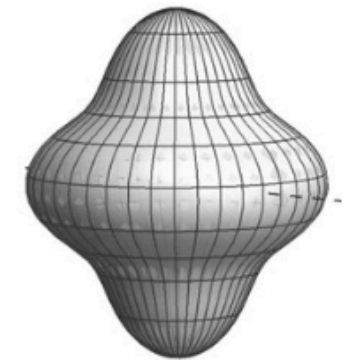
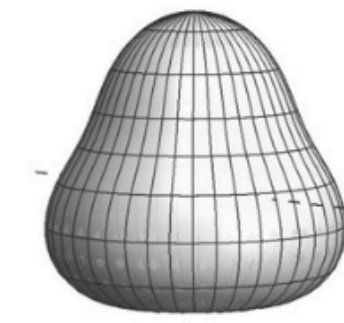
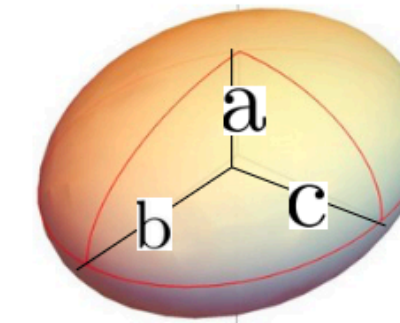
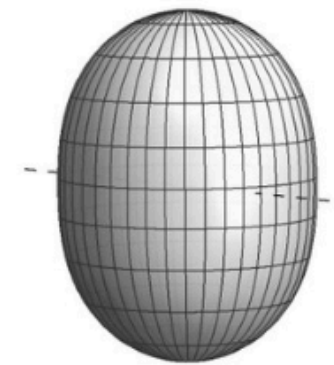
# Effects of deformation on diffractive cross sections

H. Mäntysaari, B. Schenke, C. Shen, W. Zhao, *Phys. Rev. Lett.* **131**, 062301 (2023)



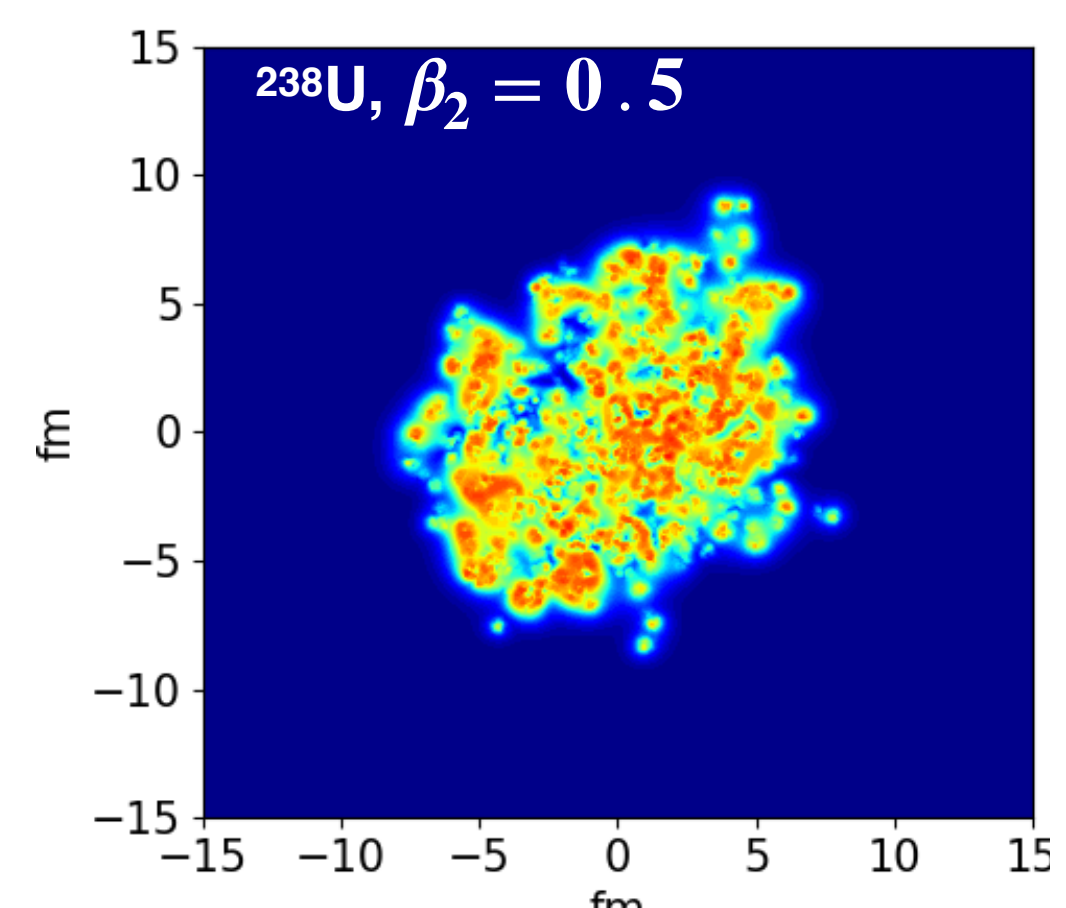
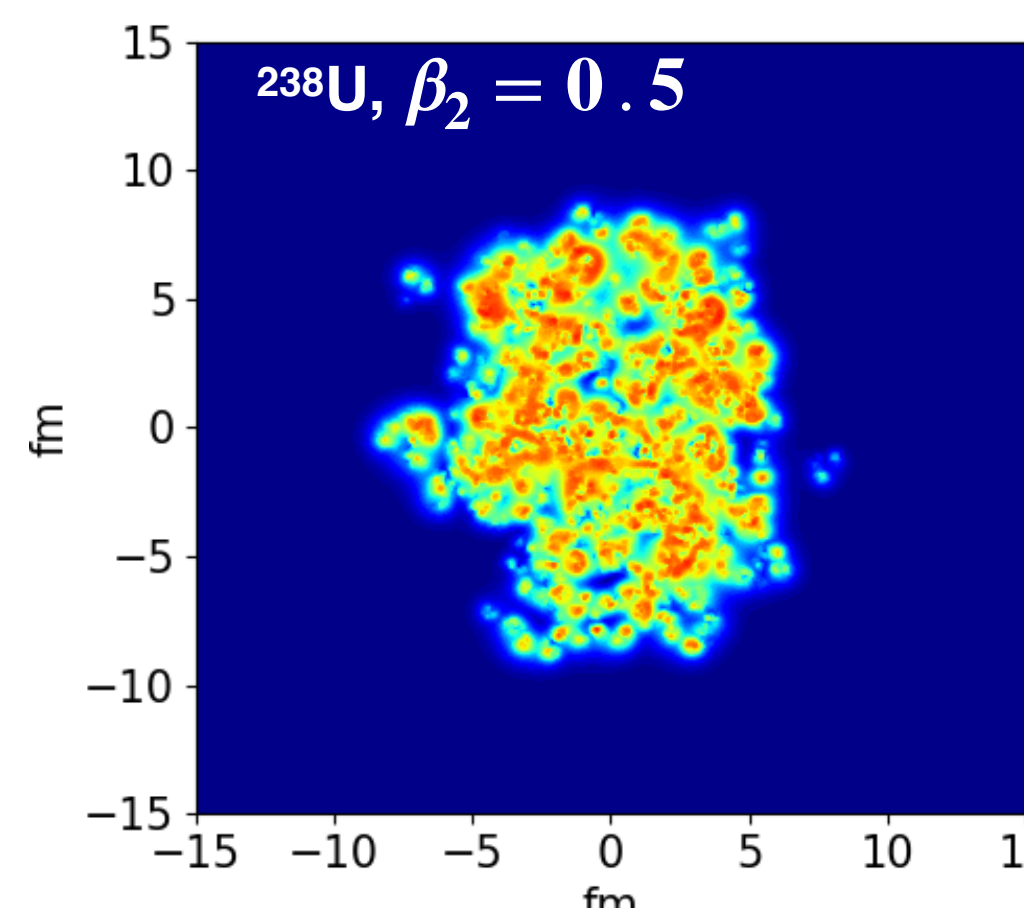
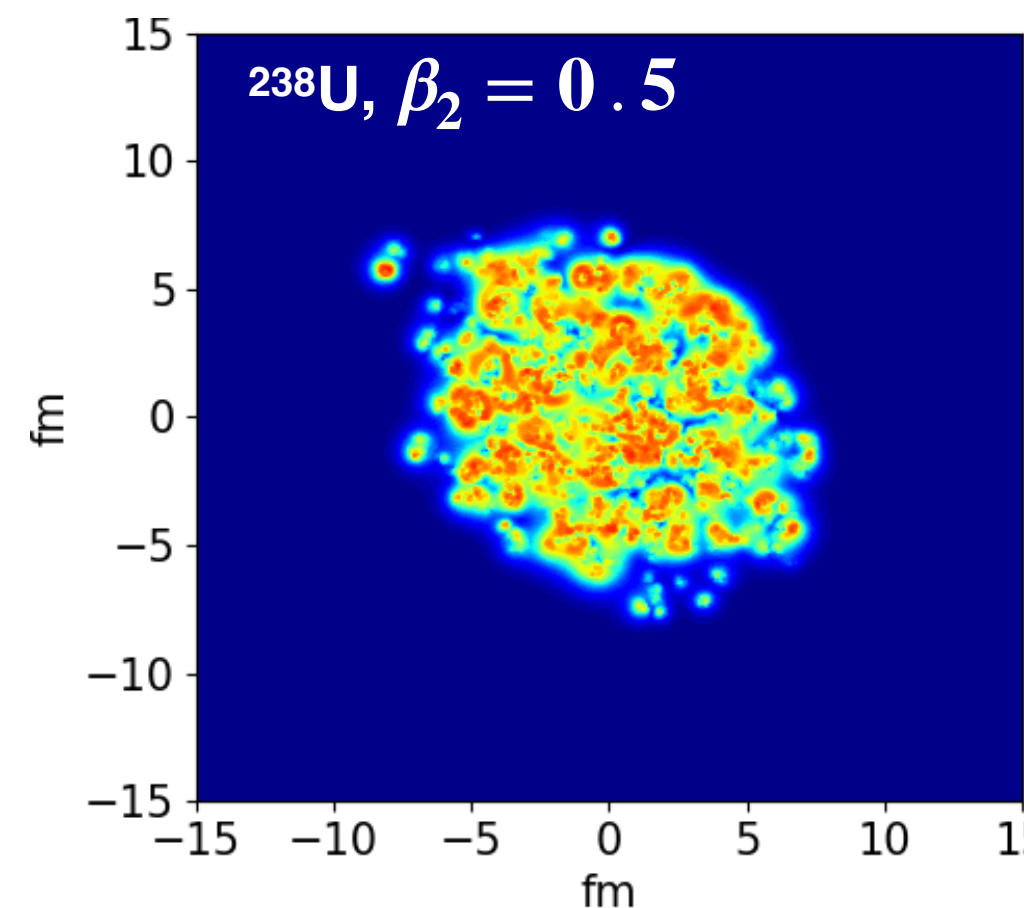
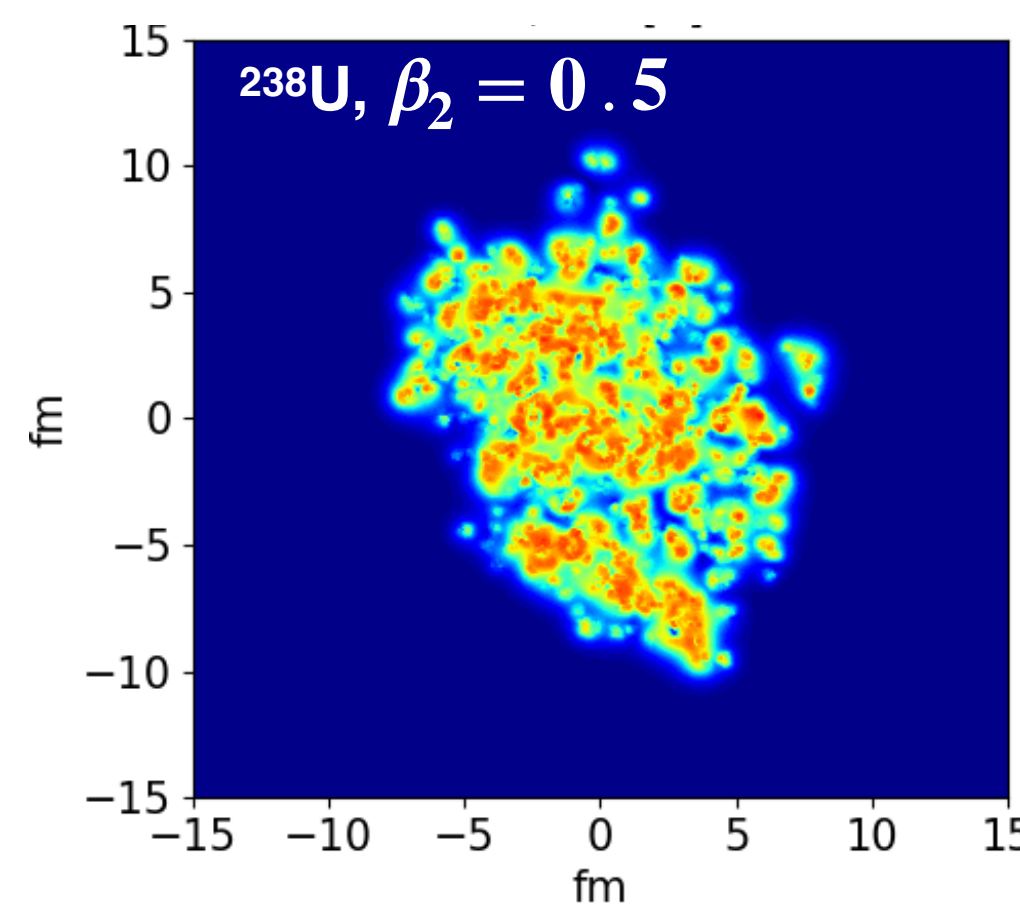
Implement deformation in the Woods-Saxon distribution:

$$\rho(r, \Theta, \Phi) \propto \frac{1}{1 + \exp([r - R(\Theta, \Phi)]/a)}, \quad R(\Theta, \Phi) = R_0 \left[ 1 + \underline{\beta_2} \left( \cos \gamma Y_{20}(\Theta) + \sin \gamma Y_{22}(\Theta, \Phi) \right) + \underline{\beta_3} Y_{30}(\Theta) + \underline{\beta_4} Y_{40}(\Theta) \right]$$



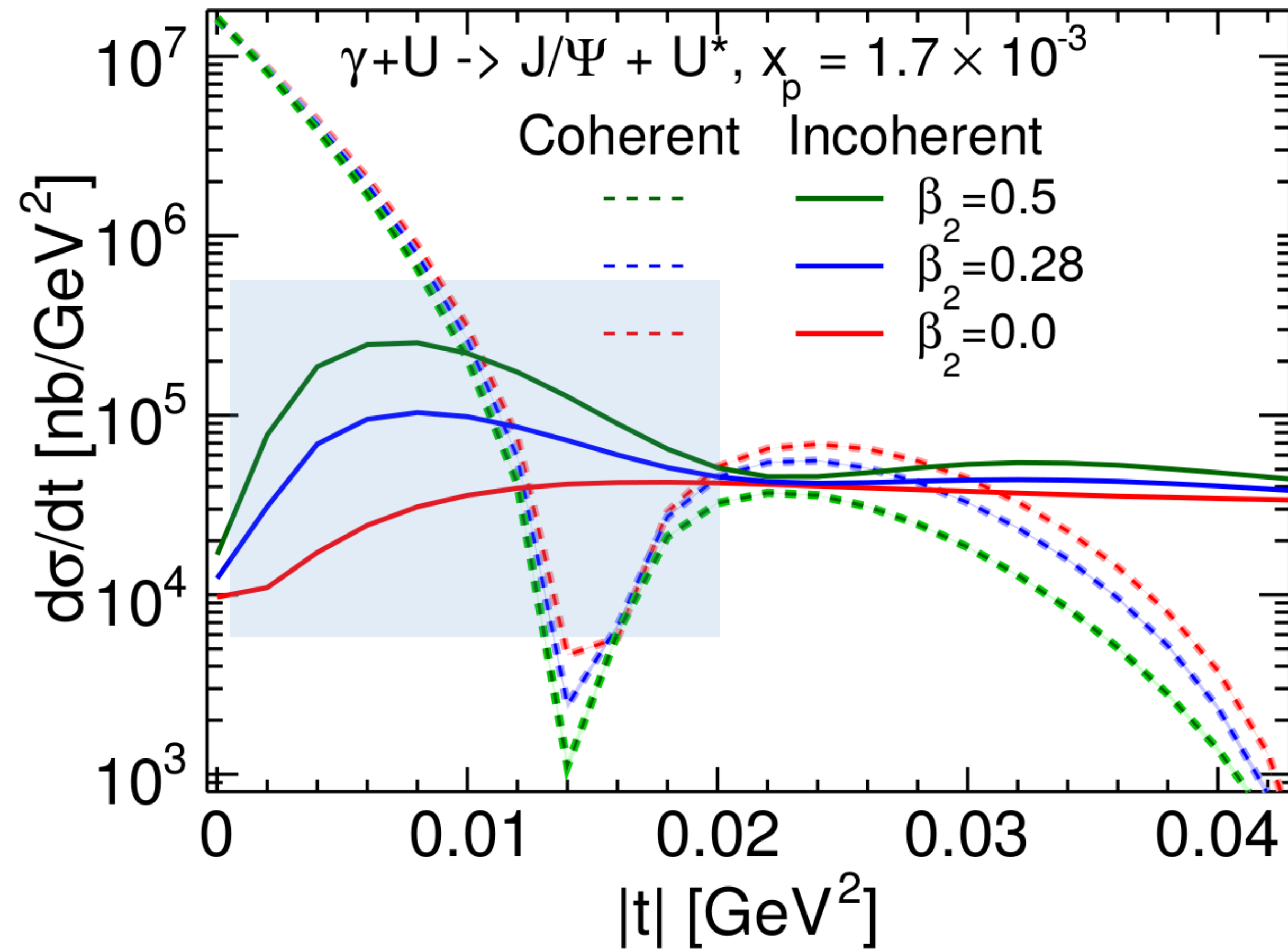
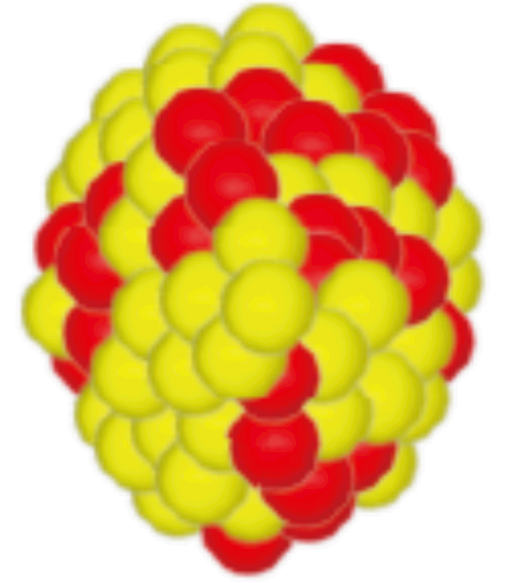
from G. Giacalone

Deformed nuclei exhibit larger fluctuation in the transverse projection:



# Effects of deformation on diffractive cross sections: Uranium

H. Mäntysaari, B. Schenke, C. Shen, W. Zhao, *Phys. Rev. Lett.* **131**, 062301 (2023)



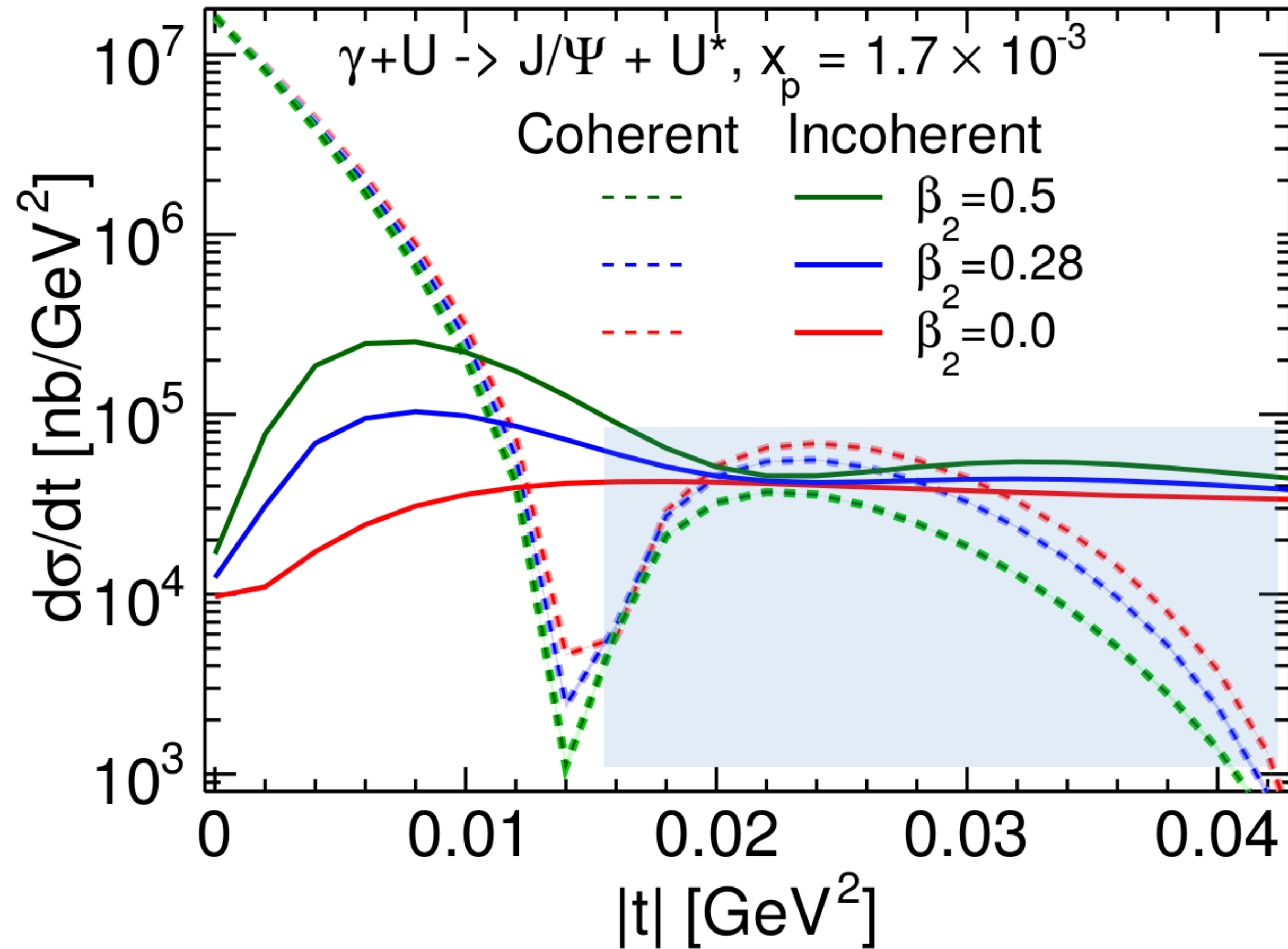
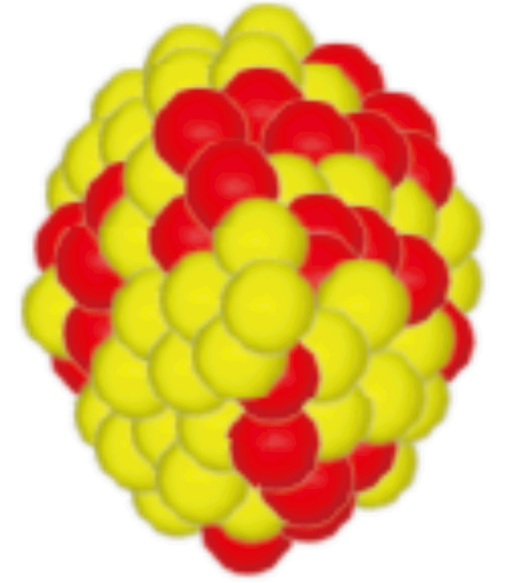
Deformation of the nucleus affects incoherent cross section at small  $|t|$  (large length scales)

This observable provides direct information on the small  $x$  structure

$$Q^2 = 0$$

# Effects of deformation on diffractive cross sections: Uranium

H. Mäntysaari, B. Schenke, C. Shen, W. Zhao, *Phys. Rev. Lett.* **131**, 062301 (2023)



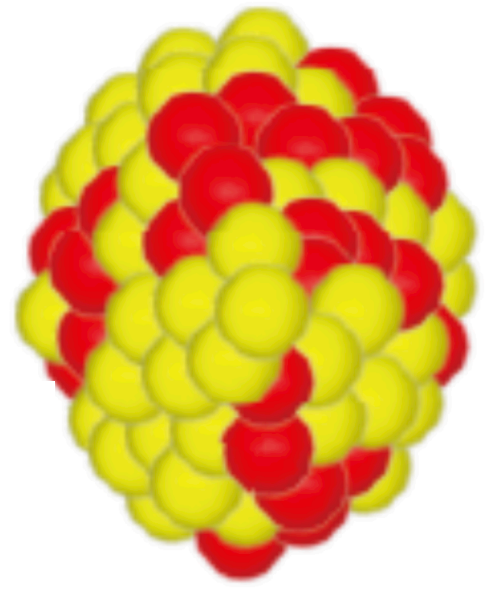
Deformation changes the shape of the average 2D projection of the nucleus



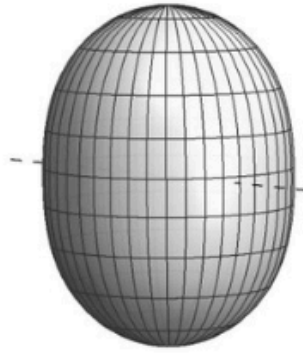
Modification of the coherent cross section

# Effects of deformation on diffractive cross sections: Uranium

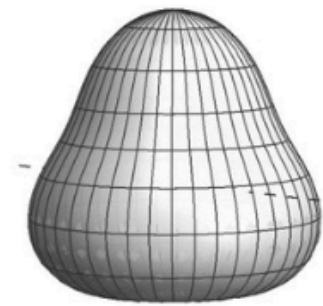
H. Mäntysaari, B. Schenke, C. Shen, W. Zhao, *Phys. Rev. Lett.* **131**, 062301 (2023)



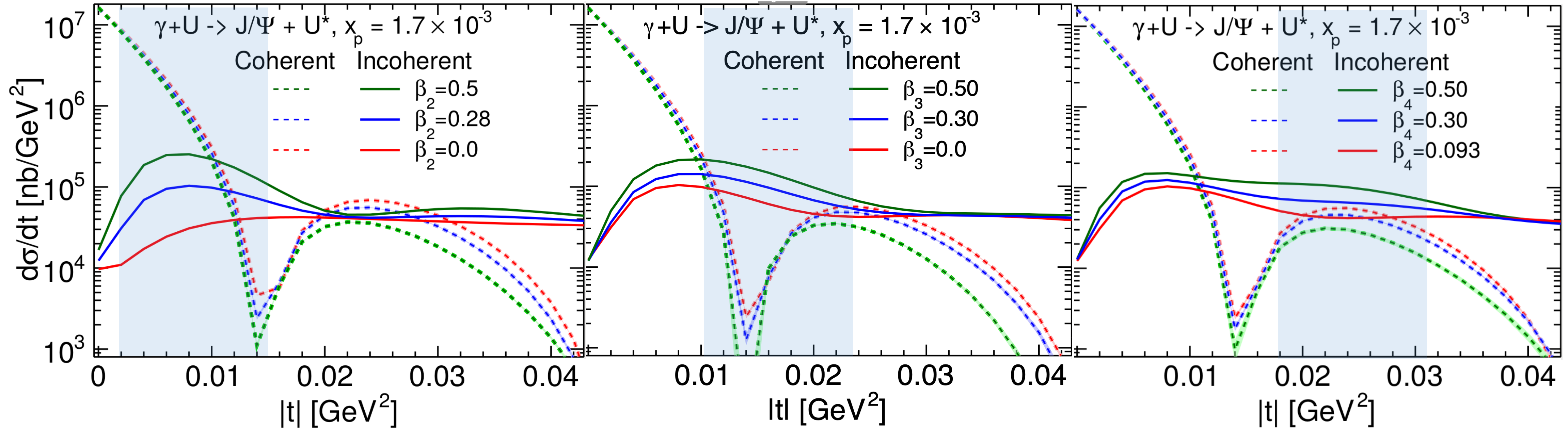
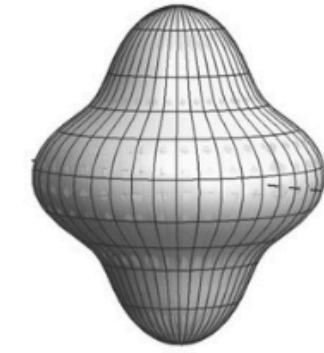
$\beta_2$



$\beta_3$



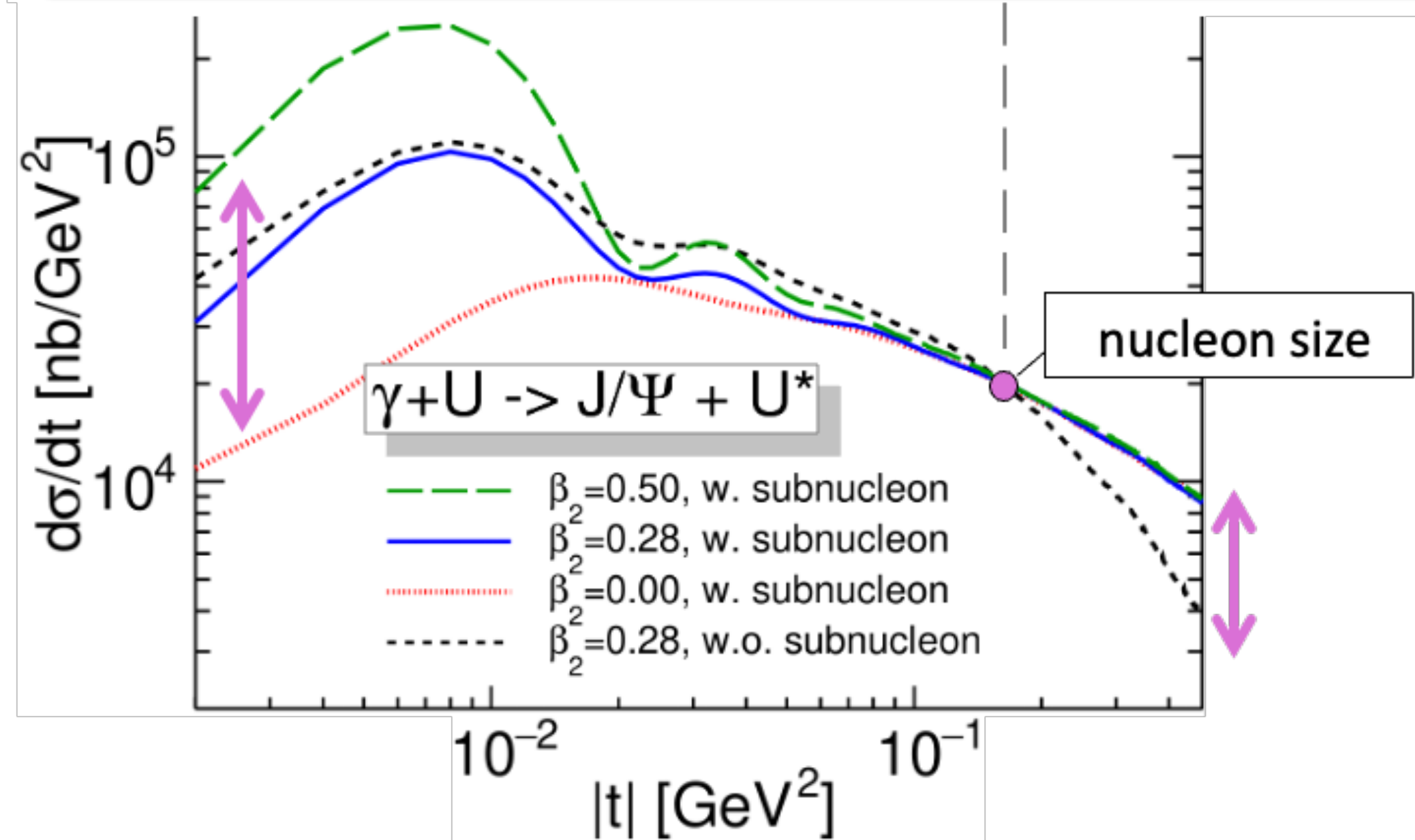
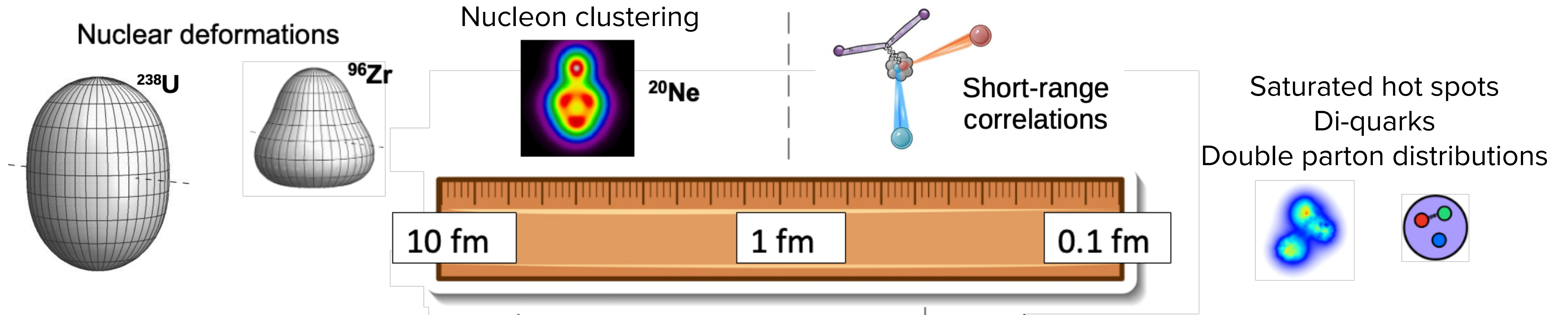
$\beta_4$



- $\beta_2$  ,  $\beta_3$  and  $\beta_4$  modify fluctuations at different length scales:  
Change incoherent cross section in different  $|t|$  regions

# Multi-scale sensitivity

H. Mäntysaari, B. Schenke, C. Shen, W. Zhao, Phys. Rev. Lett. 131, 062301 (2023)



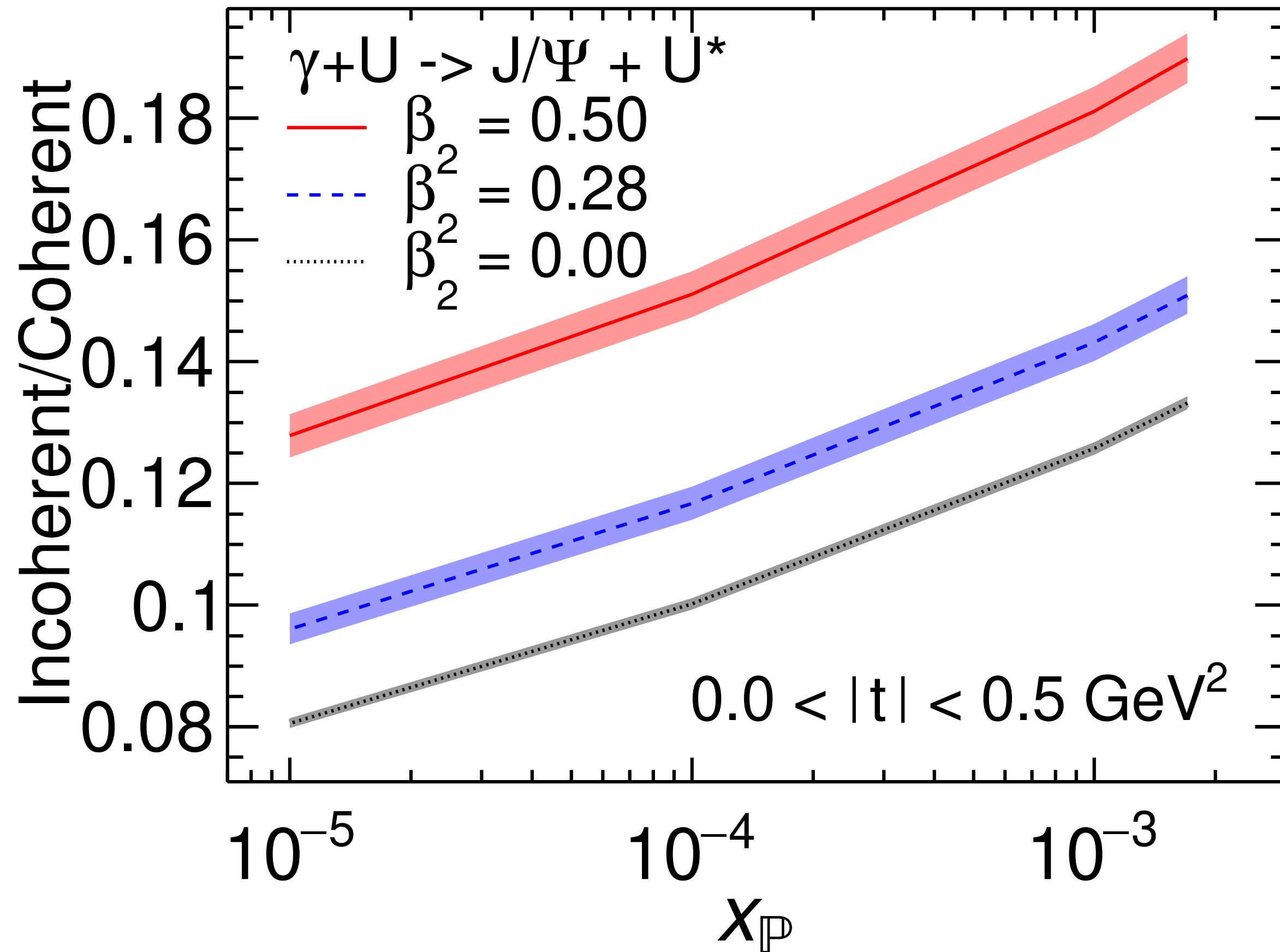
**Chiral effective field theory**  
(low-energy QCD)



**CGC effective field theory**  
(high-energy QCD)

# Towards smaller $x$

H. Mäntysaari, B. Schenke, C. Shen, W. Zhao, Phys. Rev. Lett. 131, 062301 (2023)

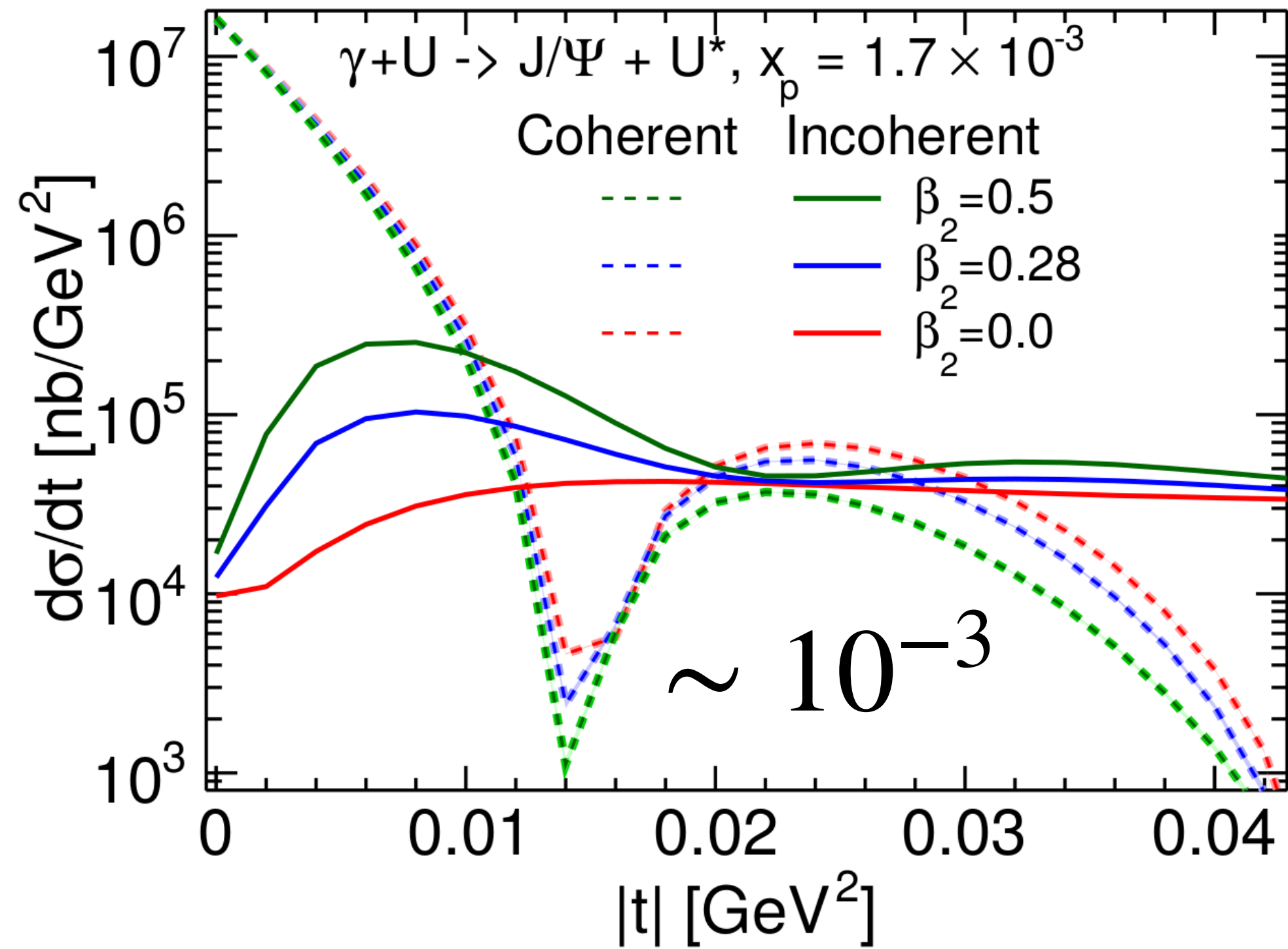


- JIMWLK evolution to smaller  $x$
- Both cross sections increase
- Ratio incoherent/coherent decreases because fluctuations are reduced (nucleus becomes smoother)
- Difference between different  $\beta_2$  does not decrease noticeably in this  $x$  range
- Is there a large enough  $x$  range we can cover at the EIC ( at least  $10^{-3} - 10^{-2}$  )?

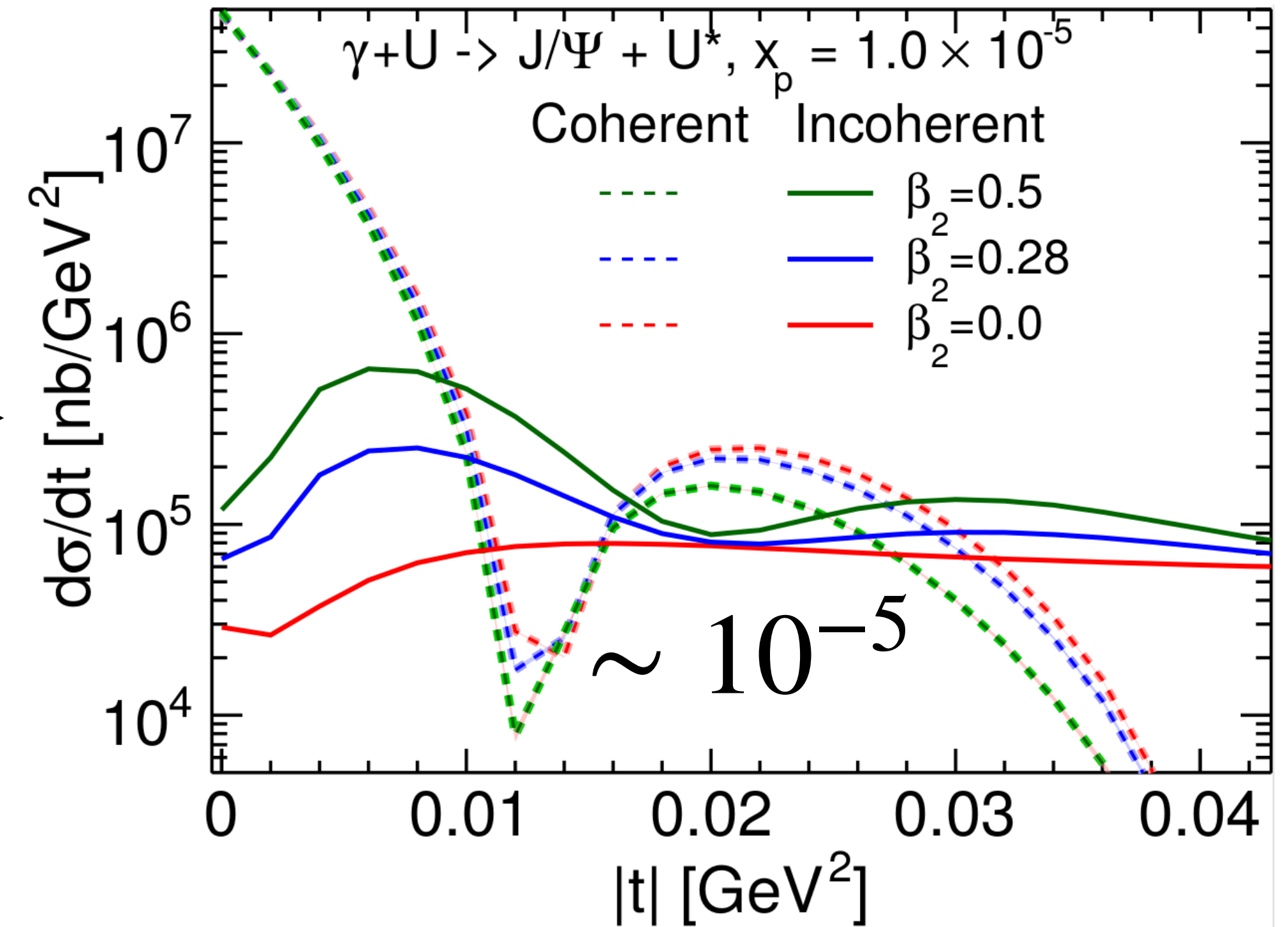


# Towards smaller $x$ : Do deformation effects survive?

H. Mäntysaari, B. Schenke, C. Shen, W. Zhao, in progress



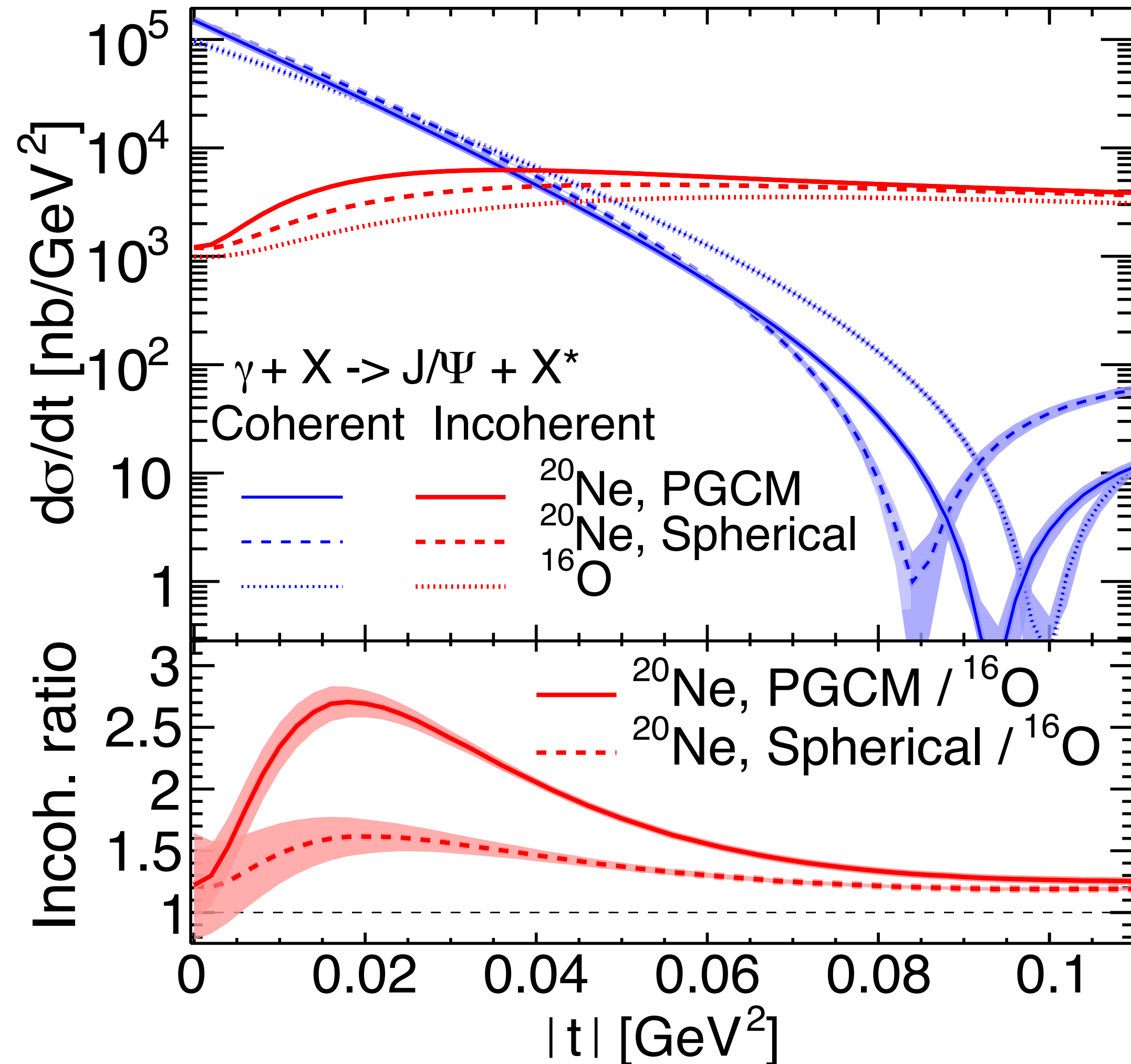
JIMWLK



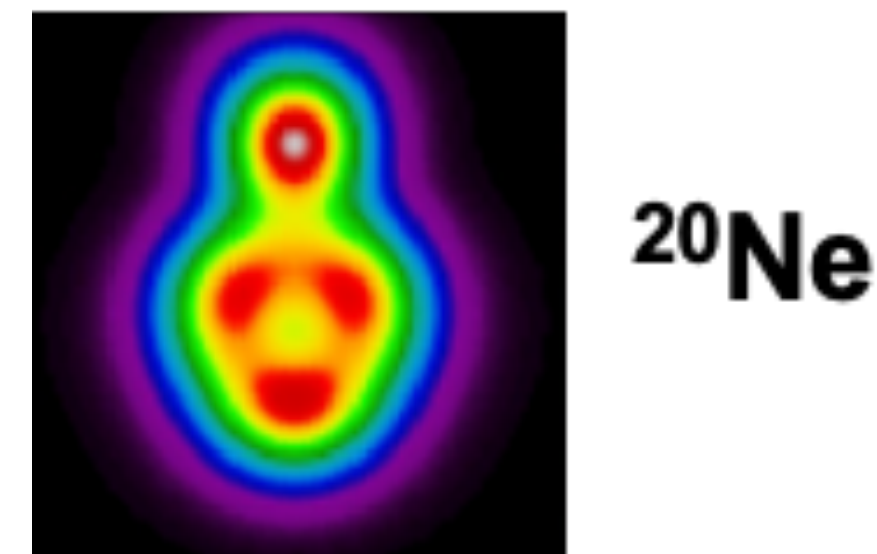
Some changes in the cross section, but deformation effects survive

# Neon and Oxygen targets

H. Mäntysaari, B. Schenke, C. Shen, W. Zhao, *Phys. Rev. Lett.* **131**, 062301 (2023)



- <sup>20</sup>Ne has a bowling pin shape that leads to an increased incoherent cross section relative to an assumed spherical (on average) neon or a spherical oxygen

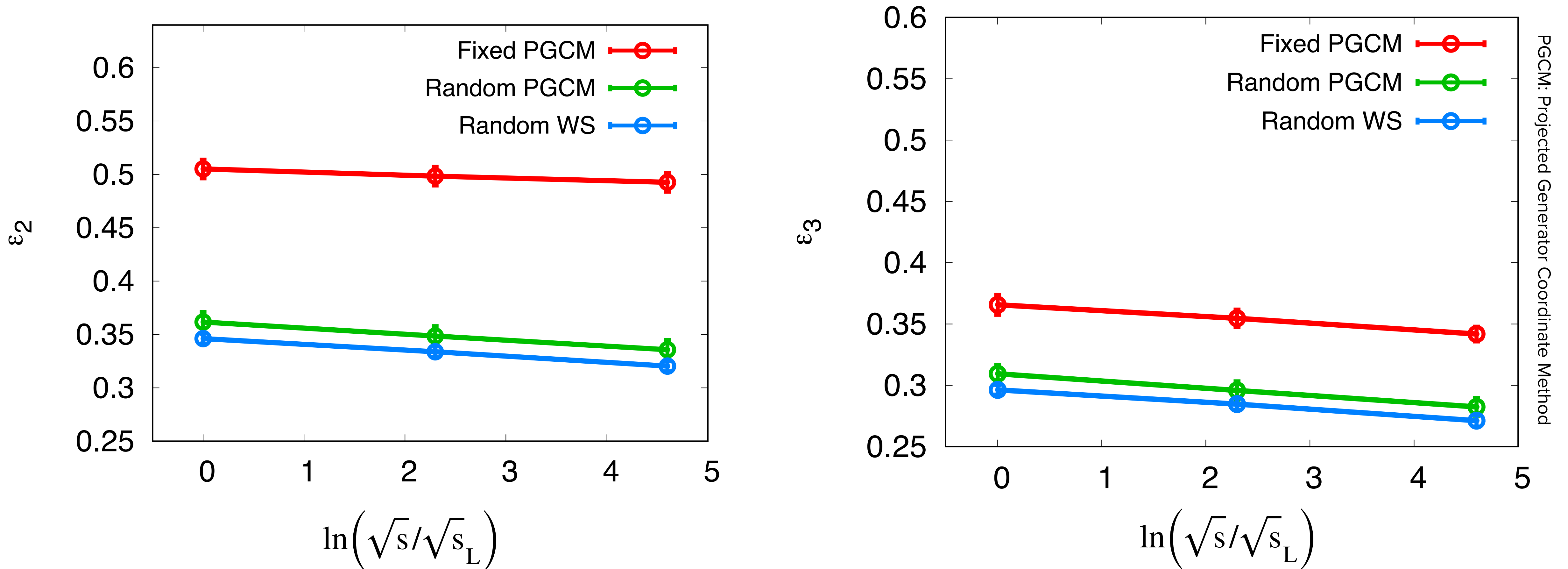


PGCM: Projected Generator Coordinate Method: B. Bally et al., “Deciphering small system collectivity with bowling-pin-shaped <sup>20</sup>Ne isotopes,” in preparation (2023); Mikael Frosini, Thomas Duguet, Jean-Paul Ebran, Benjamin Bally, Tobias Mongelli, Tomá’s R. Rodríguez, Robert Roth, and Vittorio Soma, *Eur. Phys. J. A* **58**, 63 (2022)

# Neon+Neon collisions - JIMWLK evolution

G. Giacalone, B. Schenke, S. Schlichting, P. Singh, in progress

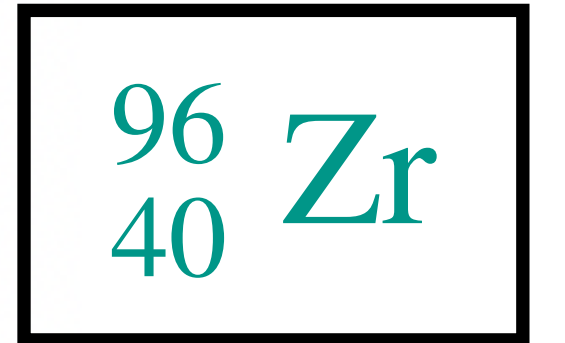
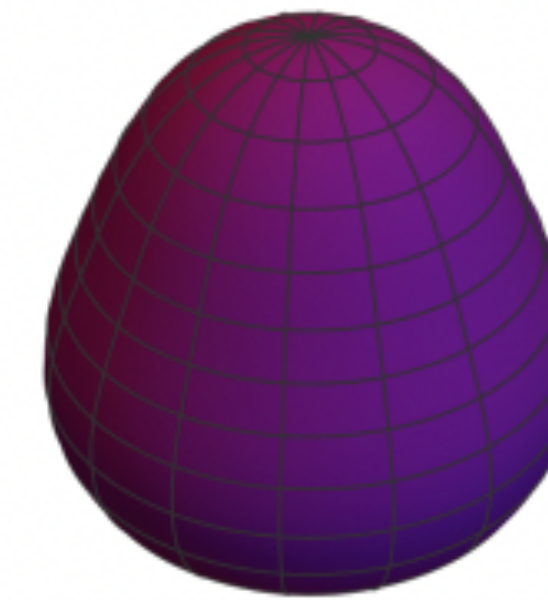
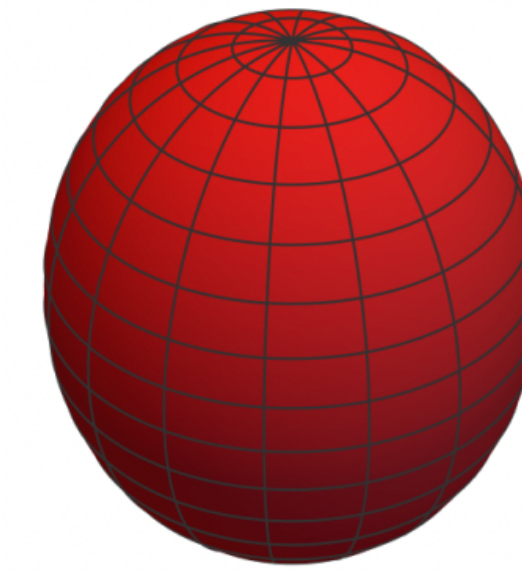
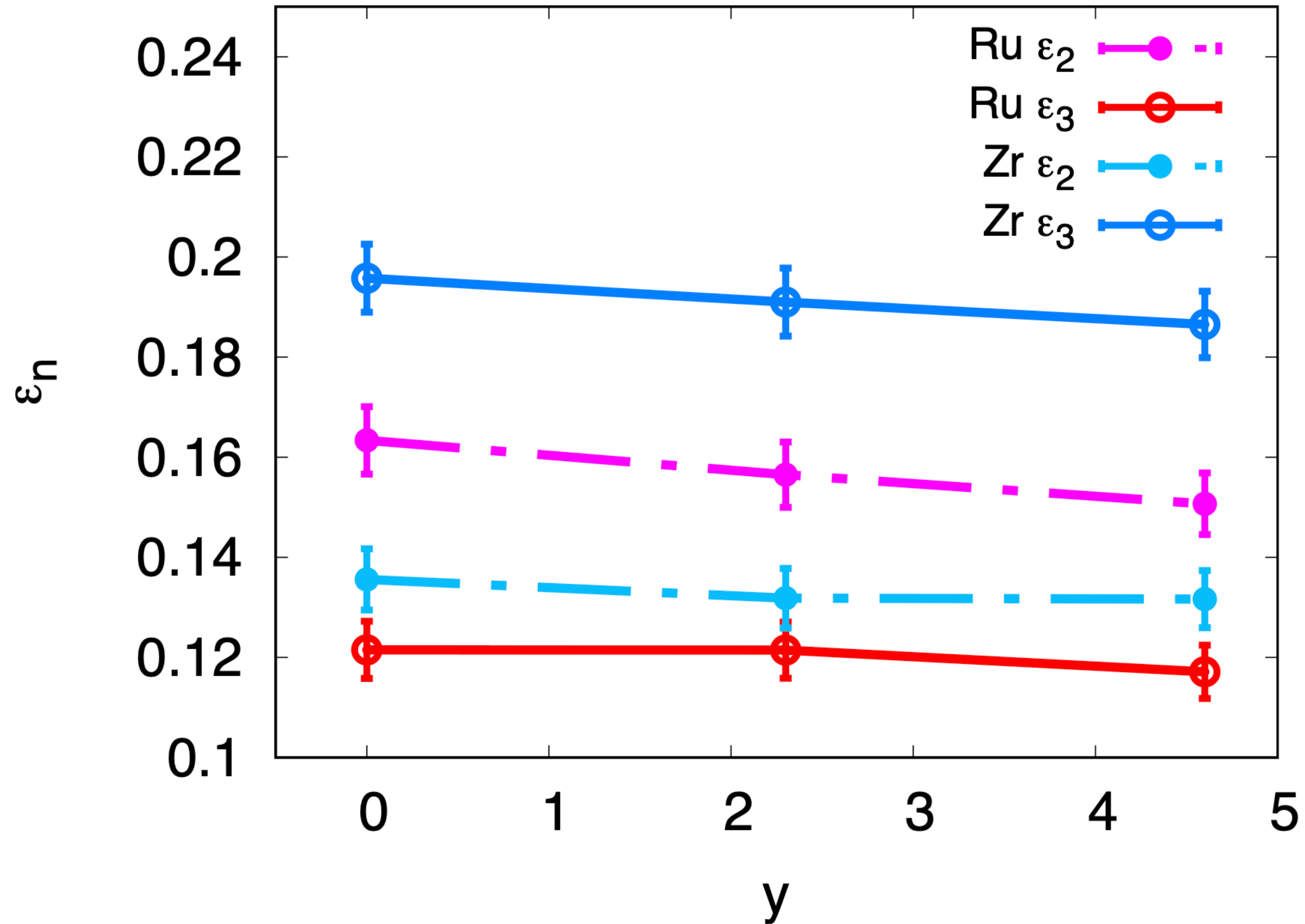
- After the collision at different energies ( $x$ ), measure the spatial eccentricities



- Expected reduction - smoother distributions, but no large change

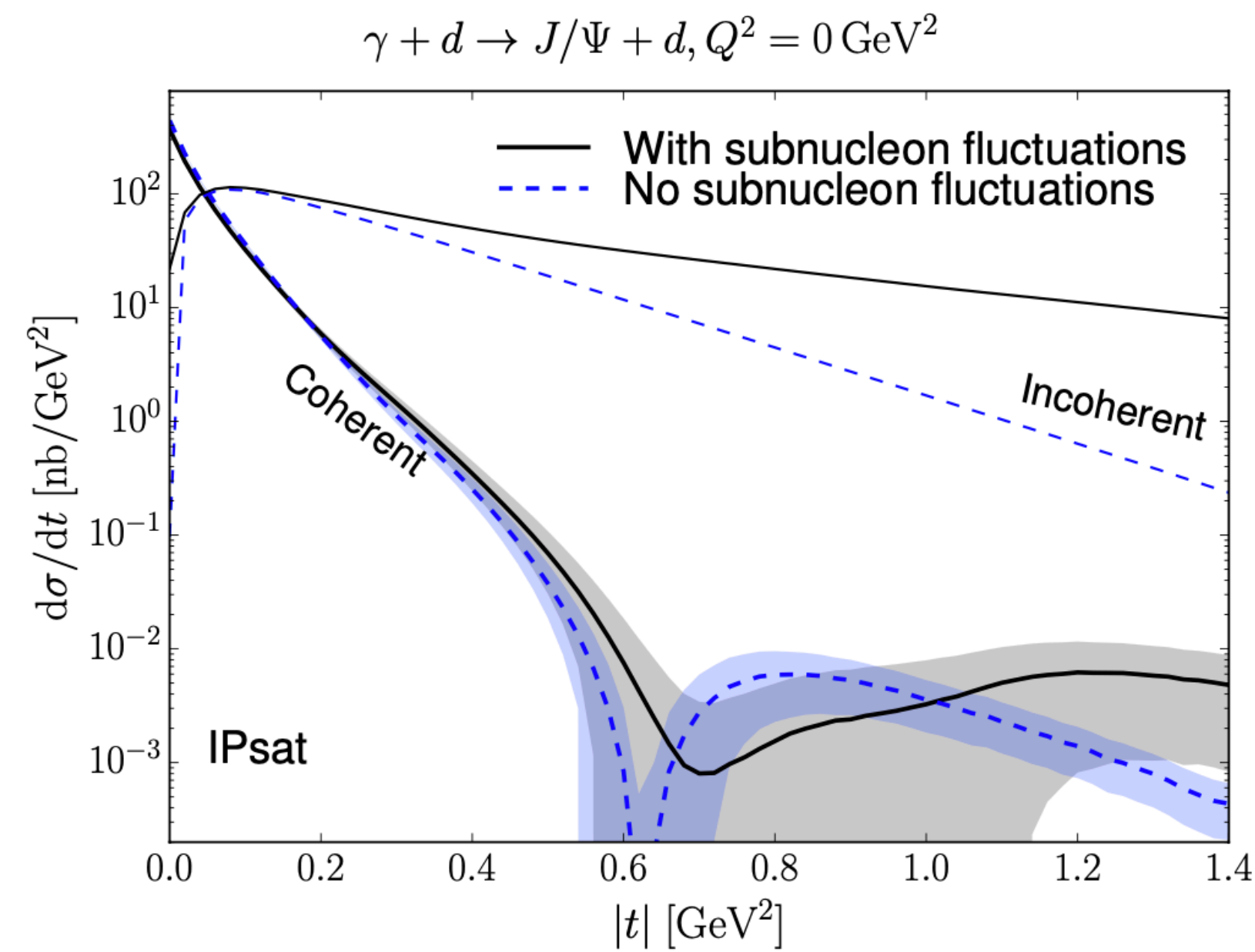
# Isobar shapes - JIMWLK evolution

G. Giacalone, B. Schenke, S. Schlichting, P. Singh, in progress

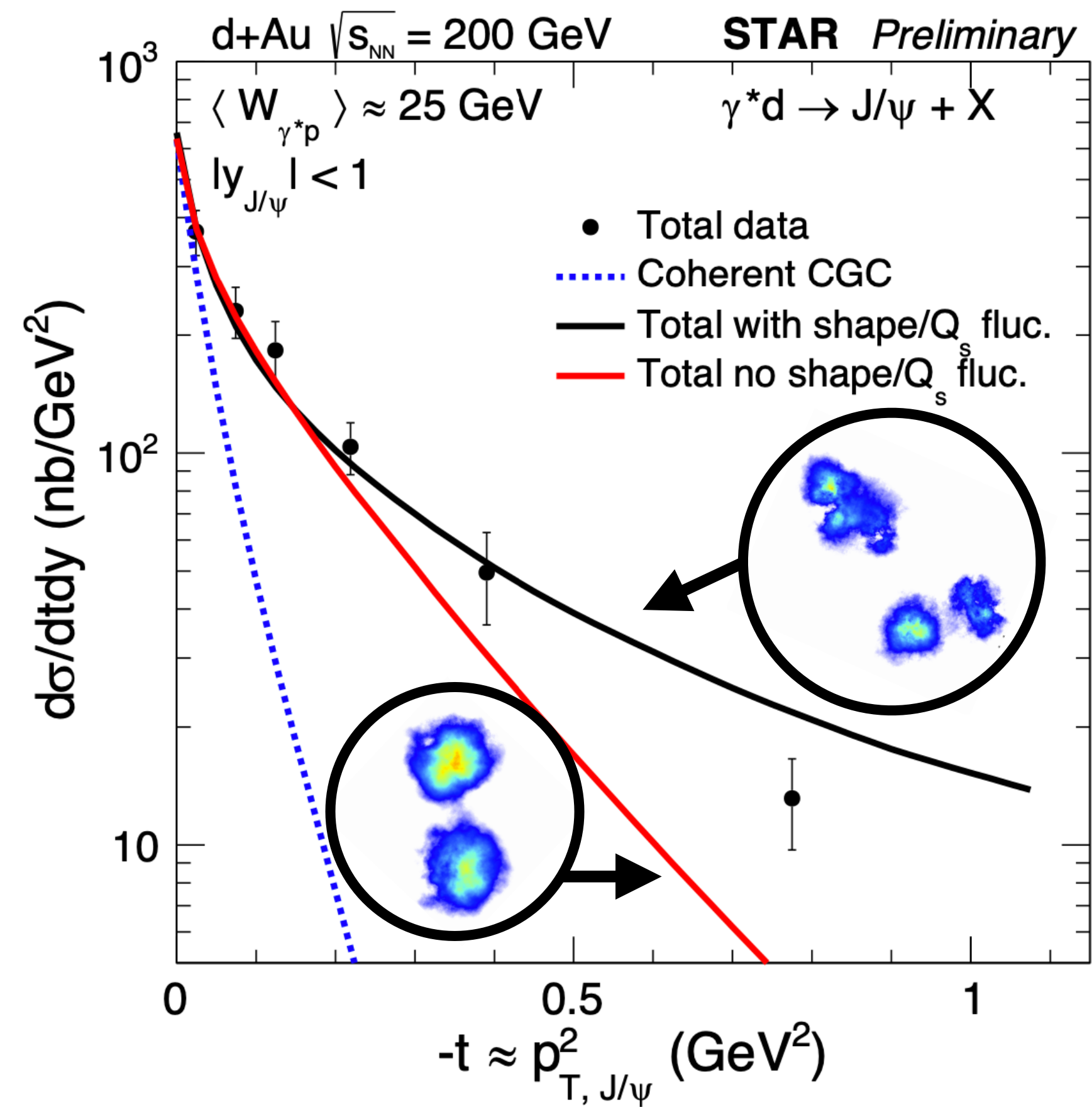


# Photoproduction of $J/\psi$ in d+Au collisions at STAR

H. Mäntysaari, B. Schenke, Phys. Rev. C101, 015203 (2020)



Can also access details of deuteron wave function (BACKUP)



Substructure: large effect on incoherent at  $|t| \gtrsim 0.25 \text{ GeV}^2$  (as in Pb)

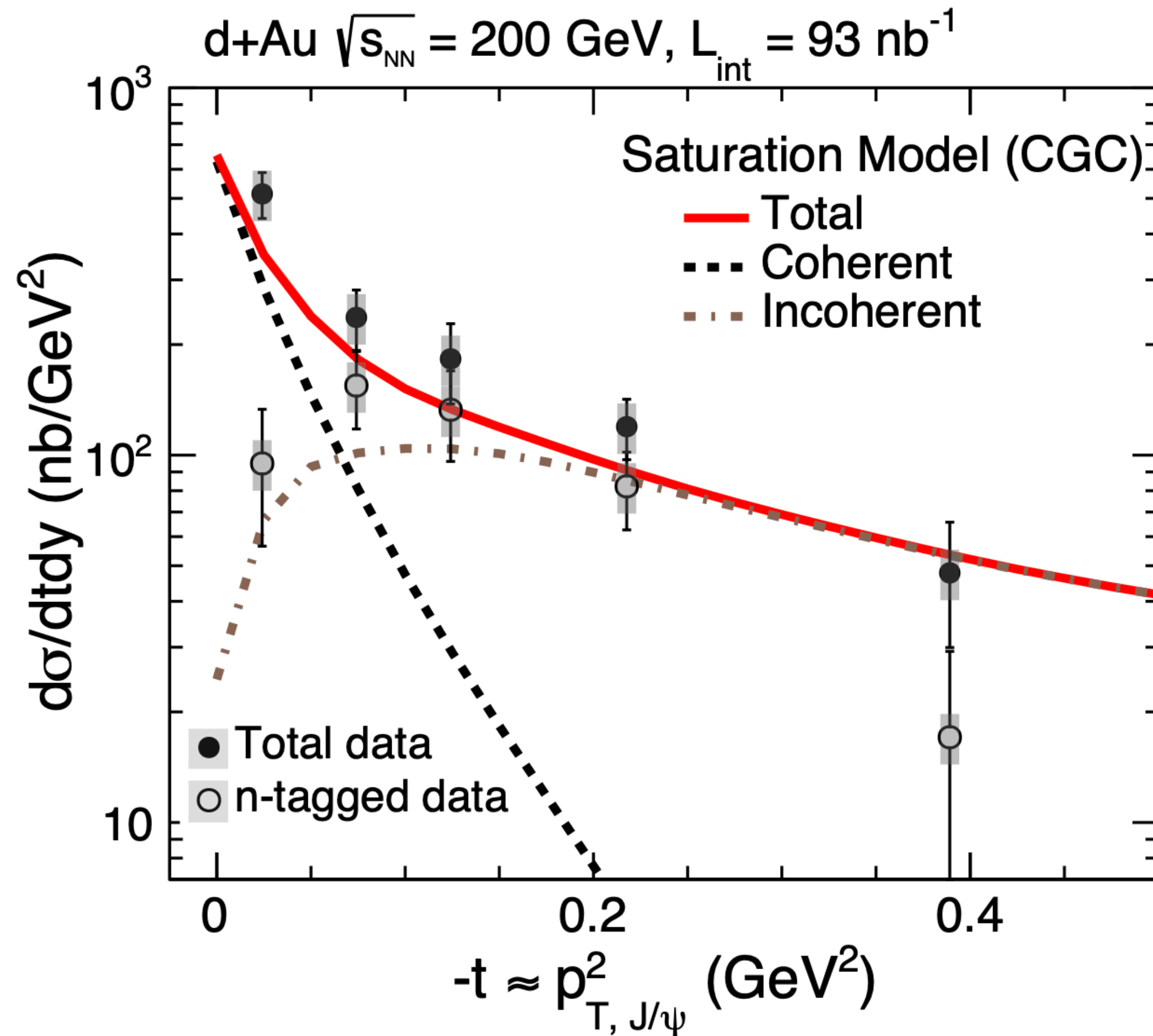
STAR data favors substructure

STAR Collaboration at Hard Probes 2020

PoS HardProbes2020 (2021) 100; arXiv:2009.04860

# Photoproduction of $J/\psi$ in d+Au collisions at STAR

H. Mäntysaari, B. Schenke, Phys. Rev. C101, 015203 (2020)

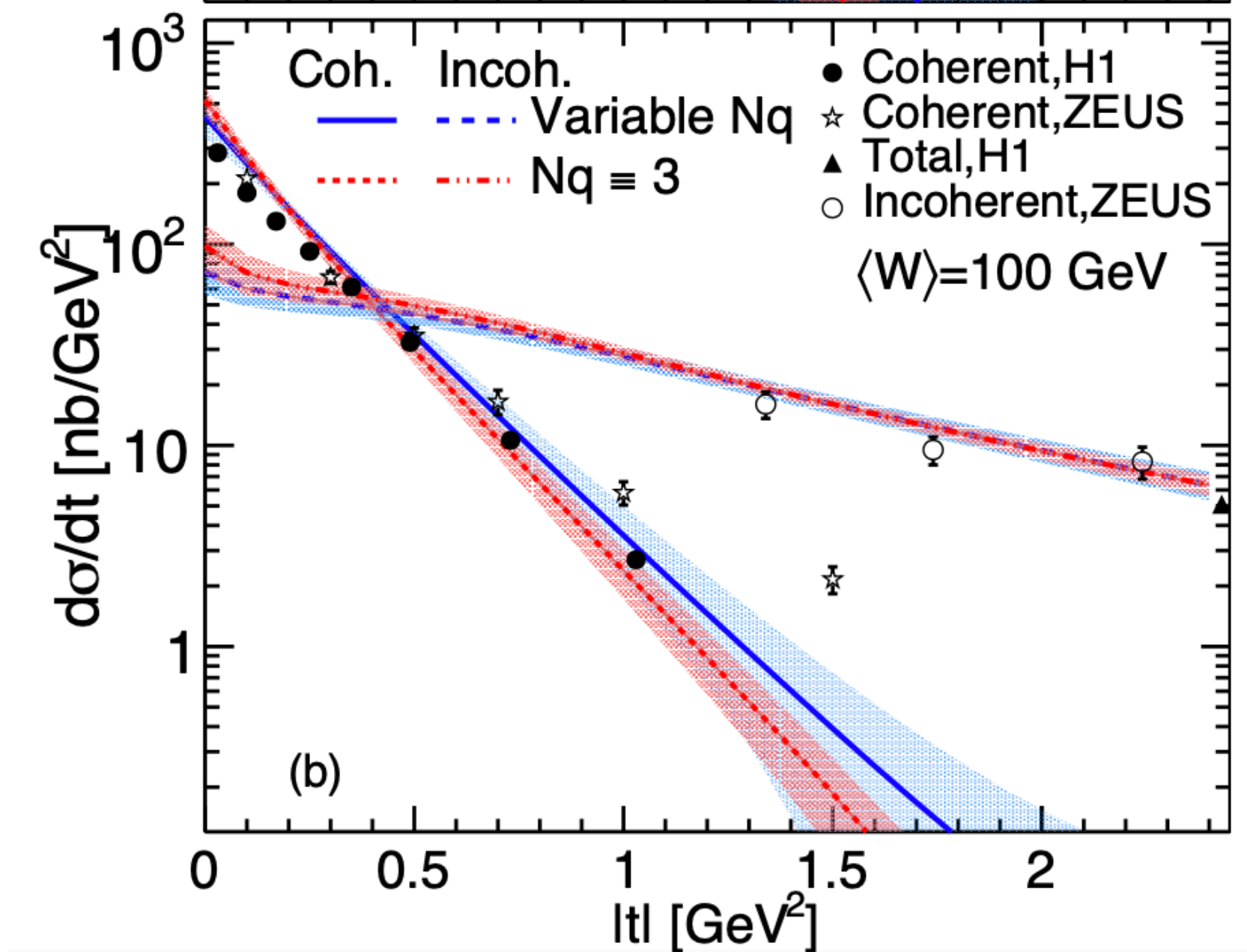
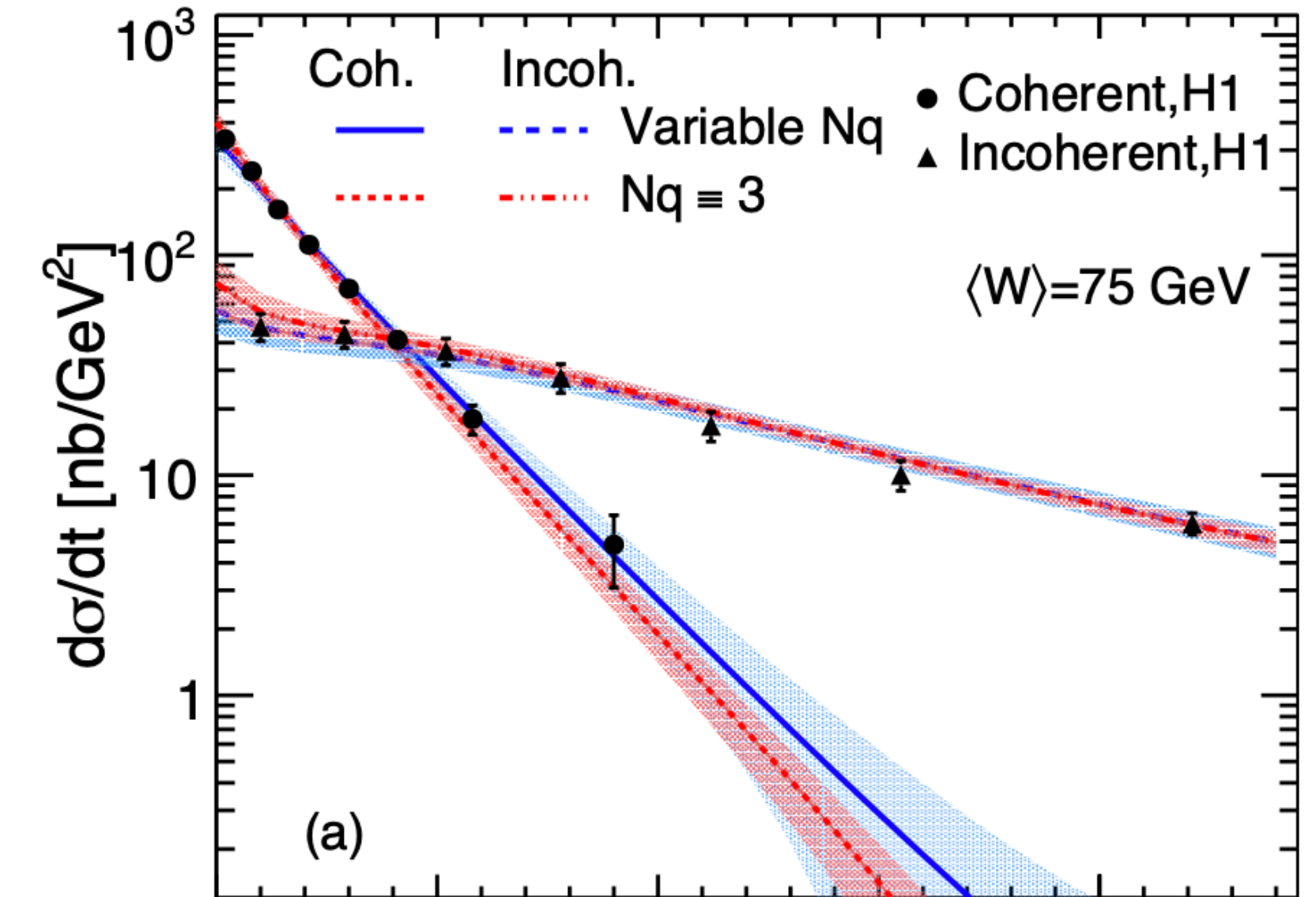
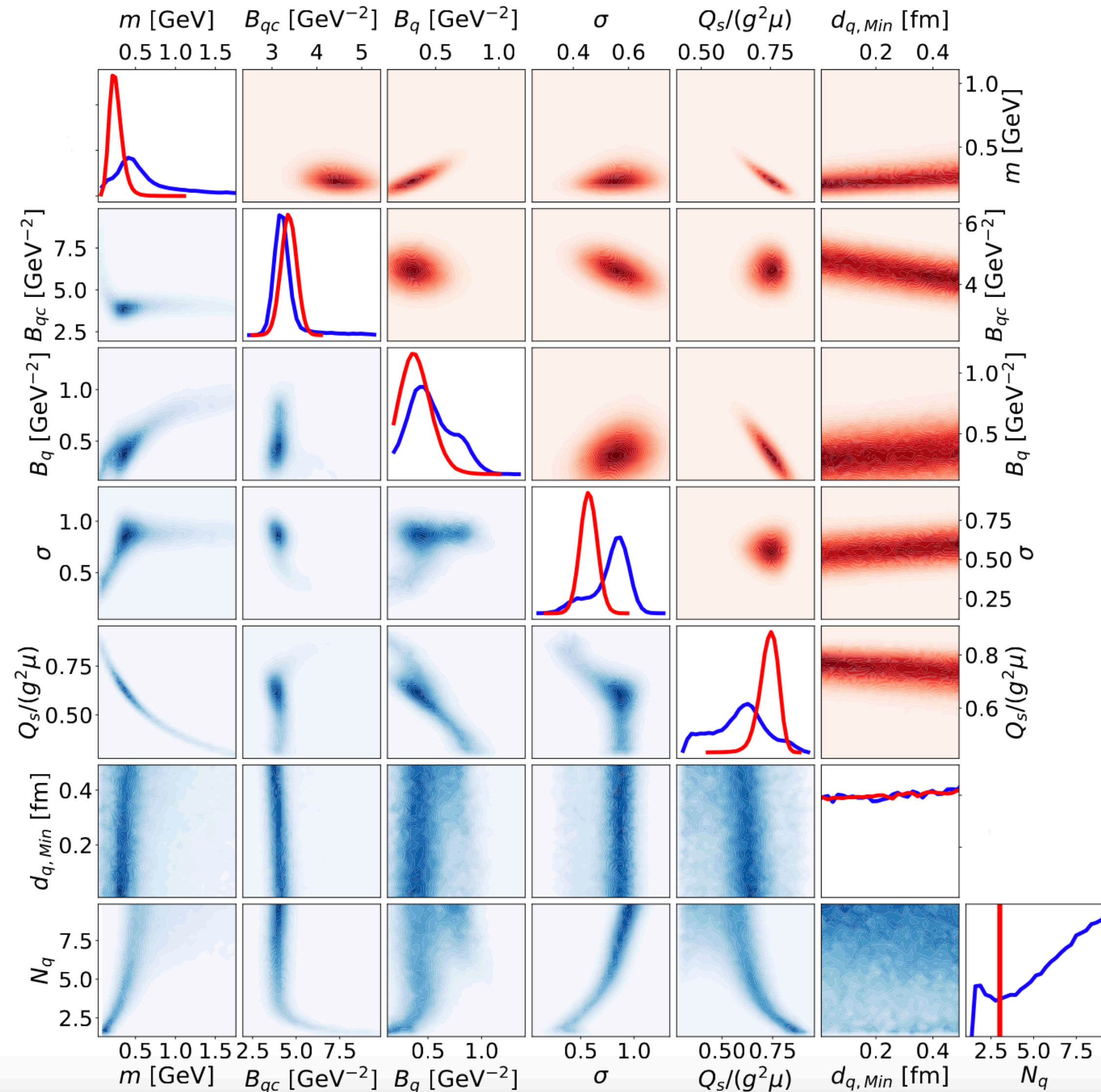


n-tagged results can be compared to incoherent cross section

STAR Collaboration, Phys. Rev. Lett. 128, 122303, (2022) e-Print: 2109.07625

# Extracting parameters using Bayesian inference

H. Mäntysaari, B. Schenke, C. Shen, W. Zhao, Phys.Lett.B 833 (2022) 137348

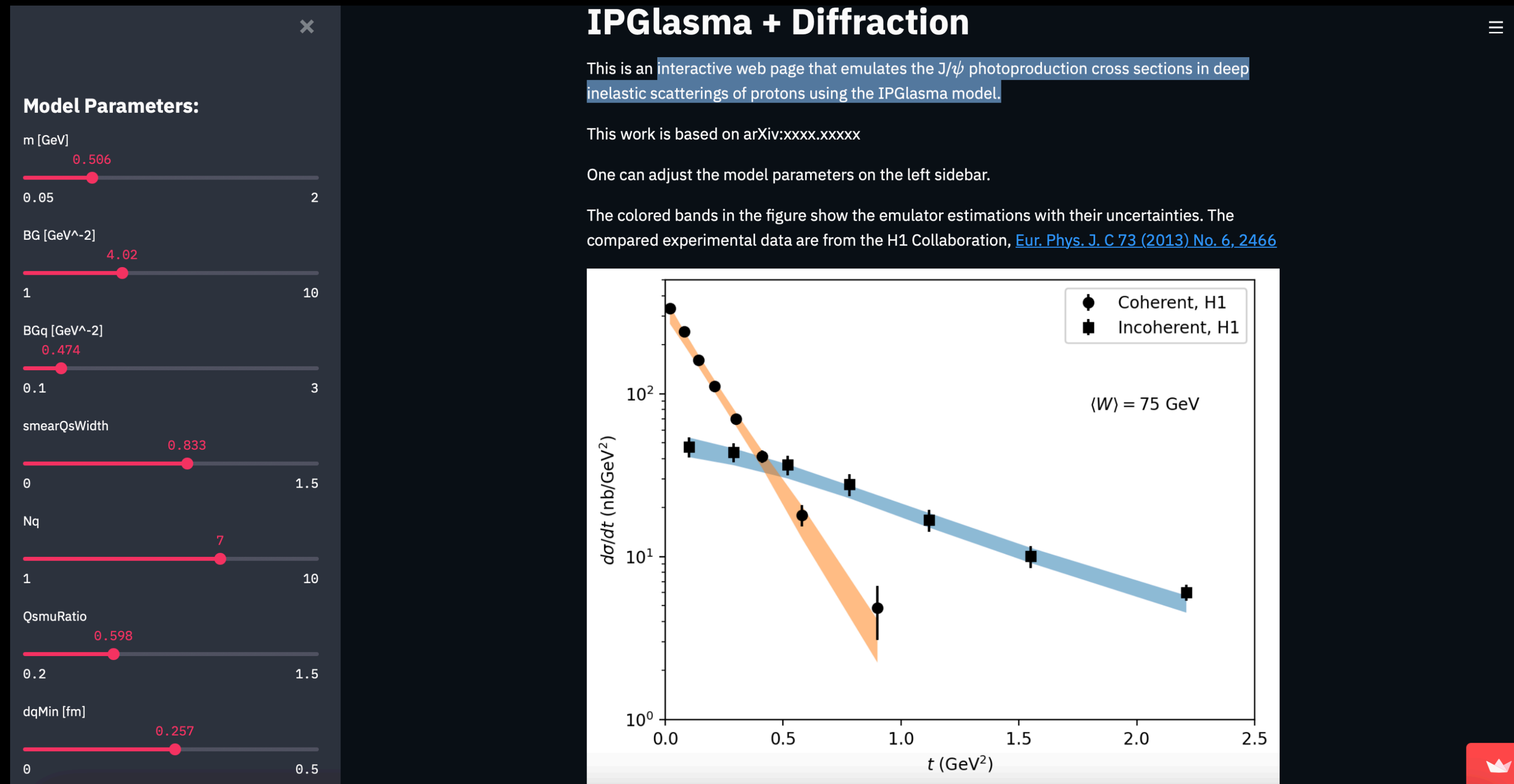


# Bayesian inference

H. Mäntysaari, B. Schenke, C. Shen, W. Zhao, [arXiv:2202.01998 \[hep-ph\]](https://arxiv.org/abs/2202.01998)

See the effect of changing parameters on the cross sections at

[https://share.streamlit.io/chunshen1987/ipglasmaidiffractionstreamlit/main/IPGlasmaDiffraction\\_app.py](https://share.streamlit.io/chunshen1987/ipglasmaidiffractionstreamlit/main/IPGlasmaDiffraction_app.py)

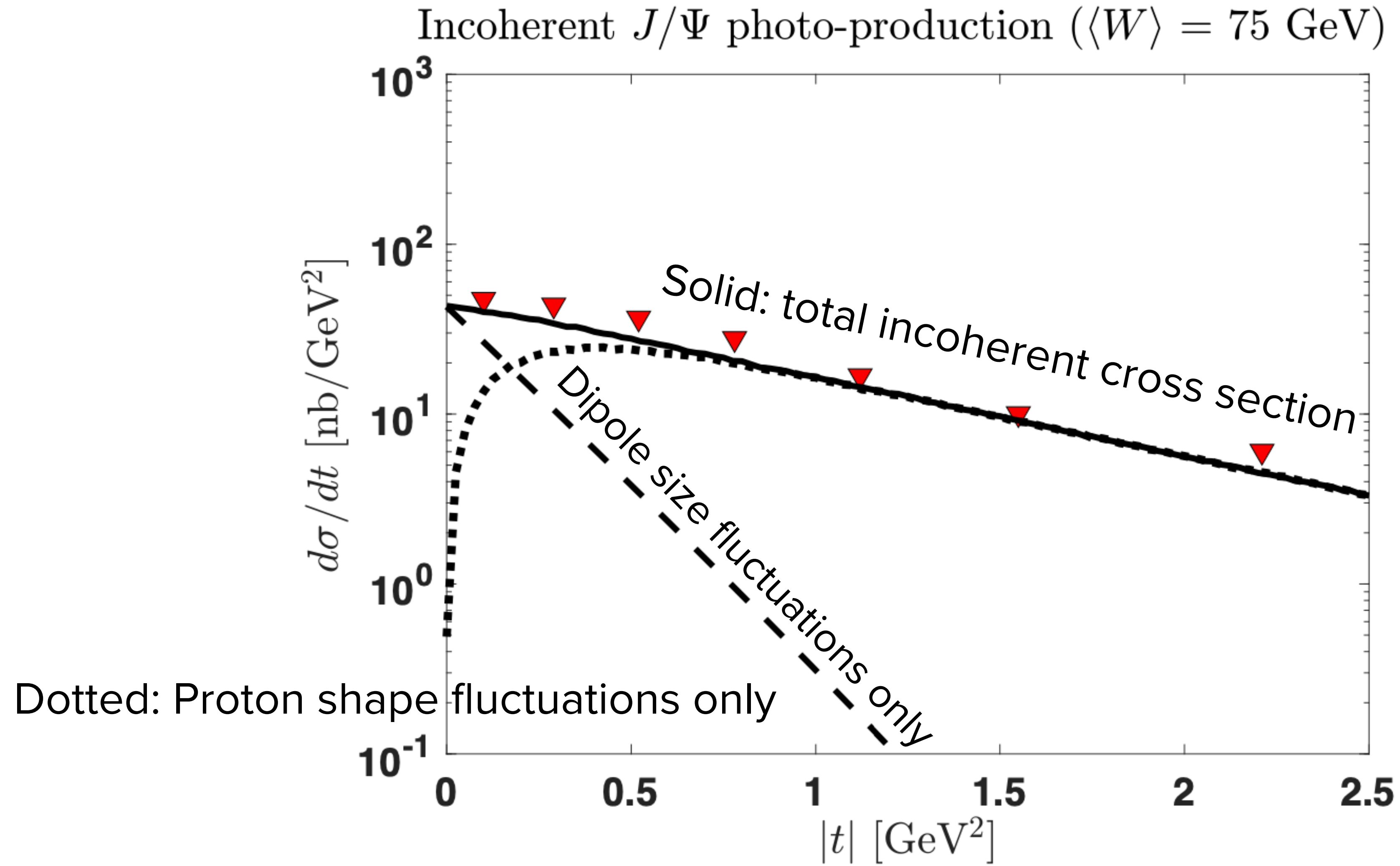


This website also provides posterior samples for your own application



# Dipole size fluctuations

Blaizot and Traini, 2209.15545 [hep-ph]



# Good-Walker/Miettinen-Pumplin

M. L. Good and W. D. Walker, Phys. Rev. 120 (1960) 1857  
H. I. Miettinen and J. Pumplin, Phys. Rev. D18 (1978) 1696

Discussing mainly diffractive scattering in p+p collisions, Miettinen and Pumplin ask two questions:

1. What are the states which diagonalize the diffractive part of the S-matrix, so that their interactions are described simply by absorption coefficients?

*Answer in their paper:* States of the parton model (fixed number  $N$ , positions  $\vec{b}_i$ , fixed  $x$ )

2. What causes the large variations in the absorption coefficients at a given impact parameter, which are implied by the large cross section for diffractive production?

*Answer in their paper:* Fluctuations in  $N$ ,  $\vec{b}_i$ ,  $x$  between the states. “Among the parton states which describe a high-energy hadron, there are some which are rich in wee partons, and are therefore likely to interact, while other states have few or no wee partons, and correspond to the transparent channels of diffraction.”

# Miettinen-Pumplin: Optical Model Formulation

H. I. Miettinen and J. Pumplin, *Phys. Rev. D*18 (1978) 1696

*Target:* Average optical potential

*Beam particle:*  $|B\rangle = \sum_k C_k |\psi_k\rangle$  (linear combination of the eigenstates of diffraction  $|\psi_k\rangle$ )

With  $\text{Im}T = 1 - \text{Re}S$  the imaginary part of the scattering amplitude operator, we have

$$\text{Im}T |\psi_k\rangle = t_k |\psi_k\rangle$$

with  $t_k$  the probability for eigenstate  $|\psi_k\rangle$  to interact with the target (absorption coefficients)

$$\text{Normalize: } \langle B | B \rangle = \sum_k |C_k|^2 = 1$$

$$\text{Elastic scattering: } \langle B | \text{Im}T | B \rangle = \sum_k |C_k|^2 t_k = \langle t \rangle$$

# Miettinen-Pumplin: Cross Sections

H. I. Miettinen and J. Pumplin, Phys. Rev. D18 (1978) 1696

*Total cross section:*

$$d\sigma_{\text{tot}}/d^2\vec{b} = 2\langle t \rangle$$

*Elastic cross section:*

$$d\sigma_{\text{el}}/d^2\vec{b} = \langle t \rangle^2$$

*Incoherent diffractive cross section:*

$$\begin{aligned} d\sigma_{\text{diff}}/d^2\vec{b} &= \sum_k |\langle \psi_k | \text{Im}T | B \rangle|^2 - d\sigma_{\text{el}}/d^2\vec{b} = \sum_k |\langle \psi_k | \text{Im}T | \sum_i C_i |\psi_i\rangle|^2 - d\sigma_{\text{el}}/d^2\vec{b} \\ &= \sum_{k,i} |\langle \psi_k | C_i t_i | \psi_i \rangle|^2 - d\sigma_{\text{el}}/d^2\vec{b} = \sum_{k,i} \delta_{ik} |C_i t_i|^2 - d\sigma_{\text{el}}/d^2\vec{b} = \sum_k |C_k|^2 t_k^2 - \langle t \rangle^2 = \langle t^2 \rangle - \langle t \rangle^2 \end{aligned}$$

$$d\sigma_{\text{diff}}/d^2\vec{b} = \langle t^2 \rangle - \langle t \rangle^2$$

# Color Glass Condensate calculation

- We study diffractive production in e+p/A (not p+p)
- The projectile can be understood as a quark anti-quark dipole (splitting from the incoming virtual photon)
- The fluctuations are included in the target wave function: Fluctuating spatial distribution of the gluon fields (normalization fluctuations correspond to  $N$  fluctuations, spatial fluctuations to  $\vec{b}_i$  fluctuations)  
(see [Blaizot and Traini, 2209.15545 \[hep-ph\]](#) for the effect of fluctuations of the dipole size)

# Fluctuations in the target

Define

$$\hat{T}_p(\vec{b}) = \sum_i^{N_q} T_G(\vec{b}_i - \vec{b}) = \int d^2\vec{x} \hat{\rho}(\vec{x}) T_G(\vec{x} - \vec{b}) \quad T_G \text{ is the gluon distribution in a hot spot}$$

$$\hat{\rho}(\vec{x}) = \sum_i^{N_q} \delta(\vec{x} - \vec{b}_i) \text{ is the hot spot density operator in the transverse plane}$$

The dipole cross section can be written as

$$N = \exp \left[ -\frac{1}{2} \sigma_{\text{dip}}(x, \vec{r}) \hat{T}_p(\vec{b}) \right] \approx 1 - \frac{1}{2} \sigma_{\text{dip}}(x, \vec{r}) \hat{T}_p(\vec{b}) \text{ in the weak field limit}$$

$$\text{The dipole cross section then is } \frac{d\sigma_{q\bar{q}}}{d^2\vec{b}} = 2[1 - N] = \sigma_{\text{dip}}(x, \vec{r}) \hat{T}_p(\vec{b})$$

# Fluctuations in the target

The dipole cross section then is  $\frac{d\sigma_{q\bar{q}}}{d^2\vec{b}} = 2[1 - N] = \sigma_{\text{dip}}(x, \vec{r}) \hat{T}_p(\vec{b})$

This operator is diagonal in the basis of states  $|\vec{b}_1, \dots, \vec{b}_{N_q}\rangle$ , where the  $\vec{b}_i$  are the positions of the individual hot spots, frozen during the collision process:

*These states can be considered the diffractive eigenstates*

Coherent diffractive cross section:

$$\int d^2\vec{b} d^2\vec{b}' e^{-i\vec{\Delta} \cdot (\vec{b} - \vec{b}')} \left\langle \frac{d\sigma^{q\bar{q}}}{d^2\vec{b}} \right\rangle \left\langle \frac{d\sigma^{q\bar{q}}}{d^2\vec{b}'} \right\rangle = \langle \Sigma_{q\bar{q}}(\vec{\Delta}) \rangle^2$$

with  $\Sigma_{q\bar{q}}(\vec{\Delta}) = \int d^2\vec{b} e^{-i\vec{\Delta} \cdot \vec{b}} \frac{d\sigma^{q\bar{q}}}{d^2\vec{b}}$  and  $\langle \cdot \rangle$  is the average over the ground state wave function

# Fluctuations in the target

Total diffractive cross section:

Allow all possible diffractive eigenstates  $|\alpha\rangle$  as intermediate states (assume dilute limit here)

$$\int d^2\vec{b} d^2\vec{b}' e^{-i\vec{\Delta}\cdot(\vec{b}-\vec{b}')} \sigma_{\text{dip}}^2 \sum_{\alpha} \left| \langle \alpha | \hat{T}_p(\vec{b}) | \psi_0 \rangle \right|^2 = \langle \Sigma_{q\bar{q}}^2(\vec{\Delta}) \rangle$$

in analogy to the optical model example

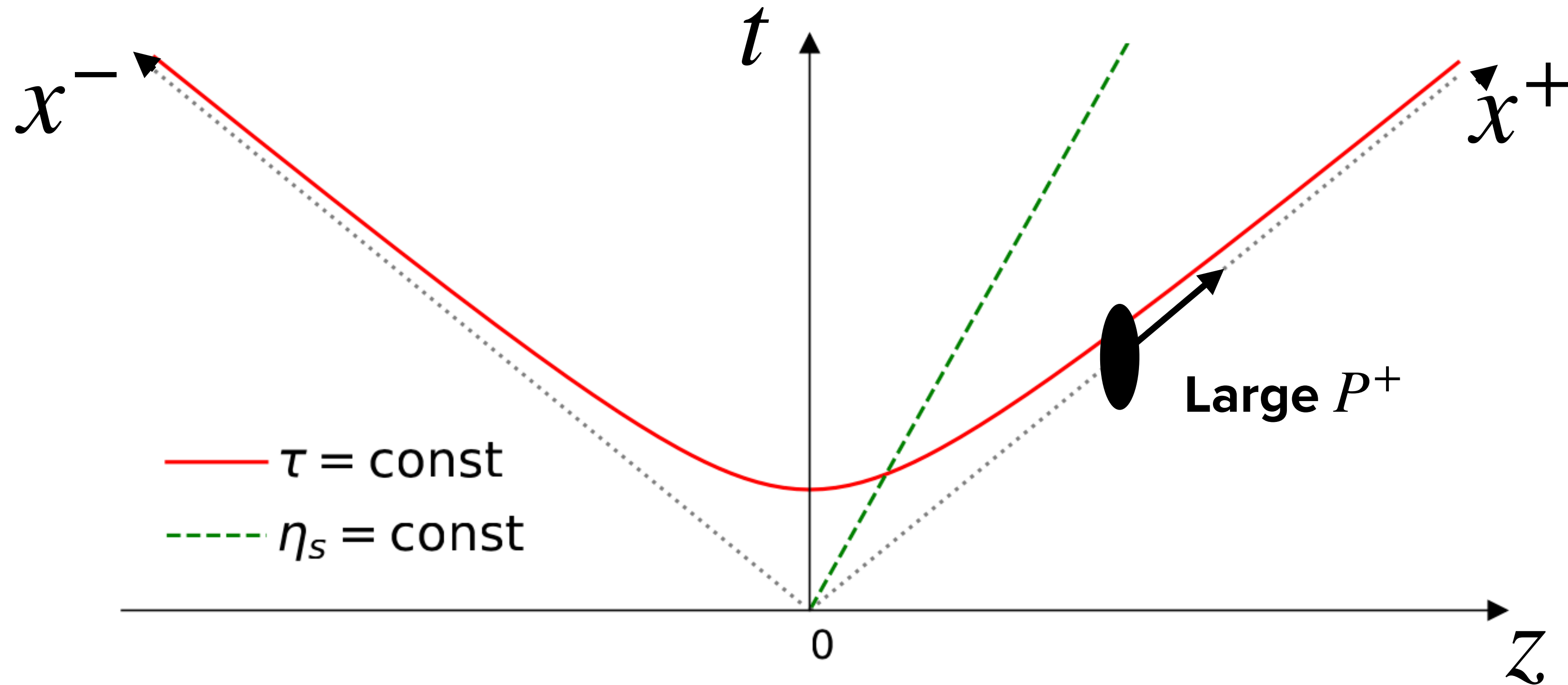
This also shows the relation to the density-density correlation function  $\langle \hat{T}_p(\vec{b}) \hat{T}_p(\vec{b}') \rangle$

and how we are sensitive to different distance scales via  $\vec{b} - \vec{b}'$

See [Blaizot and Traini, 2209.15545 \[hep-ph\]](#) for a more detailed discussion



# The scenario: Hadron moving at high momentum



**Probe hadron (or nucleus) moving with large  $P^+$  at scale  $x_0 P^+$  with  $x_0 \ll 1$**

**Separate partonic content based on longitudinal momentum  $k^+ = x P^+$**

**Large  $x > x_0$ : Static and localized color sources  $\rho$**

# Dynamic color fields

The moving color sources generate a current, independent of light cone time  $z^+$ :

$$J^{\mu,a}(z) = \delta^{\mu+} \rho^a(z^-, z_T) \quad a \text{ is the color index of the gluon}$$

This current generates delocalized dynamical fields  $A^{\mu,a}(z)$  described by the Yang-Mills equations

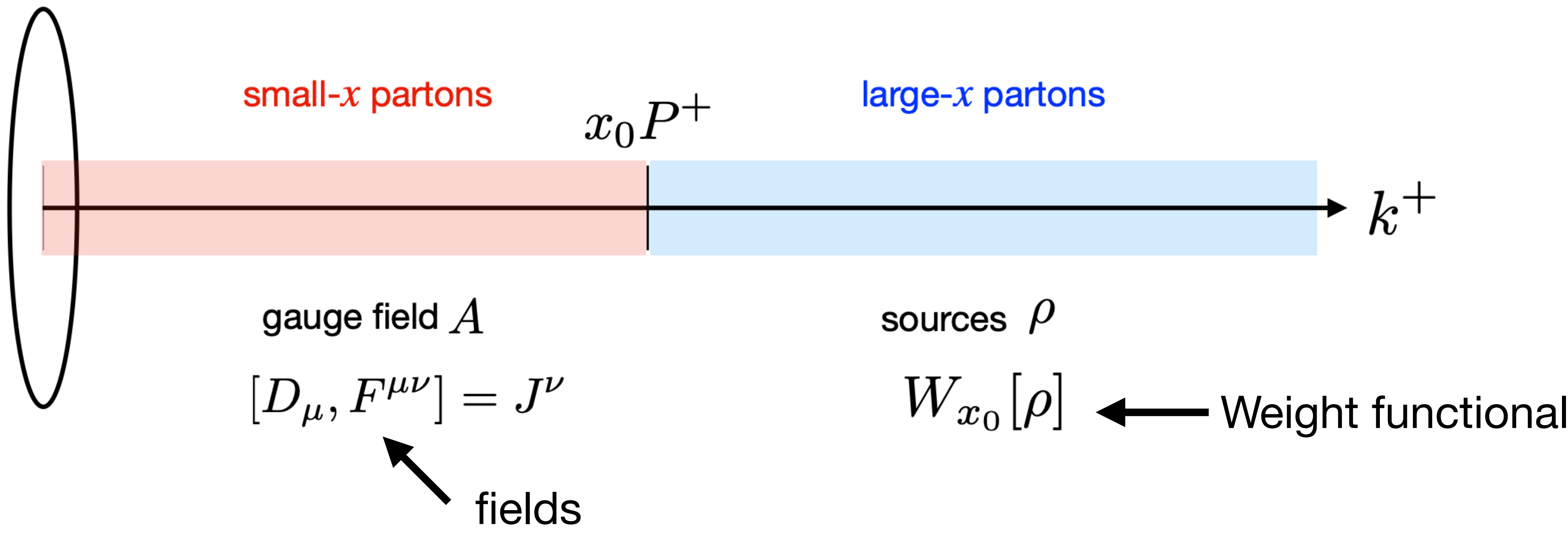
$$[D_\mu, F^{\mu\nu}] = J^\nu$$

with  $D_\mu = \partial_\mu + igA_\mu$  and  $F_{\mu\nu} = \frac{1}{ig}[D_\mu, D_\nu] = \partial_\mu A_\nu - \partial_\nu A_\mu + ig[A_\mu, A_\nu]$

These fields  $A$  are the small  $x < x_0$  degrees of freedom

They can be treated classically, because their occupation number is large  $\langle AA \rangle \sim 1/\alpha_s$

# Color Glass Condensate (CGC): Sources and fields



When  $x \lesssim x_0$  the path integral  $\langle \mathcal{O} \rangle_\rho$  is dominated by classical solution and we are done

For smaller  $x$  we need to do quantum evolution

# Wilson lines

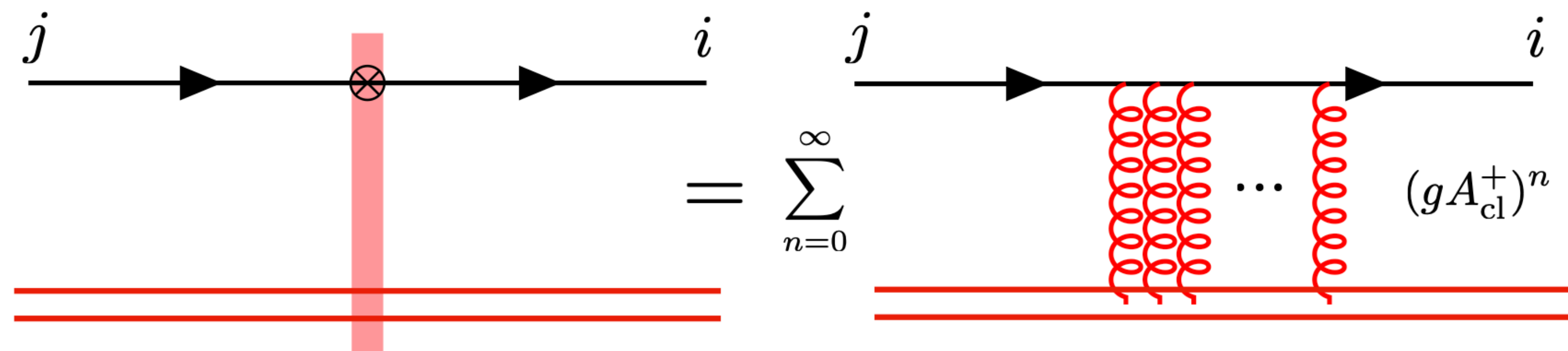
Interaction of high energy color-charged probe with large  $k^-$  momentum (and small  $k^+ = \frac{k_T^2}{2k^-}$ )

with the classical field of a nucleus can be described in the **eikonal approximation**:

The scattering rotates the color, but keeps  $k^-$ , transverse position  $\vec{x}_T$ , and any other quantum numbers the same.

The color rotation is encoded in a light-like Wilson line, which for a quark probe reads

$$V_{ij}(\vec{x}_T) = \mathcal{P} \left( ig \int_{-\infty}^{\infty} A^{+,c}(z^-, \vec{x}_T) t_{ij}^c dz^- \right)$$



**MULTIPLE INTERACTIONS NEED TO BE RESUMMED, BECAUSE  $A^+ \sim 1/g$**

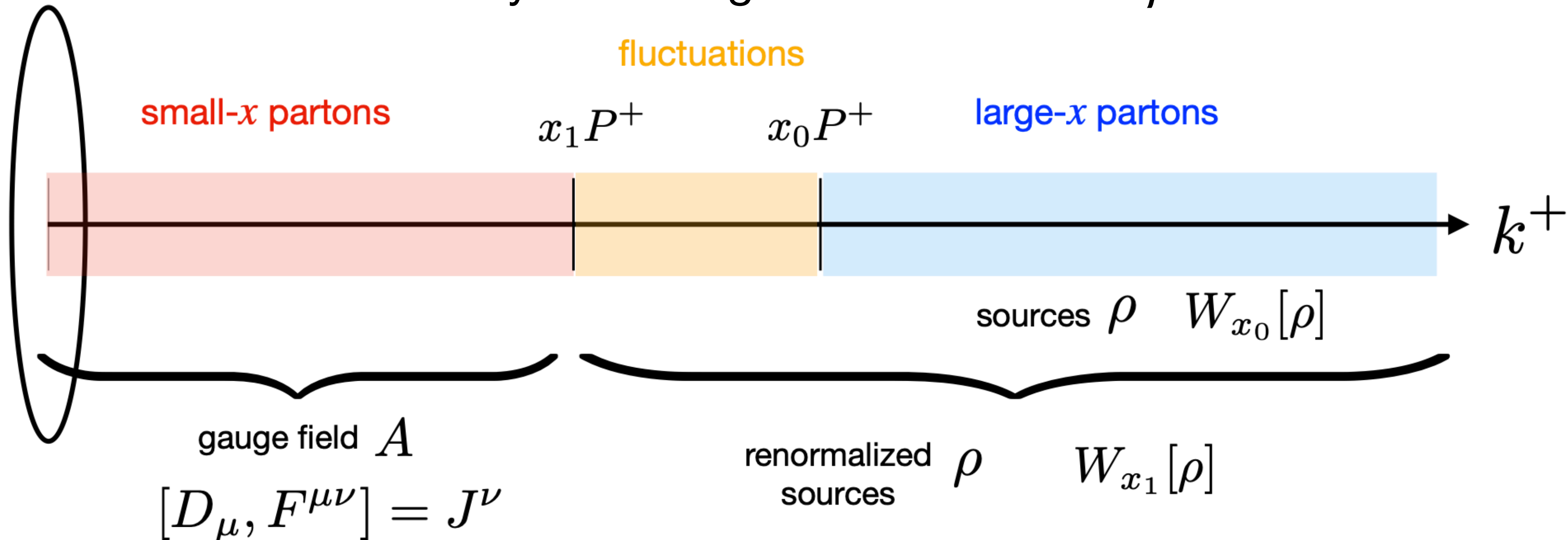
# JIMWLK evolution

Jalilian-Marian, J.; Kovner, A.; McLerran, L.D.; Weigert, H., Phys. Rev. D 1997, 55, 5414–5428, [hep-ph/9606337]  
 Jalilian-Marian, J.; Kovner, A.; Weigert, H., Phys. Rev. D 1998, 59, 014015, [hep-ph/9709432]  
 Kovner, A.; Milhano, J.G.; Weigert, H., Phys. Rev. D 2000, 62, 114005, [hep-ph/0004014]  
 Iancu, E.; Leonidov, A.; McLerran, L.D., Nucl. Phys. A 2001, 692, 583–645, [hep-ph/0011241]  
 Iancu, E.; Leonidov, A.; McLerran, L.D., Phys. Lett. B 2001, 510, 133–144, [hep-ph/0102009]  
 Ferreiro, E.; Iancu, E.; Leonidov, A.; McLerran, L., Nucl. Phys. A 2002, 703, 489–538, [hep-ph/0109115]

LO Small- $x$  evolution resums logarithmically enhanced terms  $\sim \alpha_s \ln(x_0/x)$

$$\frac{dW_x[\rho]}{d \ln(1/x)} = - \mathcal{H}_{\text{JIMWLK}} W_x[\rho]$$

Physically, one absorbs the quantum fluctuations in the interval  $[x_0 - dx, x_0]$  into stochastic fluctuations of the color sources by redefining the color sources  $\rho$



# JIMWLK evolution

Jalilian-Marian, J.; Kovner, A.; McLerran, L.D.; Weigert, H., Phys. Rev. D 1997, 55, 5414–5428, [hep-ph/9606337]  
Jalilian-Marian, J.; Kovner, A.; Weigert, H., Phys. Rev. D 1998, 59, 014015, [hep-ph/9709432]  
Kovner, A.; Milhano, J.G.; Weigert, H., Phys. Rev. D 2000, 62, 114005, [hep-ph/0004014]  
Iancu, E.; Leonidov, A.; McLerran, L.D., Nucl. Phys. A 2001, 692, 583–645, [hep-ph/0011241]  
Iancu, E.; Leonidov, A.; McLerran, L.D., Phys. Lett. B 2001, 510, 133–144, [hep-ph/0102009]  
Ferreiro, E.; Iancu, E.; Leonidov, A.; McLerran, L., Nucl. Phys. A 2002, 703, 489–538, [hep-ph/0109115]

LO Small- $x$  evolution resums logarithmically enhanced terms  $\sim \alpha_s \ln(x_0/x)$

$$\frac{dW_x[\rho]}{d \ln(1/x)} = - \mathcal{H}_{\text{JIMWLK}} W_x[\rho]$$

Physically, one absorbs the quantum fluctuations in the interval  $[x_0 - dx, x_0]$  into stochastic fluctuations of the color sources by redefining the color sources  $\rho$

Evolution is done using the Langevin formulation of the JIMWLK equations on the level of Wilson lines

K. Rummukainen and H. Weigert Nucl. Phys. A739 (2004) 183; T. Lappi, H. Mäntysaari, Eur. Phys. J. C73 (2013) 2307

Long distance tails are tamed by imposing a regulator in the JIMWLK kernel,  $m$

S. Schlichting, B. Schenke, Phys.Lett. B739 (2014) 313-319

# Connection between the initial state of heavy ion collisions and the EIC

- These Wilson lines are the building blocks of the CGC
- In heavy ion collisions, one can compute the initial state by determining Wilson lines after the collision from the Wilson lines of the colliding nuclei
- At the EIC (and HERA, and in UPCs), cross sections will be calculated as convolutions of Wilson line correlators with perturbatively calculable and process-dependent impact factors
- This allows the computation of rather direct constraints for the initial state of heavy ion collisions from electron-nucleus ( $\gamma$ -nucleus) or electron-proton collisions

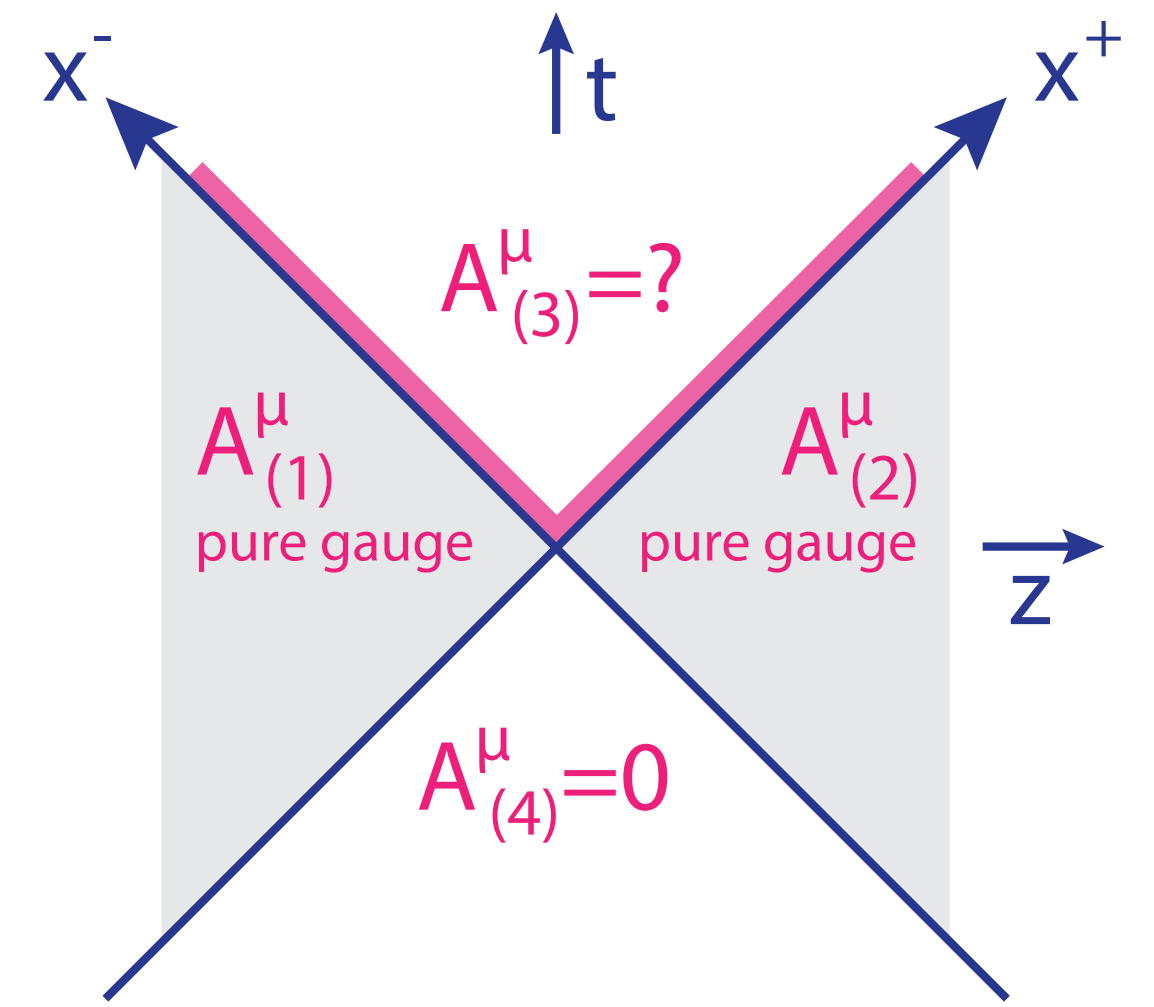
# Heavy ion collision

Compute gluon fields after the collision using light cone gauge:

$A^+ = 0$  for a right moving nucleus,  $A^- = 0$  for a left moving nucleus

gauge transformation:  $A_\mu(x) \rightarrow V(x) \left( A_\mu(x) - \frac{i}{g} \partial_\mu \right) V^\dagger(x)$

using our Wilson lines  $V^\dagger(x^-, \mathbf{x}_\perp) = \mathcal{P} \exp \left( -ig \int_{-\infty}^{x^-} dz^- A^+(z^-, \mathbf{x}_\perp) \right)$  (for the right moving nucleus)



Then, the gauge fields read (choosing  $A^\mu = 0$  for the quadrant for  $x^- < 0$  and  $x^+ < 0$ )

$$A^i(x) = \theta(x^+) \theta(x^-) \alpha^i(\tau, \mathbf{x}_\perp) + \theta(x^-) \theta(-x^+) \alpha_P^i(\mathbf{x}_\perp) + \theta(x^+) \theta(-x^-) \alpha_T^i(\mathbf{x}_\perp)$$

$$A^\eta(x) = \theta(x^+) \theta(x^-) \alpha^\eta(\tau, \mathbf{x}_\perp) \quad \text{with } \alpha_P^i(\mathbf{x}_\perp) = \frac{1}{ig} V_P(\mathbf{x}_\perp) \partial^i V_P^\dagger(\mathbf{x}_\perp) \text{ and } \alpha_T^i(\mathbf{x}_\perp) = \frac{1}{ig} V_T(\mathbf{x}_\perp) \partial^i V_T^\dagger(\mathbf{x}_\perp)$$

$$A^\tau = 0, \text{ because we chose Fock-Schwinger gauge } x^+ A^- + x^- A^+ = 0$$



# Heavy ion collision

Plugging this ansatz

$$A^i(x) = \theta(x^+)\theta(x^-)\alpha^i(\tau, \mathbf{x}_\perp) + \theta(x^-)\theta(-x^+)\alpha_P^i(\mathbf{x}_\perp) + \theta(x^+)\theta(-x^-)\alpha_T^i(\mathbf{x}_\perp)$$

$$A^\eta(x) = \theta(x^+)\theta(x^-)\alpha^\eta(\tau, \mathbf{x}_\perp)$$

into YM equations leads to singular terms on the boundary from derivatives of  $\theta$ -functions

Requiring that the singularities vanish leads to the solutions

$$\alpha^i = \alpha_P^i + \alpha_T^i \quad \alpha^\eta = -\frac{ig}{2} \left[ \alpha_{Pj}, \alpha_T^j \right] \quad \begin{aligned} \partial_\tau \alpha^i &= 0 \\ \partial_\tau \alpha^\eta &= 0 \end{aligned}$$

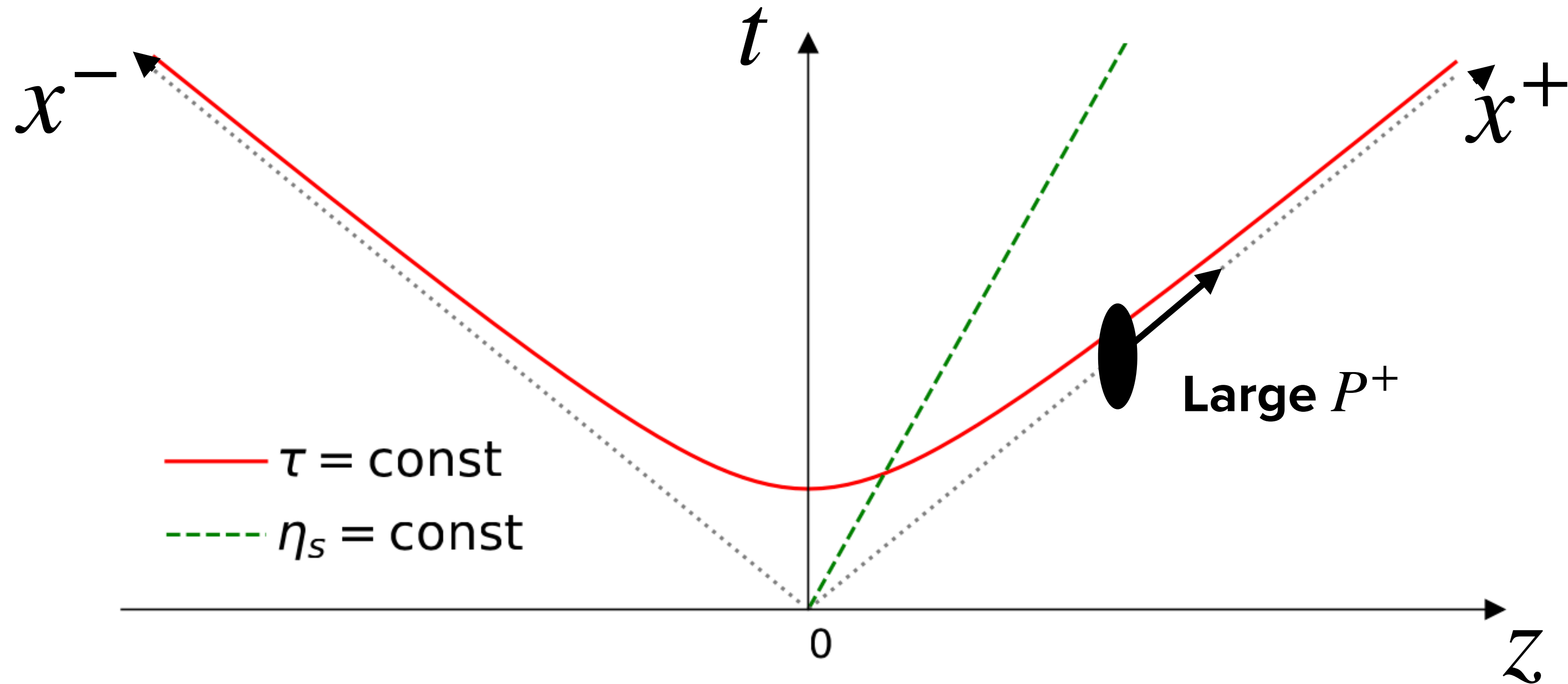
These are the gauge fields in the forward light cone.

We can compute  $T^{\mu\nu}$  from it, providing an initial condition for hydrodynamics.

# Geometry, fluctuations, ...

- All the information on geometry and nucleon and sub-nucleon fluctuations is contained in the distribution of color charges  $\rho_{P/T}^a(x^\mp, \mathbf{x}_\perp)$
- Typically, use the MV model, which gives
$$\langle \rho^a(\mathbf{b}_\perp) \rho^b(\mathbf{x}_\perp) \rangle = g^2 \mu^2(x, \mathbf{b}_\perp) \delta^{ab} \delta^{(2)}(\mathbf{b}_\perp - \mathbf{x}_\perp)$$
- The color charge distribution  $g^2 \mu(x, \mathbf{b}_\perp)$  depends on the longitudinal momentum fraction  $x$  and the transverse position  $\mathbf{b}_\perp$ . The latter needs to be modeled, the former can be modeled or obtained from e.g. JIMWLK evolution
- We factorize  $\mu(x, \mathbf{b}_\perp) \sim T(\mathbf{b}_\perp) \mu(x)$  and constrain the impact parameter  $\mathbf{b}_\perp$  dependence using input from a process sensitive to geometry, such as diffractive VM production
- The cross section for that process can be expressed with the Wilson lines of the target  
The same quantities we have used to initialize the heavy ion collision

# Color sources

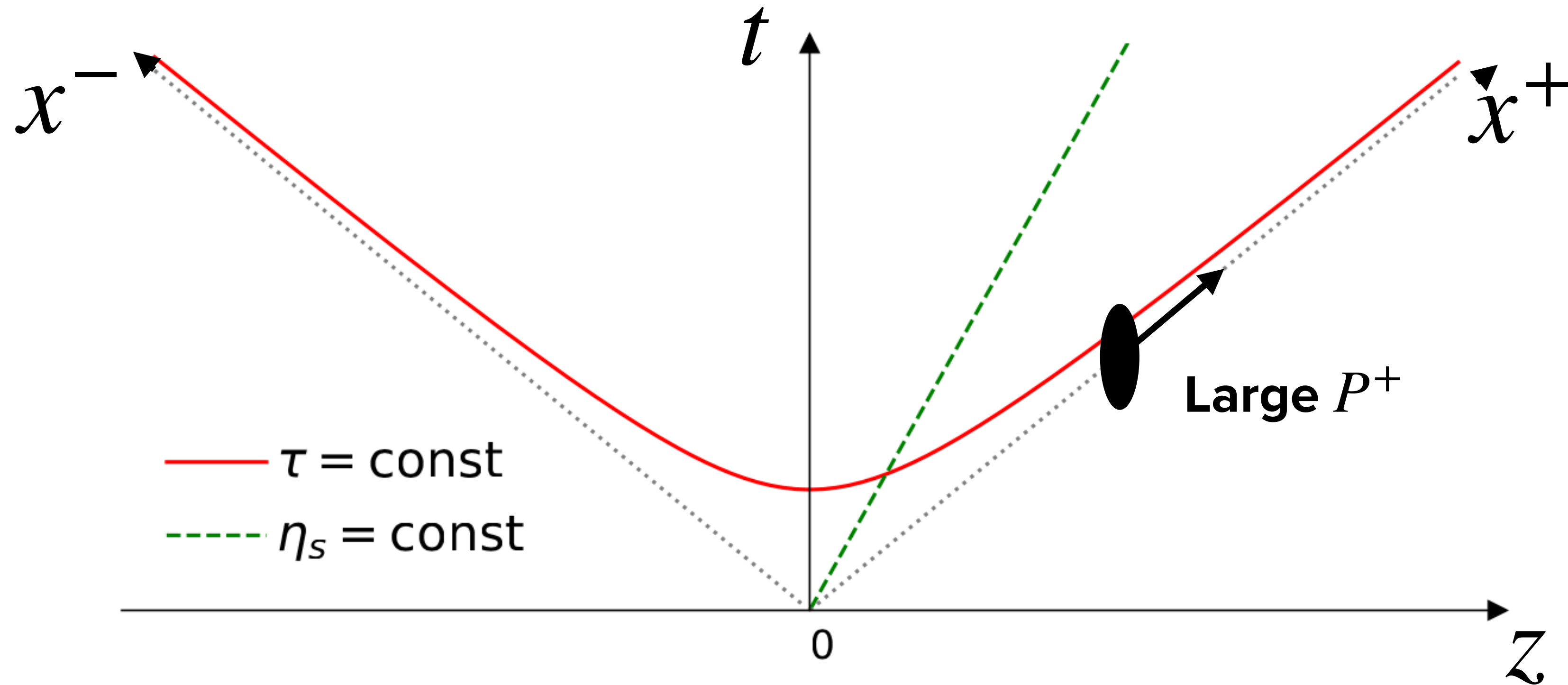


How localized are these sources?  $\Delta z^- \sim \frac{1}{k^+} = \frac{1}{xP^+}$

What is the resolution scale of the probe?  $\frac{1}{x_0 P^+} > \frac{1}{x P^+}$  for  $x > x_0$

→ Color sources look fully localized to the probe in  $z^-$

# Color sources



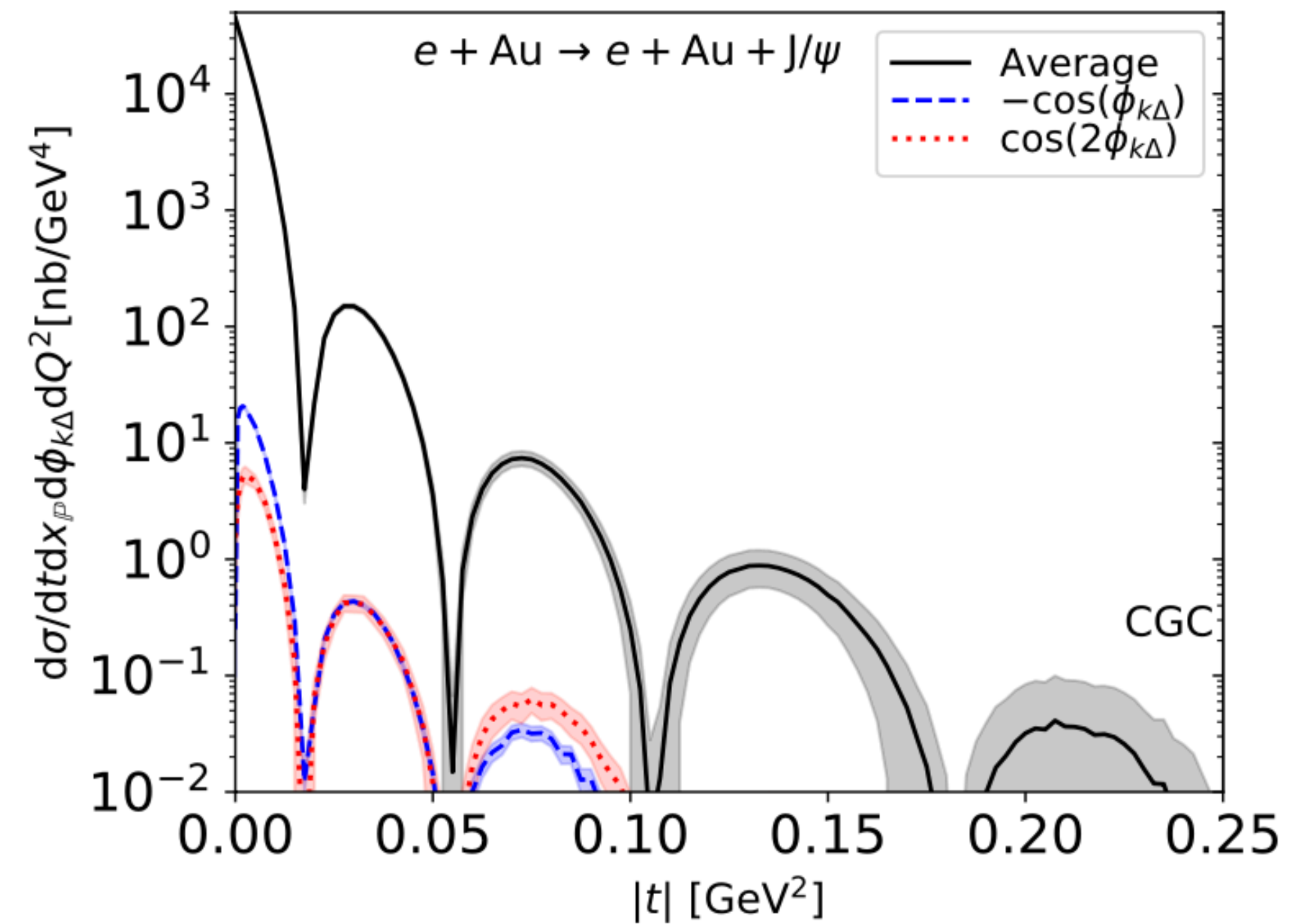
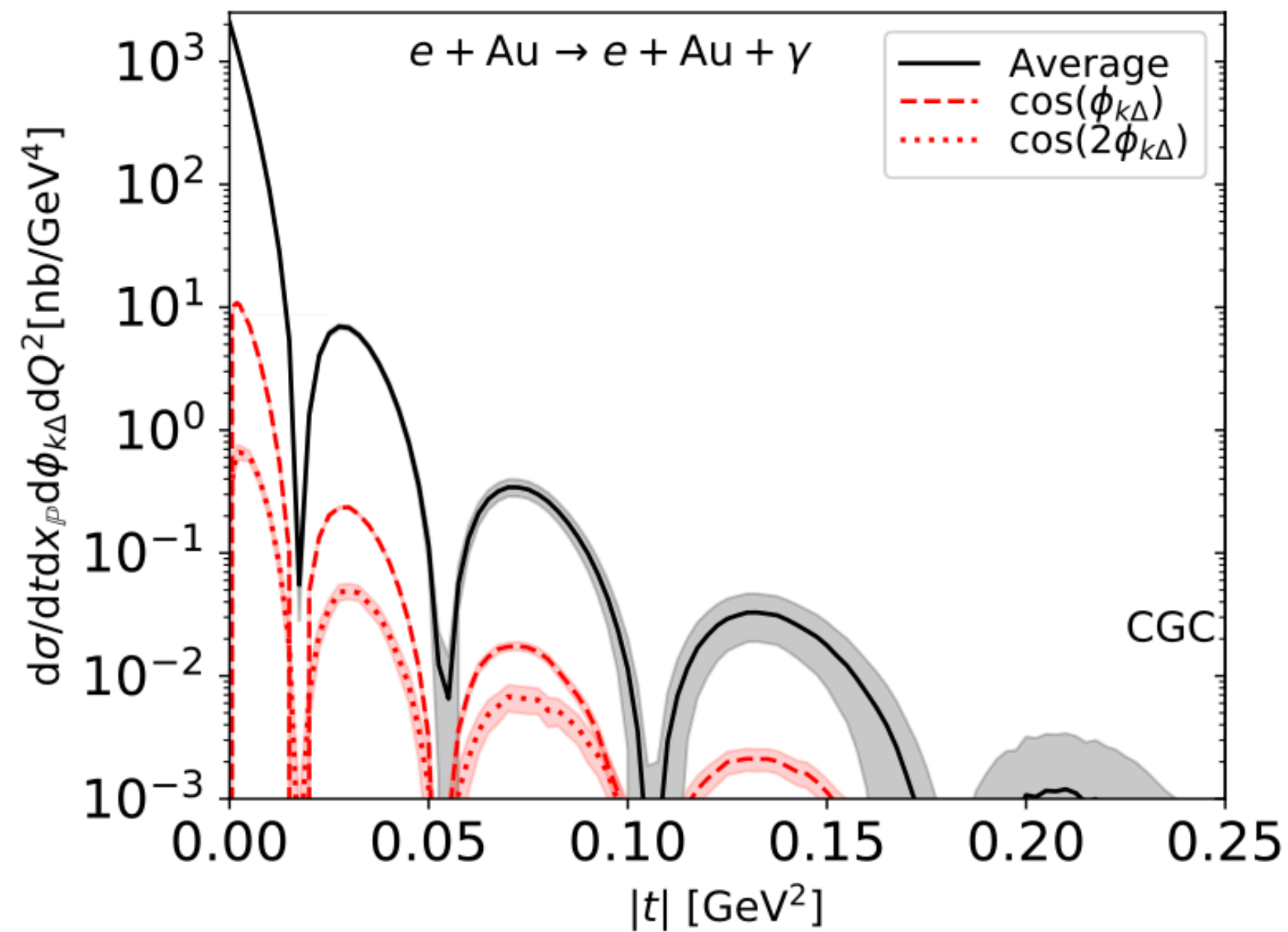
**How fast do they evolve?**  $\Delta z^+ \sim \frac{1}{k^-} = \frac{2k^+}{k_T^2} = \frac{2xP^+}{k_T^2}$  (because  $a_\mu b^\mu = a^+ b^- + a^- b^+ - \vec{a}_T \cdot \vec{b}_T$ )

**What is the time scale of the probe?**  $\tau \approx \frac{2x_0 P^+}{k_T^2} < \frac{2xP^+}{k_T^2}$

→ Color sources look static to the probe in light cone time  $z^+$

# Predictions for e-Au at the future EIC

## DVCS and exclusive $J/\psi$ : Spectra and azimuthal modulations

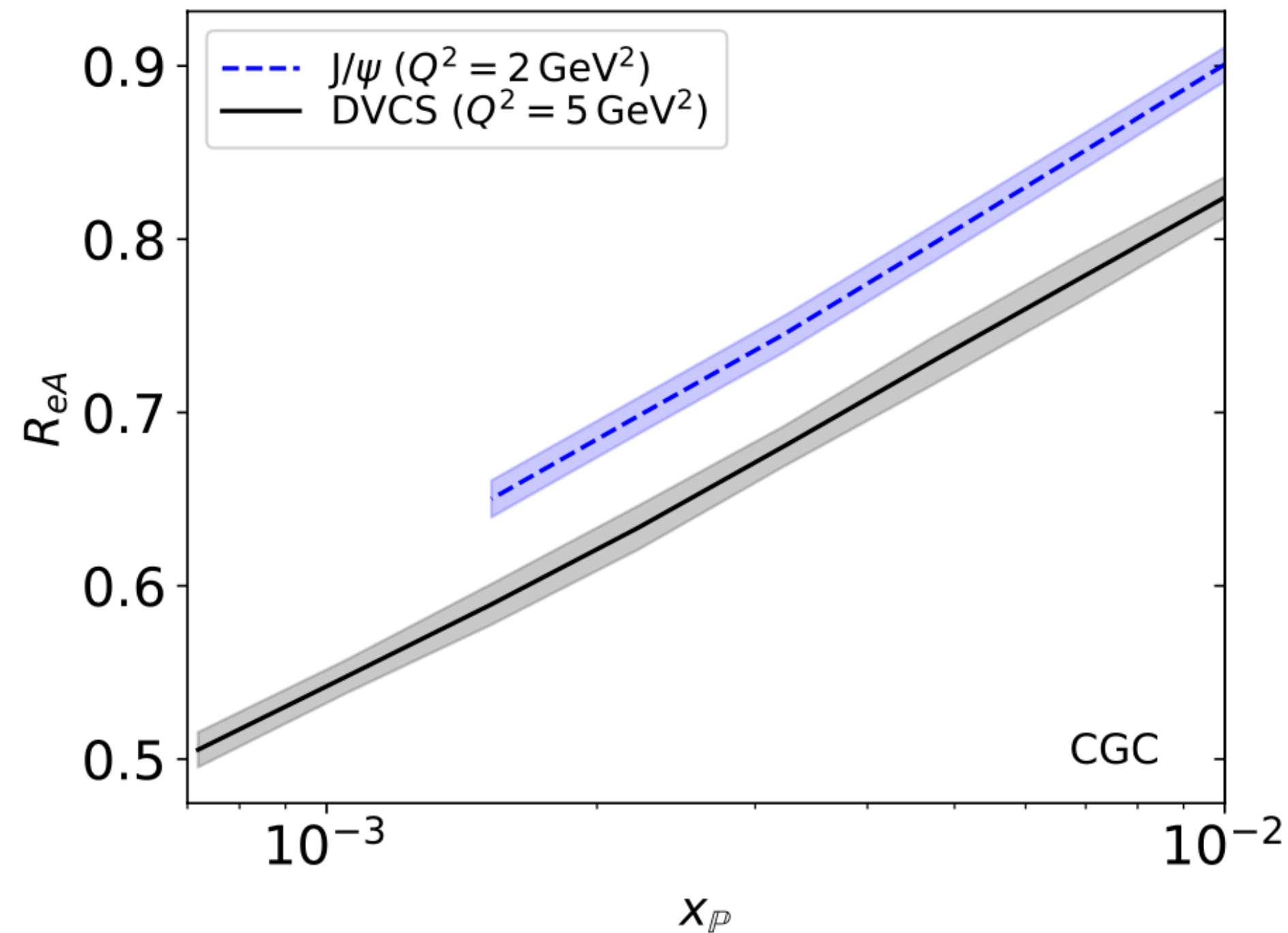


Characteristic dips in spectra due to Woods-Saxon nuclear profile

Azimuthal modulations  $v_n$  a few percent for DVCS, and less than 1% for  $J/\psi$

# Predictions for e-Au at the future EIC

## Nuclear suppressions factor for DVCS and exclusive $J/\psi$



$$R_{eA} = \frac{d\sigma^{e+A \rightarrow e+A+V} / dt dQ^2 dx_{\mathbb{P}}}{A^2 d\sigma^{e+p \rightarrow e+p+V} / dt dQ^2 dx_{\mathbb{P}}} \Big|_{t=0}$$

Expect  $R_{eA} = 1$  in the dilute limit.

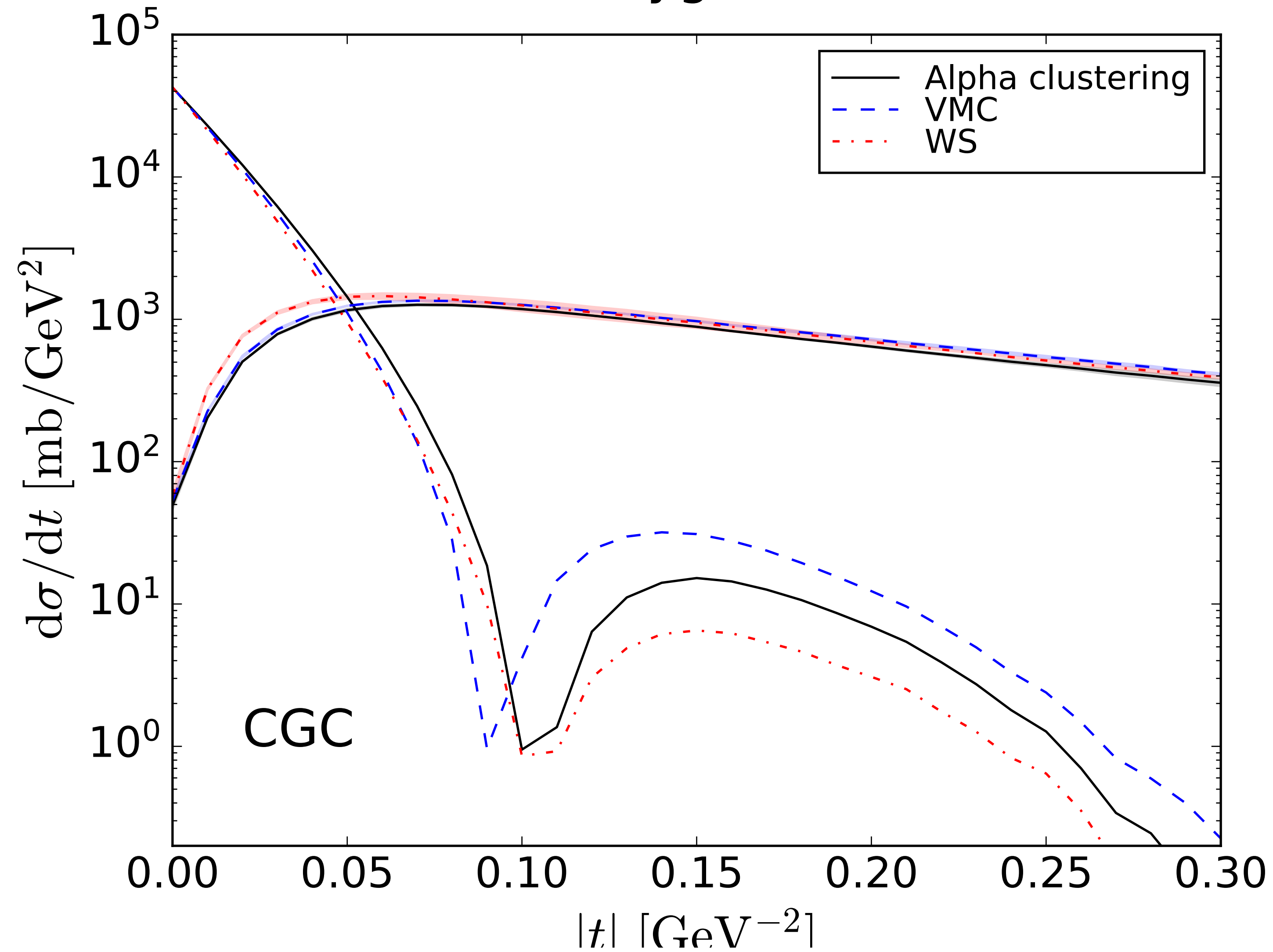
Mäntysaari, Venugopalan. [1712.02508](#)

Significant suppression that evolves with energy /  $x_{\mathbb{P}}$

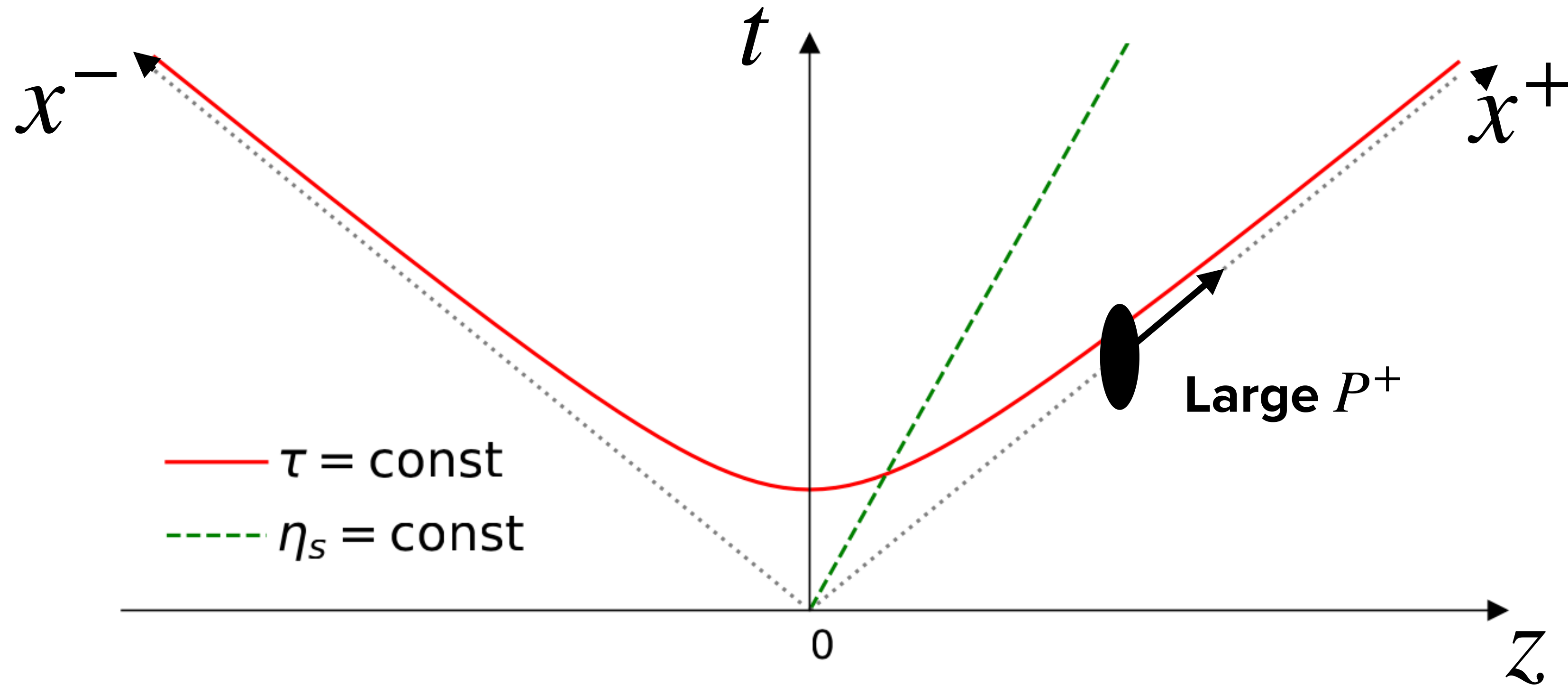
Larger suppression for DVCS due to larger dipole contributions.

# e+O: Oxygen wave function dependence

oxygen



# Light cone



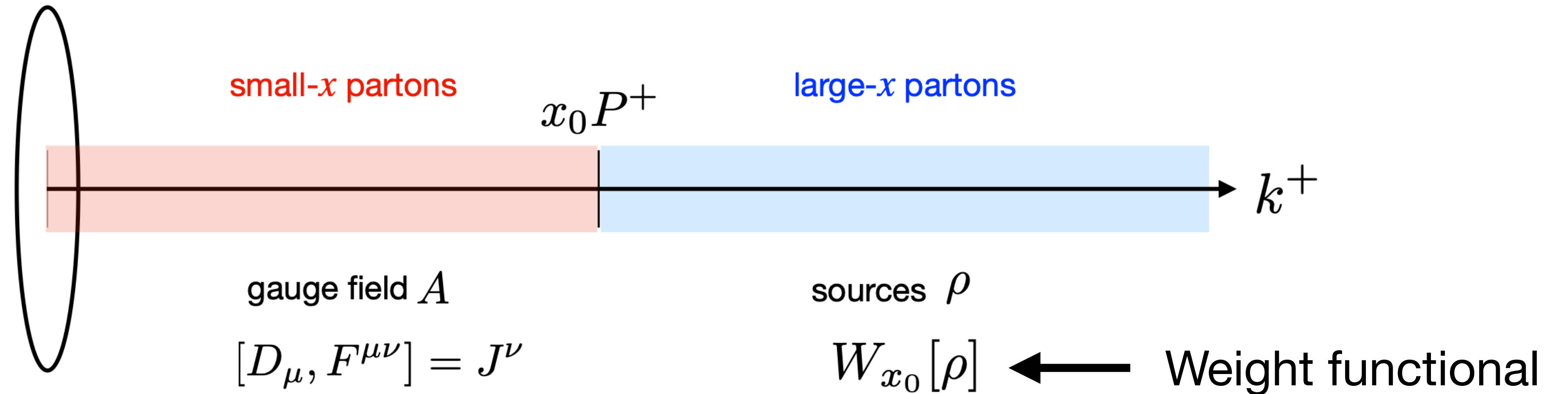
**Light cone coordinates**  $v^\pm = (v^0 \pm v^3)/\sqrt{2}$

**In the future light cone define**  $x^+ = \frac{\tau}{\sqrt{2}}e^{+\eta}$ , and  $x^- = \frac{\tau}{\sqrt{2}}e^{-\eta}$

**or inverted**  $\tau = \sqrt{2x^+x^-}$ , and  $\eta = \frac{1}{2} \ln \left( \frac{x^+}{x^-} \right)$



# Weight functional



What is the weight functional?

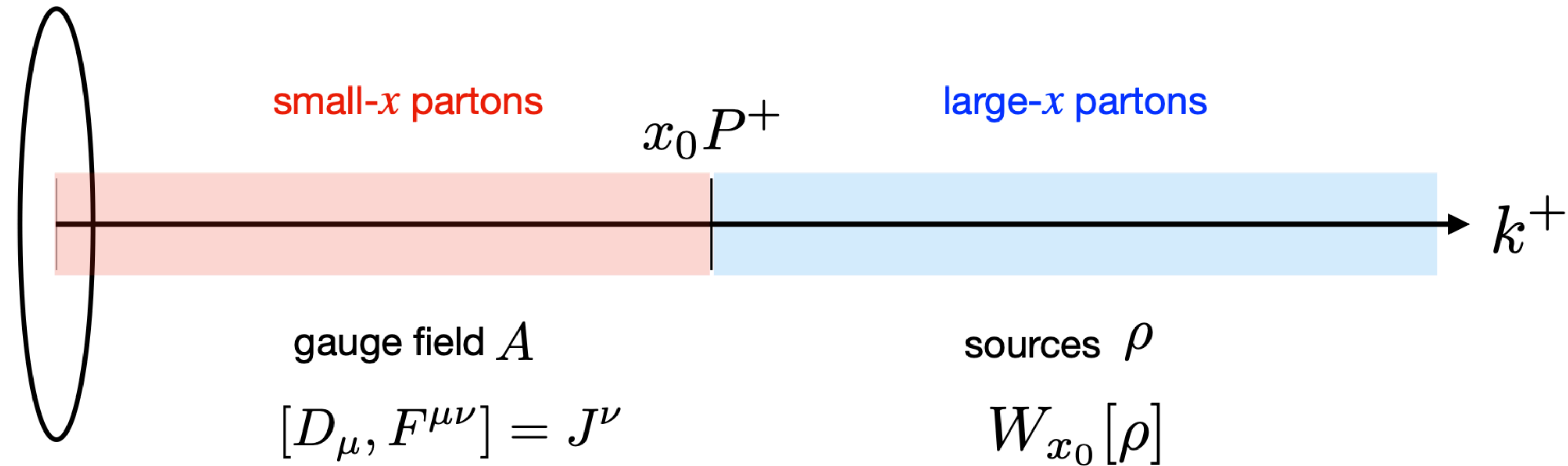
Need to model. E.g. the McLerran-Venugopalan model:

Assume a large nucleus, invoke central limit theorem. All correlations of  $\rho^a$  are Gaussian

$$W_{x_0}[\rho] = \mathcal{N} \exp \left( -\frac{1}{2} \int dx^- d^2x_T \frac{\rho^a(x^-, x_T) \rho^a(x^-, x_T)}{\lambda_{x_0}(x^-)} \right)$$

where  $\lambda_{x_0}(x^-)$  is related to the transverse color charge density distribution of the nucleus

# Weight functional



...where  $\lambda_{x_0}(x^-)$  is related to the transverse color charge density distribution of the nucleus

$$\mu^2 = \int dx^- \lambda_{x_0}(x^-) = \frac{(g^2 C_F)(AN_c)}{\pi R_A^2} \frac{1}{N_c^2 - 1} = \frac{g^2 A}{2\pi R_A^2} \sim A^{1/3}$$

That color charge density is related to  $Q_s$ , the saturation scale.

normalized per color degree of freedom